NASA-CR-192050

IN-05-CR
141631
P.175

UNIVERSITY of
NOTRE DAME

NASA/USRA UNIVERSITY ADVANCED DESIGN PROGRAM 1991-1992

UNIVERSITY SPONSOR
BOEING COMMERCIAL AIRPLANE COMPANY

FINAL DESIGN PROPOSAL

F-92 RELIANT

Air Transport System Design Simulation

May 1992

Department of Aerospace and Mechanical Engineering
University of Notre Dame
Notre Dame, IN 46556

(NASA-CR-192050) THE F-92 RELIANT: AIR TRANSPORT SYSTEM DESIGN SIMULATION Final Design Proposal (Notre Dame Univ.) 175 p

N93-18386

Unclas

G3/05 0141631

F-92 RELIANT PROPOSAL

SUBMITTED TO

UNIVERSITY OF NOTRE DAME
DEPARTMENT OF AEROSPACE AND MECHANICAL ENGINEERING

AEROSPACE DESIGN: AE 441

4 MAY 1992

GROUP F

RYAN COLLINS
CHRISTI CORBETT
MARK GILLESPIE
CESAR GONZALEZ
DAVE MERCURIO
MIKE NOSEK
SEAN O'CONNOR

Any good plan, boldly executed, is better than indecision.

- General Omar Bradley

TABLE OF CONTENTS

SECTION | PAGE #

Table of Contents i

1.0 Executive Summary 1-1

2.0 Mission Scoping and Design Requirements and Objectives 2-1
2.1 The Market 2-1
2.1.1 Distribution Goals 2-1
2.1.2 Distribution Concept 2-2
2.1.3 Daily Operating Plan 2-5
2.2 Requirements and Objectives - Performance 2-7
2.2.1 Aircraft Size, Type, and Number 2-7
2.2.2 Cruise Velocity 2-7
2.2.3 Range and Endurance 2-7
2.2.4 Take Off and Landing Distance 2-7
2.2.5 Radius of Turn and Cruise Altitude 2-8
2.2.6 Maximum Velocity 2-8
2.2.7 Weight 2-9
2.3 Requirements and Objectives - Cost 2-9
2.3.1 Construction Costs and Sales Price 2-9
2.3.2 Operating Costs 2-9
2.3.2.1 Fuel Costs 2-9
2.3.2.2 Maintenance Costs 2-10
2.3.3 Cost Per Cargo 2-10
2.4 Requirements and Objectives - Aircraft Life Span 2-10
2.5 Summary 2-11

3.0 Concept Selection Study 3-1

4.0 Aerodynamic Design Detail 4-1
4.1 Airfoil Selection 4-1
4.2 Method of Aerodynamic Wing Design 4-2
4.2.1 Aerodynamic Configuration Design Study Description 4-3
4.2.2 Aerodynamic Configuration Design Study Results 4-4
4.3 Final Aerodynamic Wing Design and Aircraft Lift Curve 4-8
4.4 Drag Breakdown and Analysis 4-10

5.0 Propulsion System Design Detail 5-1
5.1 Engine Selection 5-1
5.2 Propeller Selection 5-3
5.3 Battery Selection 5-5

6.0 Preliminary Weight Estimation 6-1
6.1 Component Weights and Center of Gravity 6-1

7.0 Stability and Control System Design Detail.......... 7-1
7.1 Directional Stability 7-1
7.1.1 Pitch Stability and Control.......... 7-1
7.1.2 Yaw Stability and Control.......... 7-3
7.1.3 Roll Stability and Control.......... 7-4
7.2 Control Mechanisms.......... 7-5
7.3 Static Stability Analysis.......... 7-6

8.0 Performance Estimation.......... 8-1
8.1 TakeOff and Landing Estimates.......... 8-1
8.2 Range and Endurance.......... 8-2
8.3 Power Required and Available.......... 8-4
8.4 Climbing and Gliding.......... 8-5
8.5 Catapult Performance Estimate.......... 8-6

9.0 Structural Design Detail.......... 9-1
9.1 V-n Diagram and Flight and Ground Load Estimation.......... 9-2
9.1.1 V-n Diagram.......... 9-2
9.1.2 Flight and Ground Load Estimations.......... 9-4
9.2 Basic Structural Components, Substructures, and Assembly.......... 9-6
9.2.1 Lifting Surface.......... 9-6
9.2.2 Fuselage.......... 9-14
9.2.2.1 Fuselage Dimensions.......... 9-14
9.2.2.2 Fuselage Side Panels.......... 9-15
9.2.2.3 Nose and Motor Mount.......... 9-16
9.2.2.4 Landing Gear Support.......... 9-17
9.2.2.5 Catapult Support.......... 9-17
9.2.2.6 Empennage.......... 9-17
9.2.2.7 Connectors, Flooring, and Cross Bracing.......... 9-18
9.2.2.8 Total Fuselage Weight.......... 9-21
9.2.3 Landing Gear.......... 9-22
9.3 Material Selection.......... 9-24

10.0 Construction Plans.......... 10-1
10.1 Major Assemblies.......... 10-1
10.1.1 Lifting Surfaces.......... 10-1
10.1.1.1 Main Wing.......... 10-1
10.1.2 Fuselage.......... 10-4
10.1.2.1 Main Body.......... 10-4
10.1.2.2 Nose and Engine Mount.......... 10-4
10.1.2.3 Empennage.......... 10-4
10.1.3 Landing Gear Assembly.......... 10-5
10.2 Complete Parts Count.......... 10-5
10.2.1 Lifting Surface.......... 10-5
10.2.2 Fuselage.......... 10-6
10.2.3 Landing Gear.......... 10-7
10.2.4 Avionics.......... 10-7
10.2.5 Propulsion System.......... 10-8
10.3 Assembly Sequence.......... 10-8
10.3.1 Main Wing.......... 10-8
10.3.2 Secondary Wing.......... 10-9
10.3.3 Fuselage.......... 10-9

11.0 Environmental Impact........ 11-1
11.1 Disposal Cost........ 11-1
11.2 Noise Characteristics........ 11-1
11.3 Waste and Toxic Materials........ 11-2

12.0 Economic Analysis........ 12-1
12.1 Production Costs........ 12-1
12.1.1 Cost Estimates........ 12-1
12.2 Maintenance Costs........ 12-3
12.3 Operation Costs........ 12-3

13.0 Technical Demonstrator 13-1
13.1 Configurational Data & Geometry........ 13-1
13.2 Weight Data & Center of Gravity........ 13-3
13.3 Technology Demonstrator Tests........ 13-5
13.3.1 Technology Demonstrator Discrepancies........ 13-5
13.3.2 Safety Considerations........ 13-6
13.3.3 Taxi Test........ 13-7
13.3.4 Flight Test........ 13-7
13.3.5 Catapult Test........ 13-9
13.4 Manufacturing Cost and Details........ 13-10

Appendix A - Request for Proposal........ A-1
Appendix B - Stability and Control Analysis........ B-1
Appendix C - Stress Reduction Factor / Life Span Tradeoff Study Procedure... C-1
Appendix D - Spar Location Analysis Program........ D-1
Appendix E - Fuselage Truss Analysis Program and Data File........ E-1
Appendix F - Catapult Analysis........ F-1
Appendix G - Primary Data Items........ G-1
Appendix H - References........ H-1

1.0 EXECUTIVE SUMMARY

Following, the reader will find the design proposal of a semester long design project by group "F" for AE 441. In formulating this design, the driving philosophy was not just to fulfill the mission requirements (discussed in chapter two), but to do so in a creative manner - this explains the unconventional aircraft design, named the F-92 RELIANT. Although unconventional, and perhaps more expensive to produce, the design has distinct advantages which could only be attained through such a creative design.

Figure 1.0.1 presents the three view drawing of the F-92 RELIANT.

Figure 1.0.2 presents a three dimensional view of the F-92 RELIANT.

Major components of the F-92 Reliant include:

Unobstructed cargo bay, 1024 in^3 capability
Loading ramp
Dual wing configuration
Polyhedral wing configuration

These design components either originated or evolved to create an aircraft that would most effectively meet the goals of cargo transportation in AeroWorld at minimum cost.

The unobstructed cargo bay and rear loading ramp allow for ease of cargo loading and unloading. These concepts were born at the initiation of the design; the rest of the aircraft developed around the fuselage cargo bay. It is not surprising that the aircraft design started here - after all, the main purpose of the Reliant is to transport cargo.

The volume cargo capacity of 1024 in^3 was established as the desired capacity based on an extensive market survey of AeroWorld. This large volume allows for a reduced number of flights required per day, yet still avoids flights with large amounts of unused cargo space. This component of the design is based on the reasoning that reducing number of flights reduces fuel costs and also increases plane longevity.

The large horizontal tail and elevator allow for a large range of center of gravity locations; this allows for flexibility in cargo loading. This feature, in combination with the open cargo bay, reduces time and costs associated with cargo balancing and planning.

To effectively utilize the large volume capacity, the Reliant also must be capable of the large weight associated with the volume. To ensure that the Reliant is capable of carrying cargo and its own structural weight, a large lifting surface was designed for the aircraft. It was determined that for a single wing, the necessary 13 square feet of wing would be very difficult to build. The dual wing configuration permits 13 ft^2 of lifting surface without resorting to the structural complication or weight penalties of a single large wing. The placement of the wings with respect to each other maximizes aerodynamic performance of the Reliant without violating stability and control requirements.

The polyhedral design, combined with a large rudder, allows for roll control of the Reliant without ailerons. This decision was based on the assumption that fixed polyhedral joints are less complex to incorporate into the plane than control-dependent ailerons, especially when considering that the wing must be segmented anyway because of packaging constraints. Furthermore, the polyhedral option, unlike the aileron option, avoids the extra costs of an additional servo.

Thus, the unique design of the Reliant grew from the most basic goal of providing a highly cost-effective, reliable means of cargo transportation. On this foundation, with the help of a team of seven engineers, the Reliant evolved to its present configuration.

More specific details about the Reliant are presented on the next pages in the critical design summary. More general information about the Reliant is presented below.

Weight : The empty weight of the aircraft is 5.5 lbs. The maximum takeoff weight is 7.5 lbs.

Range : The range of the aircraft under full cargo load is 8100 feet. This takes into account fuel necessary for ground handling.

Propulsion : The propulsion system includes a Cobalt-15 motor, a 13-inch propeller, and 12 Panasonic 1.2-volt high discharge rate batteries with 900 milliamp-hours capacity.

Avionics : Avionics include a receiver, a speed controller, one servo and one pushrod to control the elevator, and one servo and pushrod to control the rudder and tail wheel.

Landing Gear : The landing gear consists of two forward gear and a tail dragger.

FIGURE 1.0.1

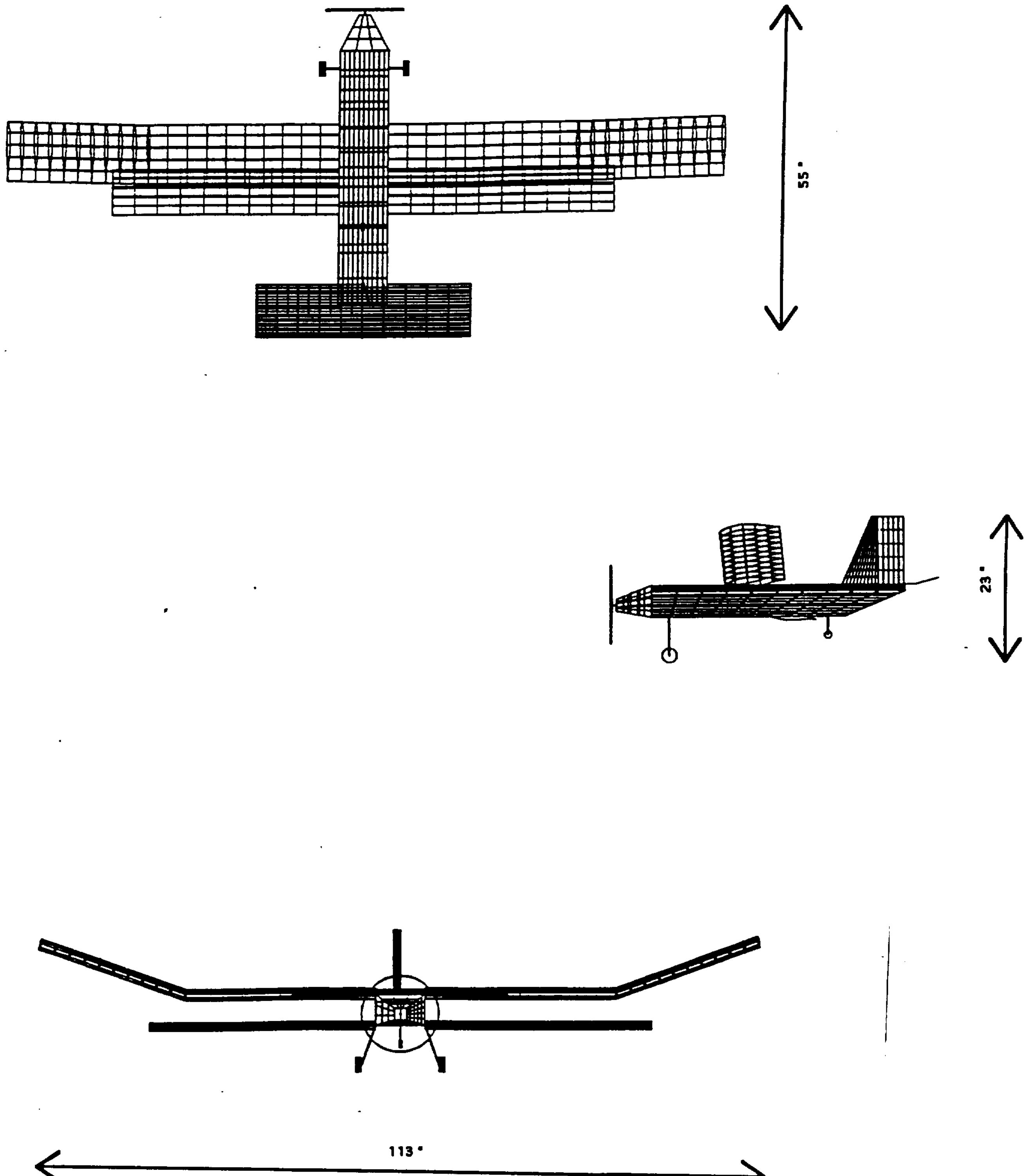

FIGURE 1.0.2

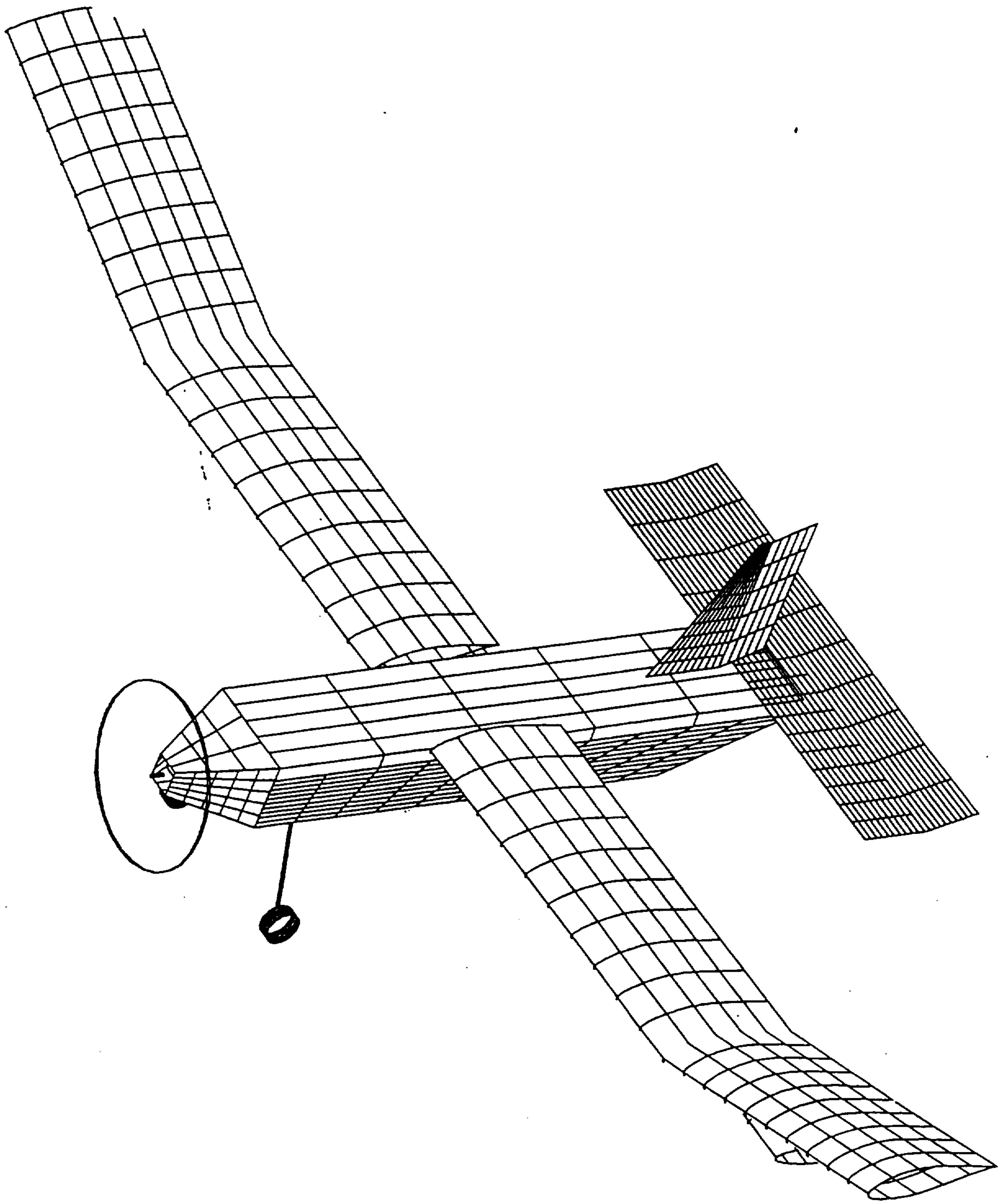

	A	B	C	D	E
1	Parameter				
2	*[all distances relative				
3	to common reference				
4	and in common units]*	Initials of RI:			
5					
6					
7	DESIGN GOALS: DR&O				
8	V cruise	MN	28		
9	Altitude cruise	MN	60		
10	Turn radius	MN	40		
11	Endurance	RC	287.43		
12	Max Payload Volume	RC	1024		
13	Range-max payload	RC	8048		
14	Payload at Max R (wgt)	CG	30.72		
15	Range-min payload	RC	10524		
16	Weight (MTO)	RC	<8.5		
17	Design life cycles	MN	600		
18	Aircraft sales price	SO	$40,568		
19	Target cost per in3 payload	SO	10.25		
20	Target cost per oz payload	SO	341		
21					
22	BASIC CONFIG.				
23					
24	Wing Area	MG	13		
25	Weight(no payload)	RC	5.58		
26	Weight(maximum)	RC	7.5		
27	Wing loading(max Wgt)MW	MG	0.65		
28	length	RC	53		
29	span	MG	10		
30	height	SO	22.5		
31	width (fuselage)	RC	8.5		
32	location of ref. axis origin	MN	x=y=0 at propeller center		
33			z=0 at cargo floor		
34					
35					
36	WING (MAIN)				
37	Aspect Ratio	MG	11.83		
38	Span	MG	10		
39	Area	MG	8.45		
40	Root Chord	MG	0.845		
41	Tip Chord	MG	0.845		
42	taper Ratio	MG	1		
43	C mac - MAC	MN	-0.06		
44	leading edge Sweep	MG	0		
45	1/4 chord Sweep *	MG	0		
46	Dihedral	MN	polyhedral	16deg2.5ft from centerline	
47	Twist (washout)	DM	none		
48	Airfoil section	MG	NACA 63-418		
49	Design Reynolds number	MG	1.5 E 5		
50	t/c	MG	0.18		
51	Incidence angle (root)	MG	neg 2 degrees		
52	Hor. pos of 1/4 MAC	MG	22.0 inches		
53	Ver. pos of 1/4 MAC	MG	4.75 inches		
54	e- Oswald efficiency	MG	0.887		
55	CDo -wing	MG	0.0105		

	A	B	C	D	E
56	CLo - wing	MG	0.0835		
57	CLalpha -wing	MG	0.059/degree		
58	alpha FRL	MG	0		
59					
60	WING (SECONDARY)				
61	Aspect Ratio	MG	10.77		
62	Span	MG	7		
63	Area	MG	4.55		
64	Root Chord	MG	0.65		
65	Tip Chord	MG	0.65		
66	taper Ratio	MG	1		
67	C mac - MAC	MG	-0.06		
68	leading edge Sweep	MG	0		
69	1/4 chord Sweep *	MG	0		
70	Dihedral	MN	0		
71	Twist (washout)	MG	none		
72	Airfoil section	MG	NACA 64-418		
73	Design Reynolds number	MG	1.5 E 5		
74	t/c	MG	0.18		
75	incidence angle (root)	MG	pos 4 degrees		
76	Hor. pos of 1/4 MAC	MG	0.0 inches		
77	Ver. pos of 1/4 MAC	MG	29.0 inches		
78	e- Oswald efficiency	MG	0.897		
79	CDo -wing	MG	0.0099		
80	CLo - wing	MG	0.186		
81	CLalpha -wing	MG	0.016/degree		
82	alpha FRL	MG	2		
83					
84	FUSELAGE				
85	Length	FC	49		
86	Width - max	FC	8.5		
87	Width - min	FC	1.25		
88	Width - avg	FC	7		
89	Finess ratio - L / Davg	FC	7.00		
90	Payload volume	FC	1024		
91	Total volume	FC	1716		
92	Planform area	FC	397		
93	Frontal area	FC	55.25		
94	CDo - fuselage	SO	0.0021		
95	CLalpha - fuselage	SO	neg 0.0019/deg		
96					
97	EMPENNAGE				
98					
99	Horizontal tail				
100	Area	CC	2.25		
101	span	CC	3		
102	aspect ratio	CC	4		
103	root chord	CC	0.75		
104	tip chord	CC	0.75		
105	taper ratio	CC	1		
106	l.e. sweep	CC	0		
107	1/4 chord sweep	CC	0		
108	incidence angle	CC	-4		
109	hor. pos. of 1/4 MAC	MN	49		
110	ver. pos. of 1/4 MAC	MN	6.5		

	A	B	C	D	E
111	Airfoil section	CC	FLAT PLATE		
112	e - Oswald efficiency	CC	0.8		
113	CDo -horizontal	CC	0.0009		
114	CLo-horizontal	CC	0		
115	CLalpha - horizontal	CC	.109654/deg		
116	CLde - horizontal	CC	1.637/rad		
117	CM mac - horizontal	CC	neg.1.72/rad		
118					
119	Vertical Tail				
120	Area	MN	0.61	ft^2	
121	span (height)	MN	0.92		
122	aspect ratio	MN	1.38		
123	root chord	MN	0.88		
124	tip chord	MN	0.46		
125	taper ratio	MN	0.52		
126	l.e. sweep	MN	0.00		
127	1/4 chord sweep	MN	0.00		
128	hor. pos. of 1/4 MAC	MN	46.00		
129	vert. pos. of 1/4 MAC	MN	11.43		
130	Airfoil section	MN	flat plate		
131					
132	SUMMARY AERODYNAMICS				
133					
134	Cl max (airfoil)	MG	1.2		
135	CL max (aircraft)	MG	0.986		
136	lift curve slope (aircraft)	MG	0.0788/deg		
137	CDo (aircraft)	SO	0.03025		
138	efficiency - e (aircraft)	SO	0.83		
139	Alpha stall (aircraft)	MG	10.00 deg		
140	Alpha zero lift (aircraft)	MG	neg 2.5 deg		
141	L/D max (aircraft)	MG	18.39		
142	Alpha L/D max (aircraft)	MG	7.0 deg		
143	Aspect Ratio eff cr (a/c)	MG	9.73		
144					
145	WEIGHTS				
146					
147	Weight total (empty)	FC	5.58		
148	C.G. most forward-x&y	FC	22.4		
149	C.G. most aft- x&y	FC	24.5		
150	Avionics	FC	8.65		
151	Payload (max)	FC	30.72		
152	Engine & Engine Controls	FC	10.5		
153	Propeller	FC	1		
154	Fuel (battery)	FC	15		
155	Structure				
156	Primary Wing	DM	14		
157	Secondary Wing	DM	7.3		
158	Fuselage/emp.	FC	18		
159	Landing gear	SO	8		
160	lcg - max weight	MN	22.4		
161	lcg - empty	MN	24.3		
162					
163	PROPULSION				
164	Type	CG	Cobalt 15		
165	number	CG	1		

	A	B	C	D	E
166	placement	CG	forward		
167	Pavail max @engine (Watt)	CG	79.1		
168	Preq cruise (Watt)	CG	14.6		
169	max. current draw	CG	13.15		
170	cruise current draw	CG	5.92		
171	Propeller diameter	CG	13		
172	Propeller pitch	CG	5		
173	Number of blades	CG	2		
174	max. prop. rpm	CG	7340		
175	cruise prop. rpm	CG	4360		
176	max. thrust	CG	2.5		
177	cruise thrust	CG	0.55		
178	battery type	CG	P-900-SCR		
179	number	CG	12		
180	individual capacity	CG	900		
181	individual voltage	CG	1.2		
182	pack capacity	CG	900		
183	pack voltage	CG	14.4		
184					
185	STAB AND CONTROL				
186	Neutral point	MN	25.8	inches	
187	Static margin %MAC	CC	9.86 - 30		
188	Hor. tail volume ratio	MN	0.44378698		
189	Vert. tail volume ratio	MN	0.12222222		
190	Elevator area	MN	1		
191	Elevator max deflection	MN	'+ 15 / -10 deg		
192	Rudder Area	MN	49.5	in^2	
193	Rudder max deflection	MN	'+/- 15 deg		
194	Aileron Area	MN	n/a		
195	Aileron max deflection	CC	n/a		
196	Cm alpha	MN	'-.02/deg		
197	Cn beta	MN	.0004/deg		
198	Cl alpha tail	MN	.11/deg		
199	Cl delta e tail	MN	0.011/deg		
200					
201	PERFORMANCE				
202					
203	Vmin	MG	12.2		
204	Vmax	CG	46.8		
205	Vstall	MG	22.2		
206	Range max - Rmax	CG	14500		
207	Endurance @ Rmax	CG	517		
208	Endurance Max -Emax	CG	546		
209	Range at @Emax	CG	13600		
210	ROC max	CG	5.36		
211	Min Glide angle	MN	3.2 deg		
212	T/O distance	CG	49.7		
213	T/O rotation angle	CG	6.9		
214	Landing Distance	MN	59		
215					
216					
217	SYSTEMS				
218					
219	Landing gear type	SO	Tail Dragging		
220	Main gear position	RC	X=10		

	A	B	C	D	E
221	Main gear length	SO	6.5 in		
222	Main gear tire size	SO	2.25 in		
223	Tail gear position	FC	X=38		
224	Tail Gear gear length	SO	4.5 in		
225	Tail gear tire size	SO	1.25 in		
226	engine speed control	CG	X=6		
227	Control surfaces	MN	1 elevator, 1 rudder, no ailerons		
228					
229	TECH DEMO				
230					
231	Payload volume	FC	1024		
232	Payload Weight	FC	30.72		
233	Gross Take-Off Weight	FC	7.90		
234	Empty Operating Weight	FC	6.00		
235	Zero Fuel Weight	FC	4.87		
236	Wing Area	MG	13		
237	Hor. Tail Area	MN	1		
238	Vert Tail Area	MN	0.61		
239	C.G. position	FC	22		
240	1/4 MAC position	MN	22		
241	Static margin %MAC	MN	more flight tests needed		
242	V takeoff	CG	26.6		
243	Range max	CG	14481		
244	Endurance max	CG	546		
245	V cruise	MG	28		
246	Turn radius	MN	More flight tests needed		
247	Airframe struct. weight	FC	46.65		
248	Propulsion sys. weight	FC	13.97		
249	Battery Weight	FC	18.13		
250	Avionics weight	FC	5.89		
251	Landing gear weight	FC	9.1		
252					
253					
254	ECONOMICS:				
255					
256	unit materials cost	SO	220		
257	unit propulsion system cost	SO	125		
258	unit control system cost	SO	272		
259	unit total cost	SO	617		
260	scaled unit total cost	SO	246800		
261	unit production manhours	SO	130		
262	scaled production costs	SO	130000		
263	total unit cost	SO	376800		
264	cargo cost ($/in3)	SO	1.77		
265	single flight gross income	SO	1812.48		
266	single flight op. costs	SO	9.64		
267	single flight profit	SO	10%		
268	#flights for break even	SO	500		
269					

2.0 MISSION SCOPING AND DESIGN REQUIREMENTS AND OBJECTIVES

The mission for which the F-92 Reliant was designed to fulfill is the overnight delivery of cargo in AeroWorld. This is to be done at a minimum cost to the operator. With no other specifications given, the design team analyzed the market and considered various other factors to set its own requirements and objectives. It was evident that key factors toward successful mission completion would be balancing various competing facets. These included balancing the percentage of the market to service versus costs of expansion, the added flexibility of employing derivative aircraft versus their cost of development, and any other means of increasing potential profit versus its costs and requirements.

2.1 THE MARKET

Figure 2.1 shows the distribution area, AeroWorld. Expected daily cargo shipments between each city were given in the request for proposal (appendix A). As would be expected, there is a wide variety of high and low volume areas, which made optimizing a distribution plan quite a challenge.

FIGURE 2.1

AEROWORLD

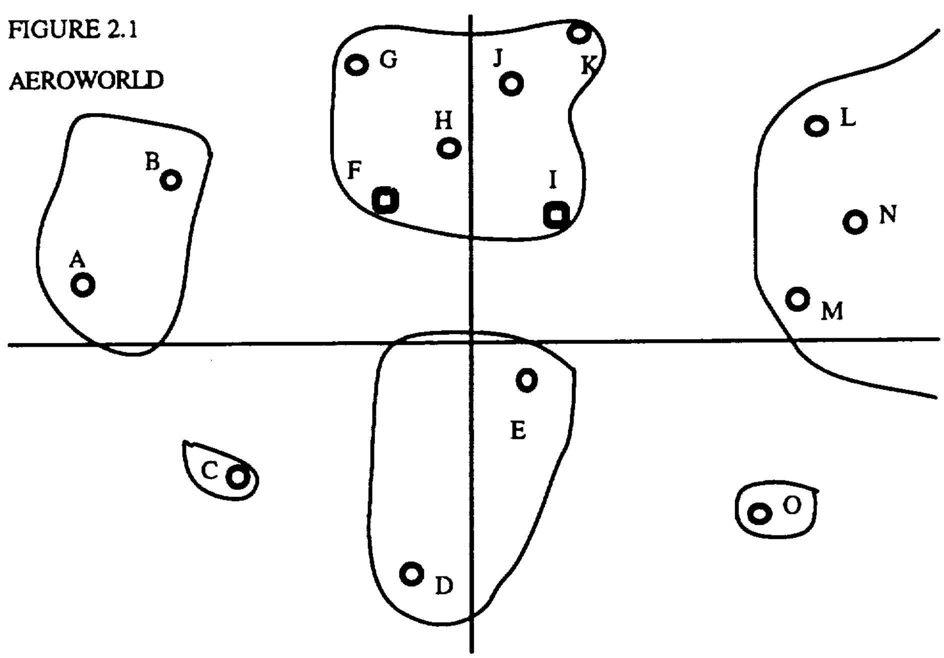

2.1.1 DISTRIBUTION GOALS

The ultimate goal of the distribution system is to provide service to every address in AeroWorld. The plan for market entry and ultimate domination is subject to the capabilities of the distribution system and its application from birth to maturity. It would be impossible to instantaneously activate an entire fleet of aircraft and their supporting infrastructure of hubs, maintenance, and ground operation facilities, not to mention to instantaneously hire and train a full contingency of personnel. Therefore, G-Dome must enter the market with a small fleet, taking advantage of the aircraft as they roll off the assembly line of AE441, Inc. Below, in the detailed description of the full-scale distribution system, two target areas are identified as likely areas for market insertion. They do not depend on a major hub, which is another facility requiring time to complete.

During this initial phase, 100% customer satisfaction will be essential to gaining loyalty and support in the market. This will require the availability of extra "standby" aircraft, capable of flying if another plane is disabled. This is also necessary to accommodate routine maintenance requirements which must be performed on the fleet.

As the fleet increases, more cities will be served, thus expanding the market. Eventually, the required hub facilities will be completed and integrated into the full scale distribution network. By this time, the original aircraft may be retired and the fleet will be continually replenished with new aircraft.

2.1.2 DISTRIBUTION CONCEPT

As stated above, the goal for the distribution system is the service of the entire AeroWorld market. Further, it should be stated that it is desirable to complete that task in the most efficient and cost effective manner possible. Primary factors in developing the distribution system were:

1) Maximizing the efficiency of every flight (avoiding empty or partially full payloads).
2) Balancing the total number of aircraft required against the required payload volume of each aircraft.
3) Ensuring that the range and endurance required did not place excessive demands on battery capacity.
4) Ensuring that the lift required for a payload weight did not necessitate wings too large for structural and shipment constraints.
5) Minimizing the number of flight cycles per plane per day in order to increase the life span of the aircraft.

As a result of AeroWorld geography and of the projected cargo expectations per city per day, a double hub system was chosen to serve as the basis of operation. The first hub, city "I", would serve all cities in the western hemisphere. The second hub, city "F", would serve all of the cities in the eastern hemisphere. Flights from each city would deliver their city's outgoing cargo to their respective hub, then flights would exchange cargo between the two hubs as required. Finally those original flights would return with the cargo to be delivered.

FIGURE 2.1.3

DAILY FLIGHTS

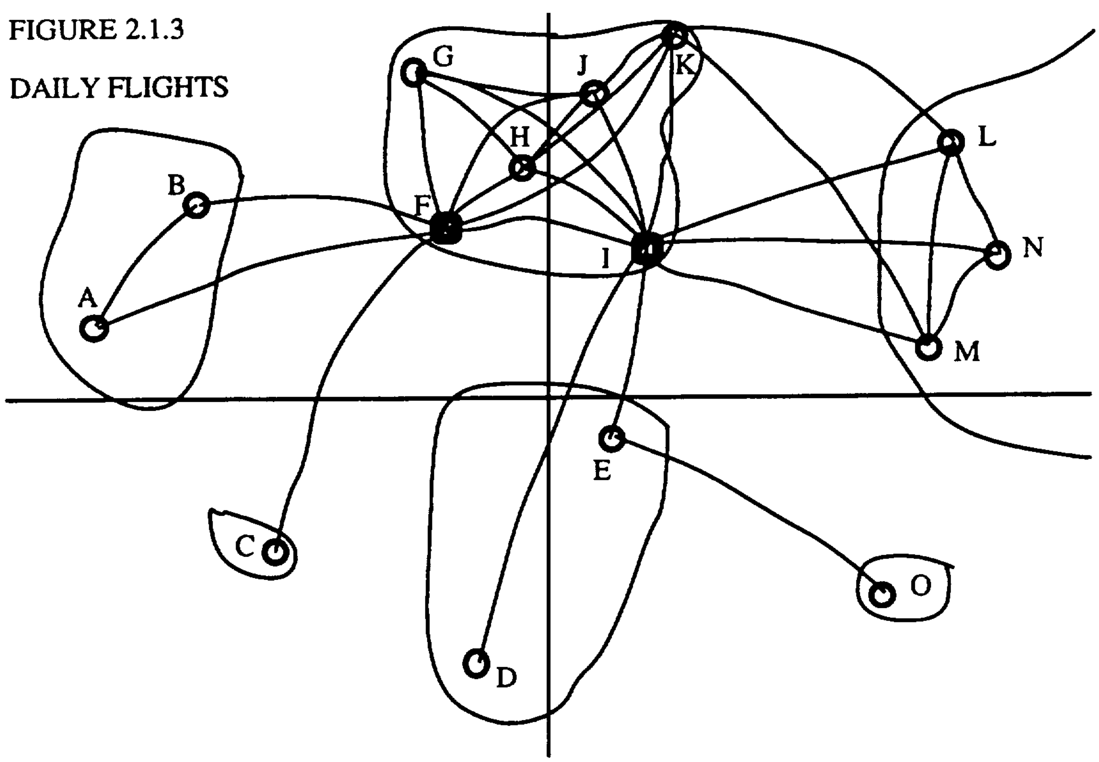

TABLE 2.1.3

FLIGHT SCHEDULE
FLIGHTS FLOWN ONE-WAY

CITY	# PLANES BY PAYLOAD SIZE 1024 (in^3)	576 (in^3)	352 (in^3)		RANGE (ft)	TOTAL (ft)
A-B		1			1697	1697
A-F	2				3493	6986
B-F	2	1			2236	6708
C-F		2			3231	6462
D-I	1				3847	3847
E-I	1		1		1612	3224
F-I	4		1		2474	12370
G-I		1			3280	3280
G-F	1	1			1414	2828
H-I		1			2059	2059
H-F			1		721	721
J-K		1			894	894
J-I	1	1			1709	3418
J-F	1				2059	2059
K-H		1			2236	2236
H-G		1			1281	1281
G-J			1		2040	2040
J-H			1		1342	1342
K-I	1				2010	2010
K-F	1				2953	2953
L-I	2		1		2884	8652
K-L	1				2236	2236
L-N	1				1281	1281
M-I	1		1		2433	4866
N-I	1	1			3256	6512
M-K		1			3256	3256
M-L			1		2000	2000
M-N			1		1281	1281
O-E			1		2720	2720
TOTAL FLIGHTS	21	13	10	44	TOTAL:	101219
TOTAL PLANES	20	12	9	41		
					AVERAGE:	2300
ROUND TRIP TOTALS:					RANGES:	
TOTAL FLIGHTS	42	26	20	88	TOTAL:	202438
TOTAL PLANES	40	24	18	82		
					AVERAGE:	4601

This plan is simple and easy to execute; however, it does not optimize all areas of the operation. Three factors in the optimization process were the reduction of the range a package must fly before reaching its destination, the reduction of the congestion at the hubs, and the reduction of the overall range capability an aircraft must possess. In areas of considerable cargo exchange between outlying cities such as "K", "L", "M", and "N", it proved to be more effective to fly a number of short hops between those cities, exchanging only their own cargo. This was also done between "G", "H", "J", and "K", and between "A" and "B". An example of the reduction of the overall range required for the aircraft was the plan for servicing city "O". Instead of flying directly to and from "I", a range of 4000 feet, the plan calls for flying to "E", and then on to "I", an overall increase in range for the payload leaving "O", but a reduction in range required for each plane, which will benefit the entire fleet. The "KLMN" and "GHJK" areas are also favorable as points of market entry. A schematic of the routes flown is shown in Figure 2.1.3. This concept calls for the use of three different size aircraft, which will be detailed in section 2.2.1. This flexibility in payload capacity allows for greater efficiency in scheduling flights, most notably in cities with lower expected daily cargo volumes .

Table 2.1.3 lists the daily schedule of flights made. A total of 88 one-way flights (or 44 round trip flights) are made daily. The majority of aircraft are scheduled for one round trip or two flight cycles per day. A flight cycle is defined as one takeoff and one landing.

2.1.3 DAILY OPERATING PLAN

The proposed plan for daily operations of the delivery business calls for all cargo to be dropped off at collection centers throughout AeroWorld prior to 4:00 PM. At that time, company operated vehicles will pick up the cargo from these collection centers as well as from any major business clients. The cargo will be delivered to the airports, sorted, balanced and loaded onto an aircraft by 6:00 PM. A four hour flight period is then allowed for all aircraft to reach their destination hub.

From midnight to 0200 AM, the cargo will be unloaded, sorted again, and reloaded onto the appropriate aircraft. Cargo that is destined for a city not serviced by its present hub will be flown on one of the exchange flights to the other hub. As the aircraft servicing their respective destination cities become full, they may takeoff. Others will be required to wait for the exchange flights. All aircraft will be at their final destination by 8:00 AM. Six hours is the time allowed for this phase.

Once at the final destination, the cargo will be unloaded and then sorted for final delivery. Delivery will require a greater number of vehicles than pickup had required because of the increased number of addresses. Depending on the number of vehicles used, all packages may be delivered by 10:00 AM. Of course, the pickup and delivery times may be shifted depending on preference of the operating company. If a delivery time of 8:00 AM was desired, pickups must be at 2:00 PM the previous day.

This daily plan typifies the operation of those aircraft which follow the hub plan. As explained earlier, some aircraft deviate from the hub centered operations. However, the same pickup / delivery target times still apply in these cases.

It should also be noted that the AeroWorld day is 30 minutes long. In the above presentation, 24-hour values were used for simplification. However, when converted to AeroWorld time, there is sufficient amount of time (in minutes) for successful operation.

2.2 REQUIREMENTS AND OBJECTIVES - PERFORMANCE

The distribution system dictates to the design team what the aircraft must be capable of doing in terms of performance and capacity. Such factors include payload volume and weight, cruise velocity, range and endurance requirements, and takeoff / landing distance. Through an iterative process used to best fulfill the goals listed above, various sizes of aircraft and derivative sizes were analyzed.

2.2.1 AIRCRAFT SIZE, TYPE, AND NUMBER

Ultimately, the results dictated that a fleet of 41 aircraft (plus a number of "standby" aircraft) will be required for the entire service of AeroWorld. These 41 aircraft will be of three sizes, depending on their payload volume. The number and payload size of each type will be 20x1024 in^3, 12x576 in^3, and 9x352 in^3. The large aircraft, designated the F-92 RELIANT, will have cargo bay dimensions capable of storing 4x8x32 in^3 in addition to whatever space is needed for loading pallets and other wrapping. The medium sized, designated the F-92 RELIANT-B, and the small sized, designated the F-92 RELIANT-C, derivative aircraft will have cargo bay dimensions of 4x4x36 in^3 and 4x4x20 in^3, respectively, with additional space as required for wrapping and loading considerations. The use of standard 4x4x2 or 4x4x4 cubic inch shipping unit allows onetime wrapping of a pallet and compatibility with any size aircraft cargo hold.

2.2.2 CRUISE VELOCITY

A cruise velocity of 28 feet per second was chosen because it allows for a lower coefficient of lift during cruise and thus, a lower induced drag yet remains below the sonic limit of 30 fps. Also, this speed assures the completion of the daily flight schedule with a sufficient amount of time left in the 30 minute AeroWorld day for pickup and delivery of the cargo.

2.2.3 RANGE AND ENDURANCE

The base maximum range required is the distance from city "I" to "D", which is 3847 feet. For safety, the distance to the next closest city, "E", is added, plus a range for one minute of loiter. The total is then 8038 feet. Using the cruise velocity as the average for the entire flight, the endurance required is then 287 seconds or 4.79 minutes.

2.2.4 TAKE-OFF AND LANDING DISTANCE

The flight schedule dictates what types of aircraft will be serving each city. Different aircraft will require different takeoff and landing distances. For most cities serviced by all three aircraft, the distance required is the 75 feet minus 15% for a factor of safety, which equals 63.75 feet. However, since the large sized plane will service "B" it will be constrained by the shorter runway, which, with a factor of safety, requires takeoff / landing in 51 feet. The medium sized plane, which will service "C", will be further constrained to use a distance of 38.25 feet. Finally, the small plane will service "O" and must take off and land in a distance of 47.8 feet.

2.2.5 RADIUS OF TURN AND CRUISE ALTITUDE

The plane should have the capability of turning with a radius of no greater than half the typical runway length. This allows for capability of the plane to effectively loiter and to make extra landing approaches if necessary. This distance, about 35 feet, also allows for maneuverability and handling qualities required to fly the technology demonstrator in Loftus Center.

Desired cruise altitude is 60 feet. This is high enough to avoid crashing into buildings in AeroWorld. For the technology demonstrator, cruise altitude required is 20 feet due to space limitations in Loftus Center.

2.2.6 MAXIMUM VELOCITY

The original maximum velocity requirement was 40 feet per second. Although the speed limit in AeroWorld is 30 fps, this may not always be the case. It is not out of the question that restrictions may change, especially when flying over water. Therefore it is desirable to have a propulsion system that could take full advantage of such a change.

It must be noted that maximum velocity is a function of excess power. Consideration must be taken to ensure enough power is available for takeoff and climbing performance.

2.2.7 WEIGHT

Original weight estimates were calculated using extensive historical data for the structural components combined with preliminary wing sizing measurements. Maximum payload weight was found according to maximum payload volume of 1024 in^3 and an estimated average cargo density of 0.03 oz/in^3. Estimates resulted in an empty weight of 6.6 pounds and maximum takeoff weight of 8.5 pounds. These estimates were conservative and little faith was placed in potential optimizations.

2.3 REQUIREMENTS AND OBJECTIVES - COST

Cost is divided into two major categories: construction costs and operating costs. Also important is the cost of the aircraft to the buyer and the cost to customer to ship his/her cargo. Detailed cost information will be presented in chapter 12.

2.3.1 CONSTRUCTION COSTS AND SALES PRICE

The estimate baseline aircraft cost was determined by using historical data from the previous two design cycles. Based on this data, the construction cost was estimated at 369,000 AeroWorld Dollars ($AW). This figure includes an estimated $AW 64,000 for construction materials, and $AW 130,000 for labor. These figures are derived from a real world expenditures of $160.00 for supplies and 130 hours of labor. Also included is $AW 175,000 for avionics, motor and batteries. From this, a selling price of $AW 406,000 was selected, which allows a 10 % profit on the aircraft.

2.3.2 OPERATING COSTS

Operating costs are the total of fuel and maintenance costs. The target for total operating cost per flight is $AW 2,960 per flight.

2.3.2.1 FUEL COSTS

The target value for fuel cost per flight is based on the average flight, 2300 feet at 28 fps for an 82 second duration. The fuel used is the total of takeoff, climb, cruise, and landing, and ground handling which equals 220 milliamp hours. At $13.00 per milliamphr, the fuel cost per average flight is $ AW 2,860.

2.3.2.2 MAINTENANCE COSTS

At a cost of $50 per labor-minute for battery exchange, maintenance costs of $100 per flight cycle were derived from an estimated time of two minutes battery exchange time. Although this process could be completed in one minute, it is felt that allowing extra time will result in people taking greater care in changing the batteries, resulting in a reduced chance of accidents due to hasty mistakes. In this way, the extra cost is justified.

2.3.3 COST PER CARGO

Cost strategy for determination of cargo shipping costs is based on the range required for the package to fly. At an average range of 2300 feet, the target cost is $1.65 per cubic inch or $55.11 per ounce. This reflects a 10 % profit for G-Dome Enterprises.

2.4 REQUIREMENTS AND OBJECTIVES - AIRCRAFT LIFE SPAN

The target life span for the aircraft was chosen as 600 flight cycles. Above 600 flight cycles, the requirements of stress reduction factor would require substantial increases in structural weight. Below 600, the cost of replacing aircraft rises with little gain in required stress reduction factor.

2.5 SUMMARY

Table 2.5 summarizes the requirements and objectives discussed in this chapter.

Number of Aircraft:	41 + Standby Aircraft
Daily Flight Cycles:	88
Cruise Velocity:	28 feet per second
Range:	8038 feet
Endurance:	287 seconds
Takeoff / Landing Distance:	51 feet
Turn Radius:	40 feet
Cruise Altitude:	60 feet
Maximum Velocity:	40 feet per second
Weight:	< 8.5 pounds
Production Time:	130 labor hours
Materials Costs:	$160
Fuel Costs:	$2860 per average flight
Maintenance Costs:	$100 per flight
Cost per Cargo:	$1.65 per cubic inch
Life Span:	600 flight cycles

TABLE 2.5

3.0 CONCEPT SELECTION STUDY

Before undertaking the concept study, it was first necessary to become familiar with the inherent constraints and requirements placed upon the design concepts as outlined in Section 2, Mission Scoping and Design Requirements and Objectives. Analysis of the constraints, requirements, and objectives as laid out in Section 2 resulted in the submission of two basic aircraft designs: a canard configuration and a conventional monoplane configuration.

The canard configuration is shown in Figure 3.1. This front loading configuration had two wing mounted engines as well as the large wing and sizeable rectangular fuselage configuration previously mentioned. The conventional monoplane configuration is shown in Figure 3.2. This configuration also had the expected large, rectangular fuselage and sizeable wing, but it is a rear loaded, single engined, puller propeller configuration. Both configurations had large empennage structures like the kind seen on large military transports, and although both configurations may have satisfied the mission constraints, both were, in the end, rejected.

The canard configuration was rejected because of problems and inexperience in dealing with the analysis of the destabilizing canard even though, as a control surface, it would have provided the benefit of positive lift as opposed to the negative lift of a conventional tail. The twin engine aspect of the canard configuration was also rejected because of the fear of asymmetric thrust difficulties. On the other hand, the conventional monoplane configuration received extended consideration. Unfortunately, the initial weight estimate for the aircraft equalled eight and a half pounds. Simple calculations showed that if this aircraft wished to cruise at a speed of 28 feet per second (2 feet per second less than the maximum allowed) and could achieve moderate cruise lift coefficients in the range of 0.6 to 0.8, it would require at least 13 square feet of wing area. Further analysis revealed that this 8.5 pound aircraft would also require 13 square feet of wing area just to barely lift off the ground within the take off constraints even with the use of a 12 inch diameter propeller.

Certainly, building a conventional monoplane with a 13 square foot wing was not impossible, but there were some concerns regarding its construction and performance. For instance, there were no 13 square foot wings in the design data base. Moreover, a 13 square foot wing would be likely to have a 12 or 13 foot wing span which could lead to a dramatic loss of lift on the inboard wing as the aircraft attempted to make a 60 foot radius turn. This loss of lift would result from the fact that in a 60 foot radius turn, the inboard wing could see a much lower relative velocity compared to that of the rest of the aircraft. This inboard lift loss would be very detrimental to an 8.5 pound aircraft, and it could even lead to a possible role from unbalanced lift forces on the inboard and outboard wings. As a result, a third configuration was brought under consideration.

This present configuration was a conventional tandem wing aircraft with a total area of 13 square feet distributed between the two wings. Two benefits resulted from the consideration of this third configuration. First, it would not require the reduction in capacity the conventional monoplane would require to reduce its weight and the required wing area. Consequently, the tandem wing configuration would not require the redesign of the predetermined distribution system planned for the 8.5 pound aircraft carrying the volume of cargo critical to the success of that distribution system. Second, a tandem wing configuration would permit use of two smaller wings of smaller spans while maintaining 13 total square feet of wing area thus alleviating concerns of a stall condition in a turn.

Unfortunately, negative aspects of this third configuration do exist. A tandem wing aircraft will have higher drag due to interference between the wings, and it will also have a lower lift coefficient as than an equivalent monoplane configuration. Additionally, it will have a lower effective aspect ratio than an equivalent monoplane. (ref. 8, pgs 60-64) However, in order to accurately determine the best choice of configuration concept, an extensive trade study analyzing wing weight, aircraft weight, lift produced, and lift to drag ratio would have to be conducted. Time was not available for a study of this sort; therefore, the tandem wing was chosen.

The tandem wing configuration was chosen because it provided the 13 square feet of wing area required to meet the velocity and take off constraints of the mission while eliminating the threat of lift loss in a 60 foot radius turn. This configuration was also chosen because the increased drag and decreased maximum lift were deemed to be preferable to redesigning the distribution system for an aircraft of lesser capacity. Initial estimates demonstrated that enough lift was still achievable to operate the aircraft. The initial tandem wing configuration is shown in Figure 3.3. This configuration is a rear loaded, single engined, puller propeller aircraft with a large wing above and to the rear of a smaller wing. This initial orientation of the wings was chosen to reduce the interference effects between the wings, but later modified as extensive aerodynamic, structural, and stability analyses took place.

TABLE 3.1 CONCEPT SELECTION STUDY SUMMARY

CONCEPT	STRENGTHS	WEAKNESSES
Concept #1 (Canard Config.)	- Canard Control provides positive lift. - Twin engines provide large thrust to transport large/heavy loads.	- Stability of canard more difficult to analyze. - Canard is a destabilizing wing. - Possibility of asymmetric thrust with twin engines.
Concept #2 (Monoplane)	- Simple concept, easy to design and build.	- Large wing needed to carry large/heavy loads. - No large wings, 13 sq. ft., in the data base. - Large wing could stall in a turn of radius 60 feet. - Smaller conv. monoplane required redesign of the mission distribution system.
Concept #3 (Tandem Wing)	- Two wings provide needed surface area to carry large/heavy loads. - Two wings of shorter wing span reduce the possibility of a stall in a turn. - Permitted use of mission distribution system as initially laid out.	- Large drag due to interference between wings. - Aerodynamic analysis is more difficult. - Construction could be more difficult and time consuming.

FIGURE 3.1: CONCEPT #1, THE CANARD CONFIGURATION

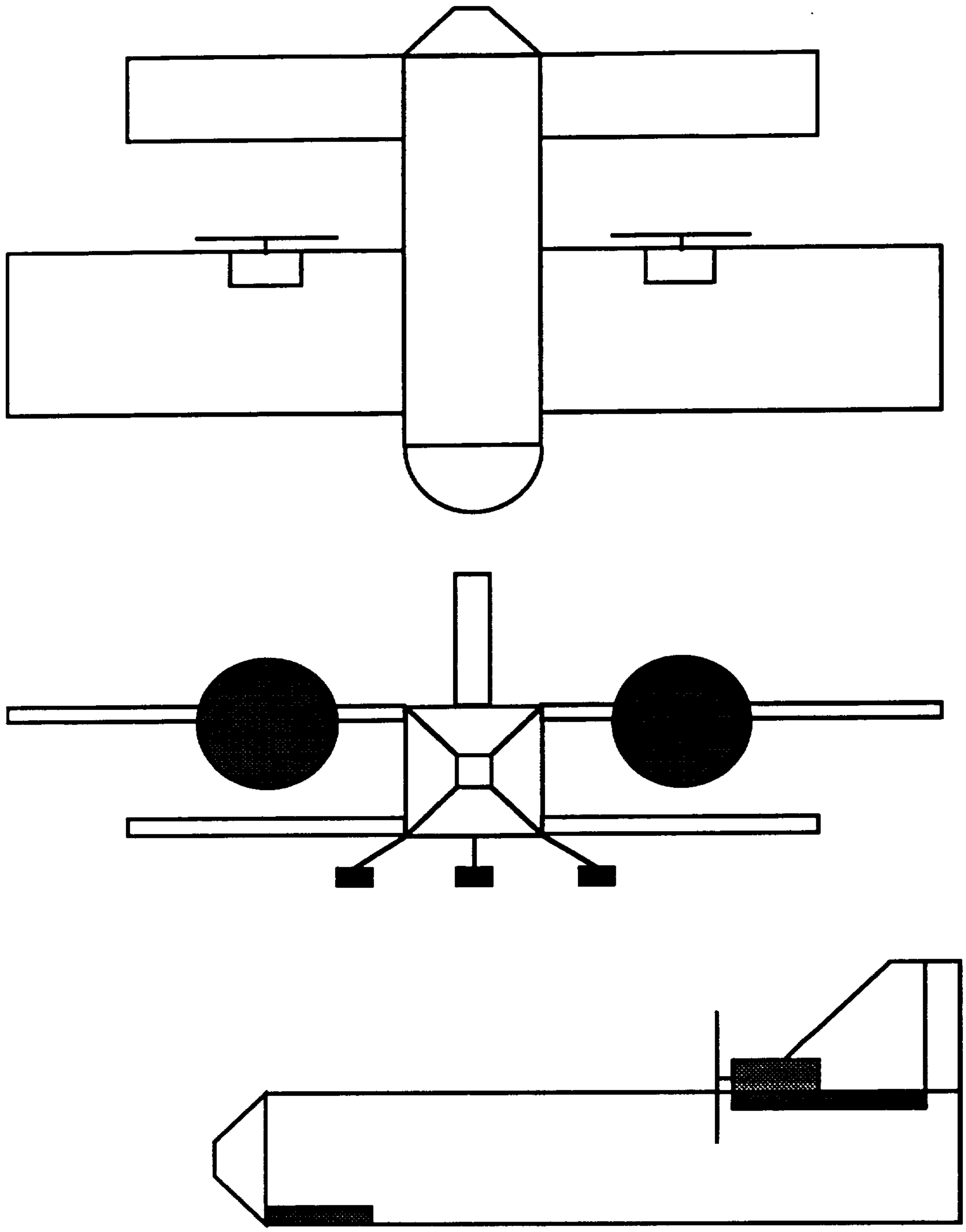

FIGURE 3.2: CONCEPT #2, THE CONVENTIONAL MONOPLANE

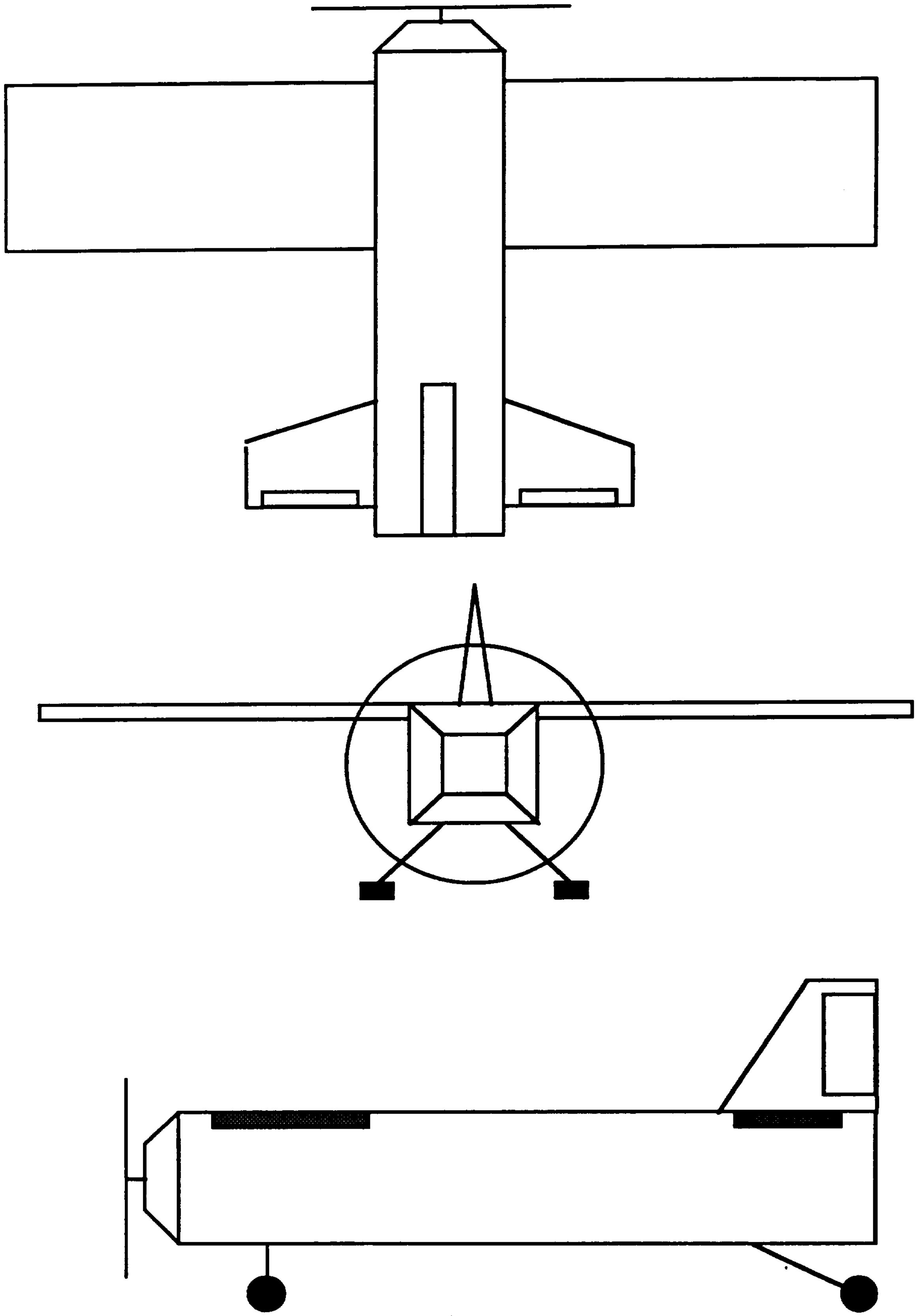

FIGURE 3.3: CONCEPT #3, THE TANDEM WING CONFIGURATION

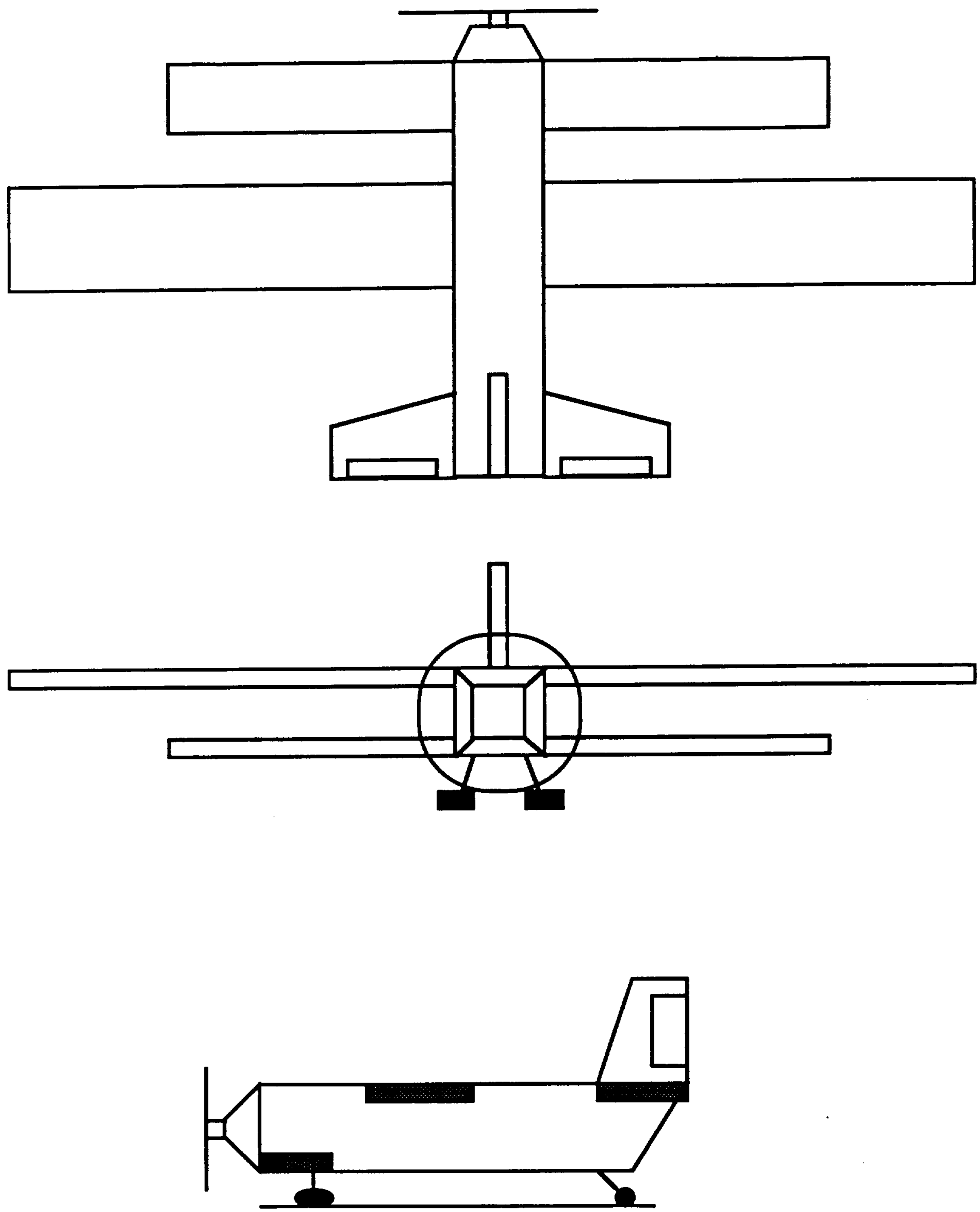

4.0 AERODYNAMIC DESIGN DETAIL

4.1 AIRFOIL SELECTION

The main factor in selecting an airfoil for the finalized tandem wing configuration was a high section lift coefficient. The maximum value desired for the section lift coefficient was 1.2 or better, and an investigation of low Reynolds number airfoils revealed two possible choices. These were the NACA 64-418 and the Wortmann FX63-137A. Both of these airfoils had high section lift coefficients at the design operating Reynolds number of $1.5X10^5$; the maximum section lift coefficient for the NACA 64-418 was 1.2 while the FX63-137A had a value of 1.6. Furthermore, both of the airfoils under consideration could be operated in the drag bucket, but the NACA 64-418 had more gradual stall characteristics. Additionally, the FX63-137A had some undesirable geometric characteristics that were considered, including a sharp cusp at the trailing edge and a concave undersurface. It was determined that because of these geometric characteristics the FX63-137A would be less desirable for manufacturing because of potential difficulties in attaching the Monokote surface to the bottom of the wings. Consequently, the NACA 64-418 airfoil section was selected over the Wortmann FX63-137A because its shape will make it more amenable to construction and its stall characteristics are better; however, it does have a lower maximum section lift coefficient. Finally, the conclusion was made that the same airfoil section, NACA 64-418, should be used as the airfoil shape for both wings to simplify construction and ease of aerodynamic analysis. The lift and drag characteristics for the airfoil are shown in Figures 4.1.1 and 4.1.2. (Reference 9) (Note, the Reynolds number data was only available for a value of $1.7X10^5$.)

FIGURE 4.1.1: NACA 64-418 LIFT CURVE

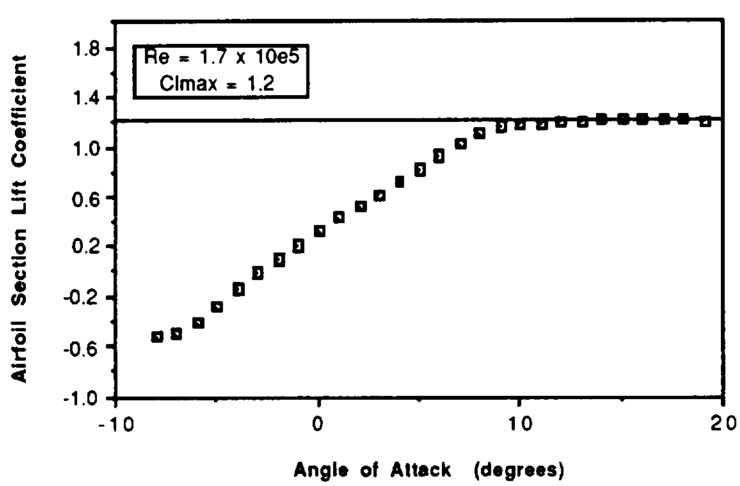

FIGURE 4.1.2: NACA 64-418 DRAG POLAR

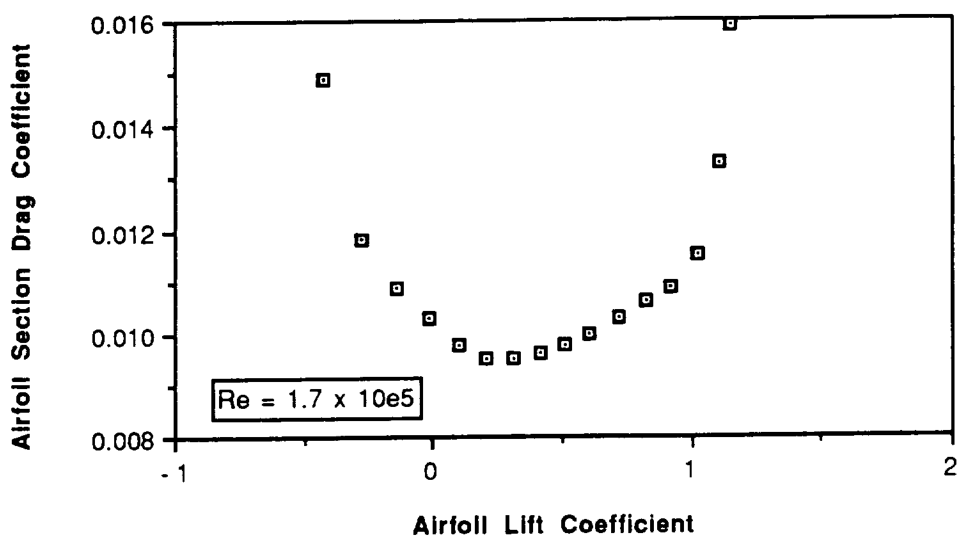

4.2 METHOD OF AERODYNAMIC WING DESIGN

In order to determine the best configuration for the tandem wing concept, Linair was used. Linair is a simple application that makes use of the vortex lattice method, an ideal aerodynamic analysis that does not include viscous effects. In this method, a lattice of horseshoe vortices of unknown strengths is used to model wings under normal flow conditions. The method then makes use of the Biot-Savart law and the flow tangency criterion to solve for the vortex strengths by reducing the system to a series of simultaneous algebraic equations. This then allows for the determination of wing lift distributions, total lift coefficient for a configuration, and induced drag. Linair also allows for the inclusion of interference effects, and according to the application's manual the results from a Linair analysis would be a reasonable approximation of those achieved through experiment.

Unfortunately, because Linair is an inviscid analysis, it will allow for an increase in total lift coefficient with any increase in angle of attack, i.e. stall does not occur. Therefore, while using Linair, the limit on total lift coefficient, C_{Lmax}, was determined by checking the lift distributions of the wings. When the section lift coefficient of a wing in the Linair analysis reached the maximum section lift coefficient of the airfoil section, increases in angle of attack were discontinued because this was an indication that stall was occurring. Therefore, the angle of attack at which the maximum section lift coefficients of the wing and airfoil were equal was taken to be the maximum angle of attack of the configuration, and the total lift coefficient at this angle was taken to be C_{Lmax} for the configuration. Figure 4.2.1 provides an indication of the output Linair can generate for a single wing.

FIGURE 4.2.1: EXAMPLE OF LIFT DISTRIBUTION AS DETERMINED BY LINAIR

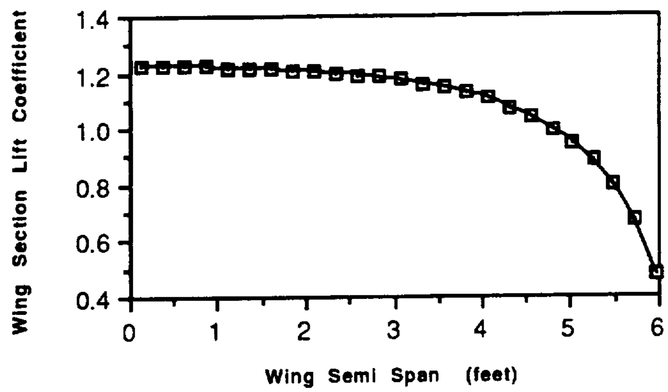

4.2.1 AERODYNAMIC CONFIGURATION DESIGN STUDY DESCRIPTION

Using Linair in the manner described, a study was undertaken to determine the configuration of the tandem wings that would optimize C_{Lmax} as well as the ratio of lift to induced drag. (The ratio of lift to total drag was not considered because Linair is an inviscid analysis.) In this study, the distribution of area between the wings, the aspect ratio of the wings, the angle of inclination of the wings, and the quarter chord separation of the wings were considered. To begin, a base configuration of 10 square feet for the main wing and 3 square feet for the secondary wing was chosen. The respective spans for these wings were 10 feet at an aspect ratio of 10 and 6 feet at an aspect ratio of 12. Neither wing was mounted at an angle of inclination relative to the fuselage, and their quarter chords were separated by 10.5 inches. This separation corresponded to a two inch separation between the trailing edge of the secondary wing and the leading edge of the main wing. As the study progressed, each parameter under consideration was varied individually until the total lift coefficient and the maximum value of lift to induced drag were maximized. When this occurred, the configuration was deemed optimal, and the value of the parameter at which optimization occurred was added to the base configuration and another parameter was varied. When all the parameters had been varied, the final configuration was fine tuned with minor variations in parameters being checked to ensure maximum performance. As a final note, in this study, the maximum value of the ratio of coefficient of lift to coefficient of induced drag was used as a means of evaluating a configuration. In fact, the maximum value of that ratio at a possible cruise condition, as opposed to the overall maximum, should have been considered because the ratio at cruise will be more important to the performance of the aircraft design.

4.2.2 AERODYNAMIC CONFIGURATION DESIGN STUDY RESULTS

The aerodynamic analyses by Linair revealed that the optimal area distribution between the two wings of the tandem wing configuration should be 65% in the main wing and 35% in the secondary wing. This result corresponded to 8.45 square feet of area in the main wing and 4.55 square feet of area in the secondary wing. The analyses also demonstrated that the aspect ratio of the two wings should be 11.83 and 10.77 respectively. These values corresponded to wing spans of 10 feet for the main wing and 7 feet for the secondary wing.

The angles of incidence of the wings and the separation of the quarter chord points were then considered. These two parameters were the most crucial in the aerodynamic analysis because of their influence on interference effects. Results showed that the forward wing should be mounted at an incidence angle of negative two degrees relative to the fuselage reference line, while the rearward, main wing should be inclined at an angle of positive four degrees relative to the fuselage reference line. The reason for this orientation of the wings resulted from an induced upwash of the rear wing on the forward wing causing it to see a higher relative angle of attack than it normally would. Consequently, it was mounted at a negative angle of incidence. On the other hand, the rear, main wing experienced a downwash from the forward, secondary wing causing it to experience a lower angle of attack than it would if the interference between the two wings were not present. As a result, the rear, main wing was inclined four degrees to account for the downwash. Figures 4.2.2.1 and 4.2.2.2 demonstrate how variation in incidence angles affect the values of maximum lift to induced drag ratio and maximum lift coefficient. From these two figures, it is apparent that the positive four, negative two orientation was chosen because it provided the best maximum lift coefficient at the best ratio of lift to induced drag.

FIGURE 4.2.2.1: EFFECT OF ANGLE OF INCLINATION ON L/D

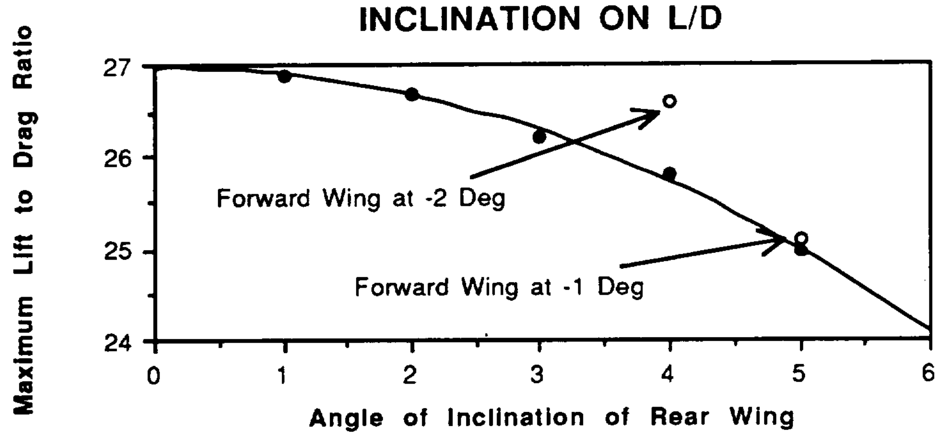

FIGURE 4.2.2.2: EFFECT OF INCIDENCE ANGLE ON MAXIMUM LIFT COEFFICIENT

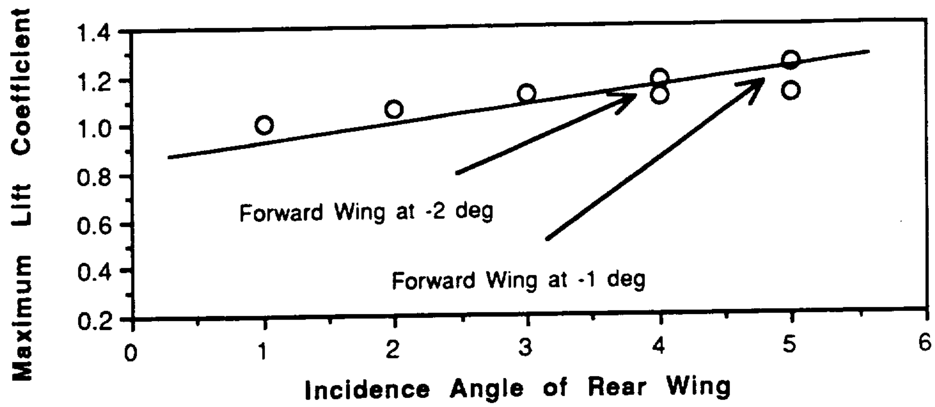

Lastly, the aerodynamic analyses revealed that optimal separation of the quarter chord points of the wings was six inches. This is verified by Figures 4.2.2.3 and 4.2.2.4 which reveal how the ratio of lift to induced drag steadily increase with separation distance up to six inches while maintaining a maximum lift coefficient consistent with other values of quarter chord separation. However, these figures also indicated that any separation greater than six inches does not significantly decrease aerodynamic performance.

FIGURE 4.2.2.3: EFFECT OF QUARTER CHORD SEPARATION ON L/D

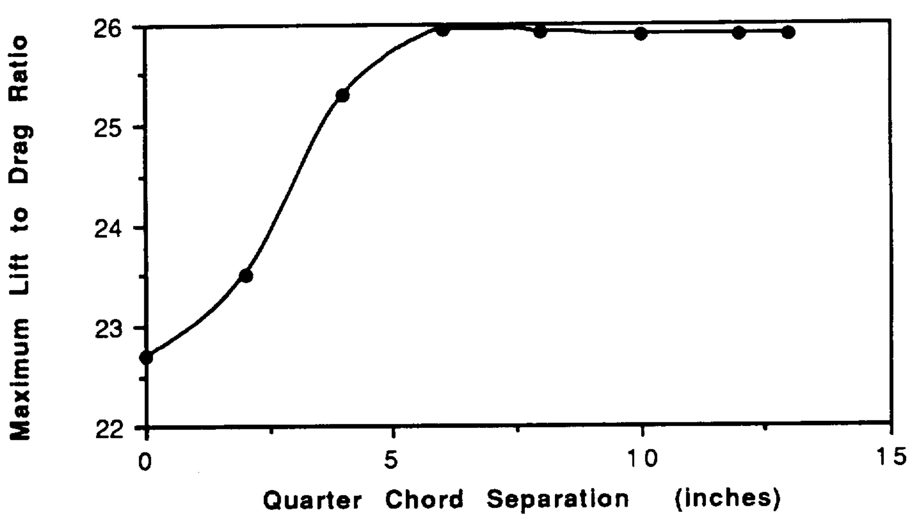

FIGURE 4.2.2.4: EFFECT OF QUARTER CHORD SEPARATION ON MAXIMUM LIFT

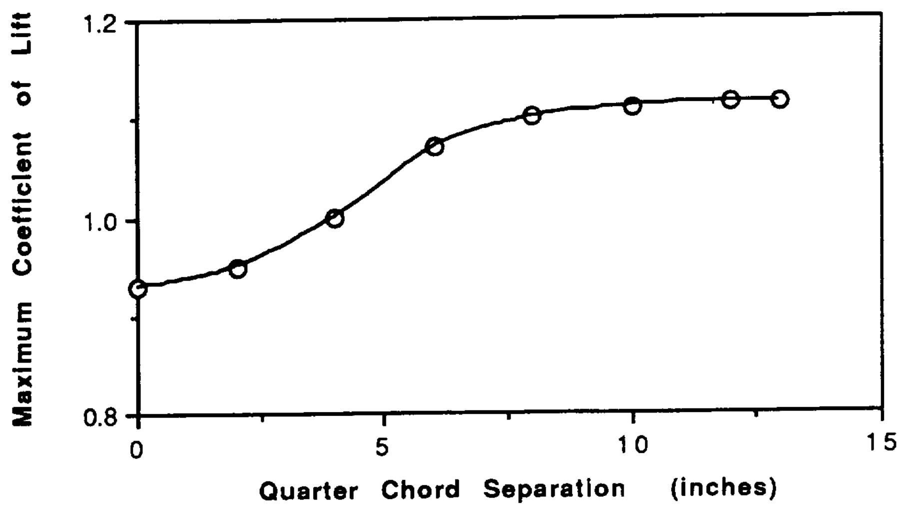

The aerodynamic analyses thus indicated that the optimal tandem wing configuration would provide the main, rear wing with 8.45 square feet of area and an aspect ratio of 11.83. They also indicated that this wing should be inclined four degrees relative to the fuselage reference line and its quarter chord should be six inches from the quarter chord of the secondary, forward wing. This secondary wing, according to the analyses, should have 4.55 square feet of area at an aspect ratio of 10.77 and it should be declined by two degrees relative to the fuselage reference line. However, this was not the final concept configuration; structural and stability considerations mandated changes.

The lift distributions of this configuration with the main wing in the rear, upper position and the secondary wing in the forward, lower position were found to be undesirable because the upwash of the secondary wing on the main wing. This upwash was evidenced by very high section lift coefficients on the outboard portion of the larger, main wing. This situation was deemed unacceptable for two reasons. First, in this orientation, the highest aerodynamic loads occurred on the outside of the wing near the tip instead of at the inside near the root where the wing is strongest. Second, if the aircraft was near its stall lift coefficient and attempted to turn, the tip of the inboard wing could easily stall resulting in an unbalanced loading on the wing causing the aircraft to roll out of control. Furthermore, if the wing incorporated any form of dihedral, the stall and loss of lift at the tip would be exacerbated. Therefore, it was deemed necessary to change the orientation of the wings.

Essentially, the change in wing orientation was manifested in an exchange of the lateral positions of the wings. The main wing was moved forward and the secondary wing was moved aft, but the main wing remained above the secondary wing. The angles of incidence were then altered to accommodate this configuration change and account for the upwash and downwash effects discussed earlier. The main, now forward, wing was declined two degrees and the secondary, now rear, wing was inclined four degrees. Static stability analysis then required that the quarter chord separation be increased by one inch to seven inches, but as noted earlier, this increase in separation distance did not greatly affect aerodynamic performance. No other parameters were required to change since they did not affect stability and they did not improve aerodynamic performance above that of this new configuration. Unfortunately, the new configuration with the new orientation of the wings saw the maximum lift coefficient and the maximum lift to drag ratio decreased slightly from that of the previous configuration. This change in wing orientation finalized the configuration of the tandem wings so that now instead of a tandem wing configuration, the aircraft appeared to be more of a biplane. (The new wing lift distribution and the old lift distribution that necessitated the changes in wing orientation may be seen in Figures 4.2.2.5 and 4.2.2.6 respectively.)

FIGURE 4.2.2.5: OLD ORIENTATION LIFT DISTRIBUTION AT 10 DEGREES AOA

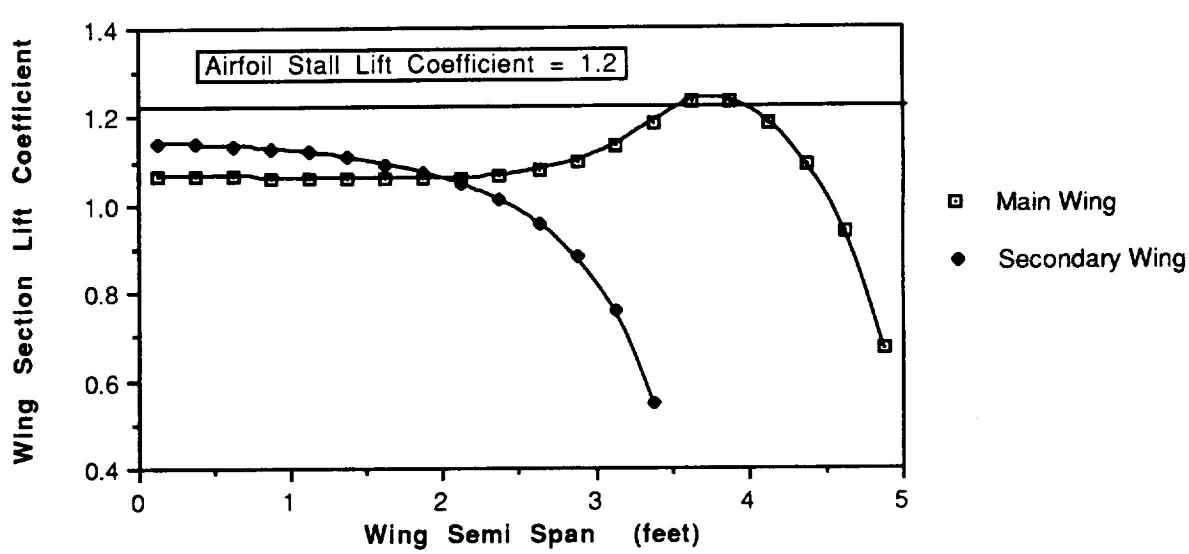

FIGURE 4.2.2.6: NEW ORIENTATION LIFT DISTRIBUTION AT 10 DEGREES AOA

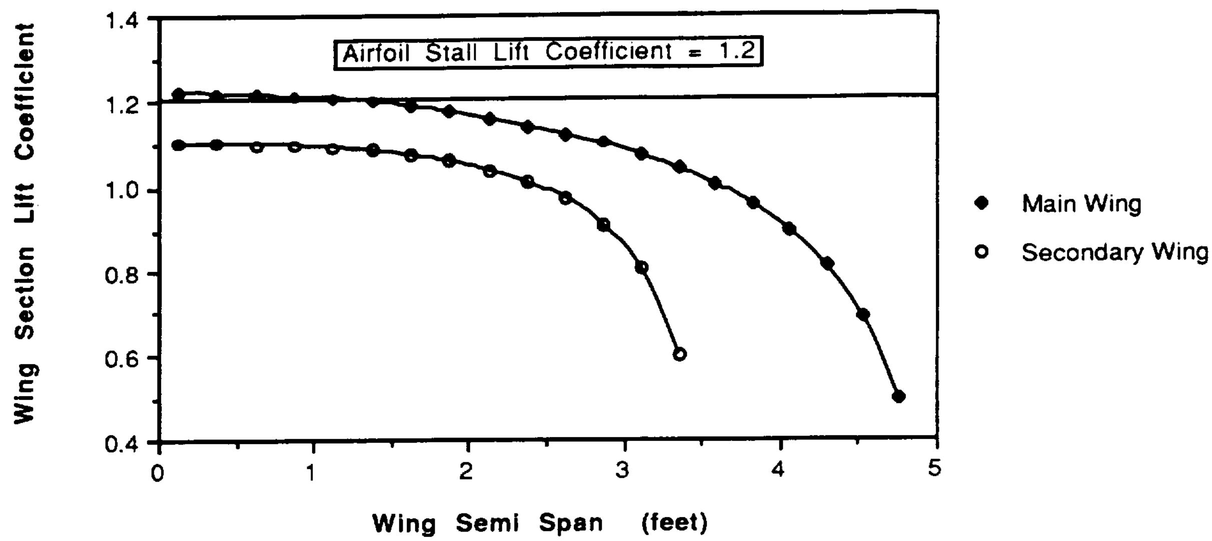

4.3 FINAL AERODYNAMIC WING DESIGN AND AIRCRAFT LIFT CURVE

The parameters for the finalized configuration are listed below in Table 4.3.1.

TABLE4.3.1 FINAL VALUES FOR THE TANDEM WING CONFIGURATION

	Main/Forward Wing	Secondary/Rear Wing
Aspect Ratio	11.83	10.77
Area (ft^2)	8.45	4.55
Span (ft)	10.0	7.0
Chord (ft)	0.845	0.65
Incidence Ang.	-2 degrees	+ 4 degrees
Quarter Chord Locations (in)	22.0	29.0

With this information, a static stability analysis revealed the need for a horizontal tail of 2.25 square feet and a 3.0 foot span mounted at -4 degrees incidence to the fuselage. This tail was incorporated into the Linair input file, and then, a lift curve was generated using a Linair sweep of angle of attack. Maximum lift coefficient for the curve and maximum angle of attack were determined as previously described. This lift curve was then modified for fuselage effects with the following relationship. (Reference 3, pg 145)

$$C_{L\,\text{with fuselage}} = C_{L\,\text{without fuselage}} \times \left(1 - \frac{S_{fus}}{S_{ref}}\right)$$

S_{fus} for the above relationship was determined by the desired volume of cargo the aircraft was required to carry in order to satisfy the mission. This value was found to be 0.31 square feet, and the final lift curve for the entire aircraft, determined from the above relationship, is shown in Figure 4.3.1. This curve shows a maximum lift coefficient of 0.986, a lift curve slope of 0.198 per degree, and a zero lift angle of attack of -2.51 degrees.

FIGURE 4.3.1: AIRCRAFT LIFT CURVE

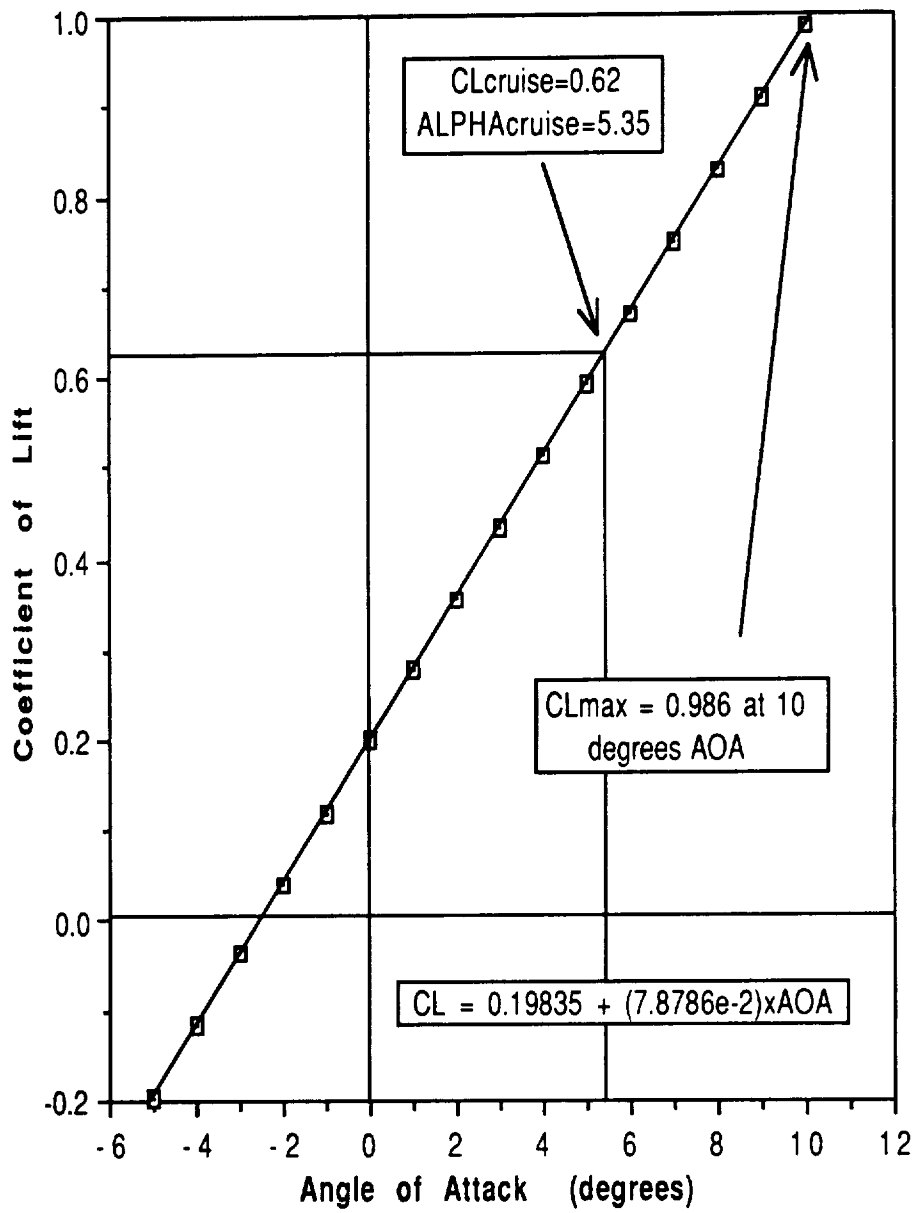

4.4 DRAG BREAKDOWN AND ANALYSIS

The drag prediction for the chosen configuration was performed using Daniel T. Jensen's thesis on drag prediction for low Reynolds numbers. Specifically, Method II was used. In this method, drag was broken down into a parasite drag coefficient for all components excluding the wing, a profile drag coefficient, and a wing lift-induced drag coefficient. Explicitly, the drag equation is as follows:

$$C_D = C_{Do} + C_{Dp} + (1 + \delta)\frac{C_L^2}{\pi AR}$$

In this equation, the first term is the parasite term, the second is the profile term, and the third is the lift-induced term.

The first term, the parasite term, (C_{Do}) was defined for each component with the following equation:

$$C_{Do} = \Sigma \frac{C_{f\pi} FF_{\pi} S_{wet\pi}}{S_{ref}}$$

In this relationship, $C_{f\pi}$ is the skin friction coefficient of each aircraft component, FF_{π} is the form factor of each component, and $S_{wet\pi}$ is the wetted area of each component. S_{ref} is the reference area, the total wing area of 13 square feet. For calculation of the parasite term, the value of the skin friction coefficient was governed by whether or not the flow over the component was laminar or turbulent and the distance at which transition occurred. It was calculated in the following manner:

$$C_{f\pi} = \frac{x_{trans}\,(C_{f_{laminar}}) + (l_{\pi} - x_{trans})\,(C_{f_{turbulent}})}{l_{\pi}}$$

On the other hand, the form factor for each component was determined through the use of these equations:

$$\text{Empennage:} \quad FF_{\pi} = [1.0 + \frac{0.6}{(x/c)_m}(\frac{t}{c}) + 100(\frac{t}{c})^4][1.34M^{0.18}(\cos\Lambda_m)^{0.28}]$$

$$\text{Body:} \quad FF_{\pi} = \left(1.0 + \frac{60.0}{(l/d)^3} + \frac{(l/d)}{400}\right)$$

Together, these equations provided the parasitic drag breakdown for the aircraft, and the results of this breakdown are presented in Table 4.4.1.

TABLE 4.4.1 PARASITIC DRAG BREAKDOWN

	$C_{f\pi}$	FF_{π}	$S_{wet\pi}$	$C_{Do\pi}$
Fuselage	0.0027	1.1075	9.131	0.0021
Horizontal Tail	0.0036	0.7317	4.500	0.0009
Vertical Tail	0.0039	0.7010	1.220	0.00025
Landing Gear				0.00066
			$C_{Dototal}$	**0.00985**

The landing gear contribution seen in Table 4.4.1 was handled in a different manner than that described above because it was not explicitly covered in Jensen's thesis. Therefore, the value for the landing gear contribution was determined to be 0.00066 as shown above based on a method given in Aerodynamics, Aeronautics, and Flight Mechanics by B.W. McCormick. (Reference 3, pg 196)

The profile and induced components of drag, however, were determined as stipulated by Jensen:

$$C_{Dwing} = (C_{Dmin} + kC_L^2) + (1 + \delta)\frac{C_L^2}{\pi AR}$$

For this equation, C_{Dmin} was the coefficient of drag of the airfoil at zero lift and k was the slope of a plot of C_d versus C_l^2 for the airfoil. The δ in the equation is a characteristic of the wing planform and it was easily determined from graphical information. However, because the tandem wing configuration incorporated two wings, it became necessary to slightly modify the profile and induced drag coefficient components for contributions from both wings. The following equation illustrates how this was done:

$$C_{Dwings} = \frac{S_{mw}}{S_{ref}}\left((C_{Dmin} + kC_{L_{mw}}^2) + (1 + \delta_c)\frac{C_L^2}{\pi AR_c}\right) + \frac{S_{sw}}{S_{ref}}\left((C_{Dmin} + kC_{L_{sw}}^2) + (1 + \delta_c)\frac{C_L^2}{\pi AR_c}\right)$$

In this equation, the subscript mw denotes a value corresponding to the main wing, sw denotes a value corresponding to the secondary wing, and c denotes a value of combined main and secondary influence. Therefore, use of this equation necessitated determination of the individual lift coefficients for each wing at various angles of attack as well as combined values of δ and aspect ratio.

The lift coefficients for each wing were easily determined from Linair and Figure 4.4.1 shows how those values varied with changes in angle of attack of the aircraft. Unfortunately, the determination of a combined δ and aspect ratio for the configuration were more difficult. First, the δ value for each wing was determined based on their respective aspect ratios. Then using the empirical summation method

$$\frac{1}{e_c} = \frac{1}{e_{mw}} + \frac{1}{e_{sw}}$$

an efficiency for the wing combination was determined. (Note, efficiency, e, equals $1/(1+\delta)$.) Now, using the induced drag data from Linair and the relationship that:

$$AR_c = \frac{C_L^2}{\pi e_c C_{Di}}$$

the combined aspect ratio of the wing combination was determined. Finally, a δ for the wing combination was determined based on the combined aspect ratio that was just calculated. Table 4.4.2 briefly summarizes the results of this analysis.

TABLE 4.4.2 SUMMARY OF DATA FOR PROFILE AND INDUCED DRAG CALCULATION

	δ	C_{Do}	k	AR
Main Wing	0.1253	0.0095	0.005	11.83
Secondary Wing	0.1147	0.0095	0.005	10.77

Combined efficiency, $e_c = 0.446$
Combined aspect ration based on e_c, $AR_c = 9.73$
Combined delta based on AR_c, $\delta_c = 0.1035$

Finally, the parasite drag coefficient, profile drag coefficient, and lift-induced drag coefficient were combined to yield the overall drag equation.

$$C_D = 0.00338 + 0.65\left((0.0095 + 0.005C_{L_{mw}}{}^2) + (1 + 0.1035)\frac{C_L{}^2}{\pi 9.73}\right) + 0.35\left((0.0095 + 0.005C_{L_{sw}}{}^2) + (1 + 0.1035)\frac{C_L{}^2}{\pi 9.73}\right)$$

This equation was then used to calculate the drag polar for the entire aircraft as seen in Figure 4.4.2, and from this drag polar, the aircraft's curve of lift to drag ratio was easily determined. This lift to drag curve is shown in Figure 4.4.3. Note that the aircraft's maximum lift to drag ratio equals 18.39 at a lift coefficient of 0.750 for which the angle of attack is 7.0 degrees.

FIGURE 4.4.1: LIFT COEFFICIENTS FOR THE INDIVIDUAL WINGS

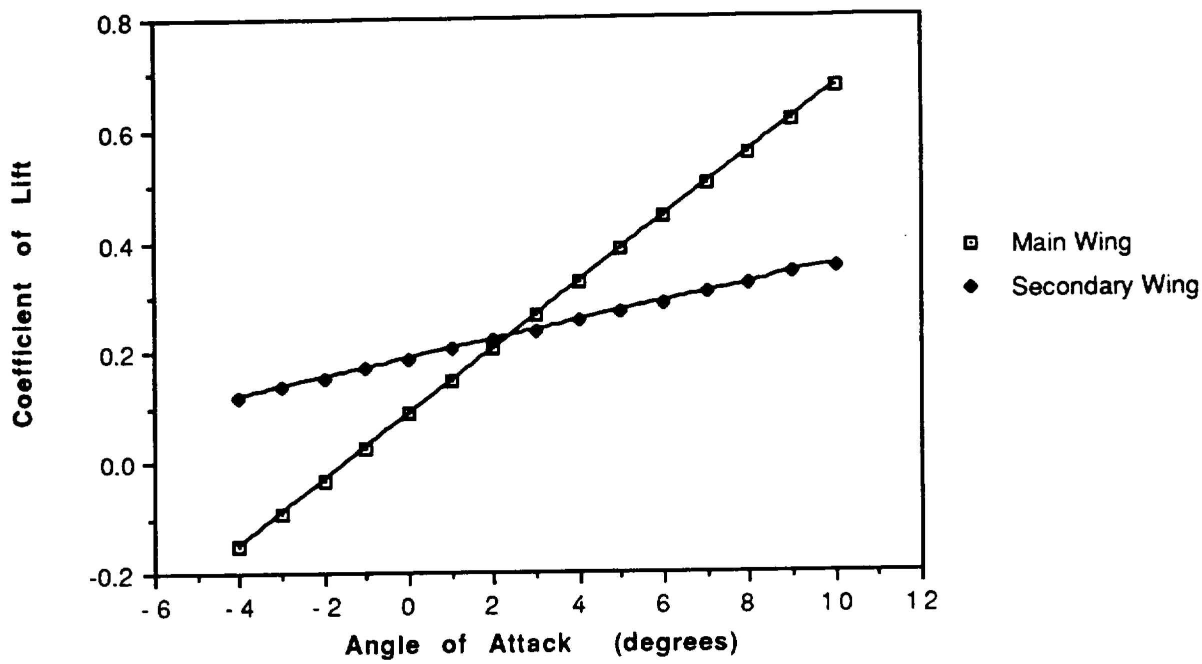

FIGURE 4.4.2: AIRCRAFT DRAG POLAR

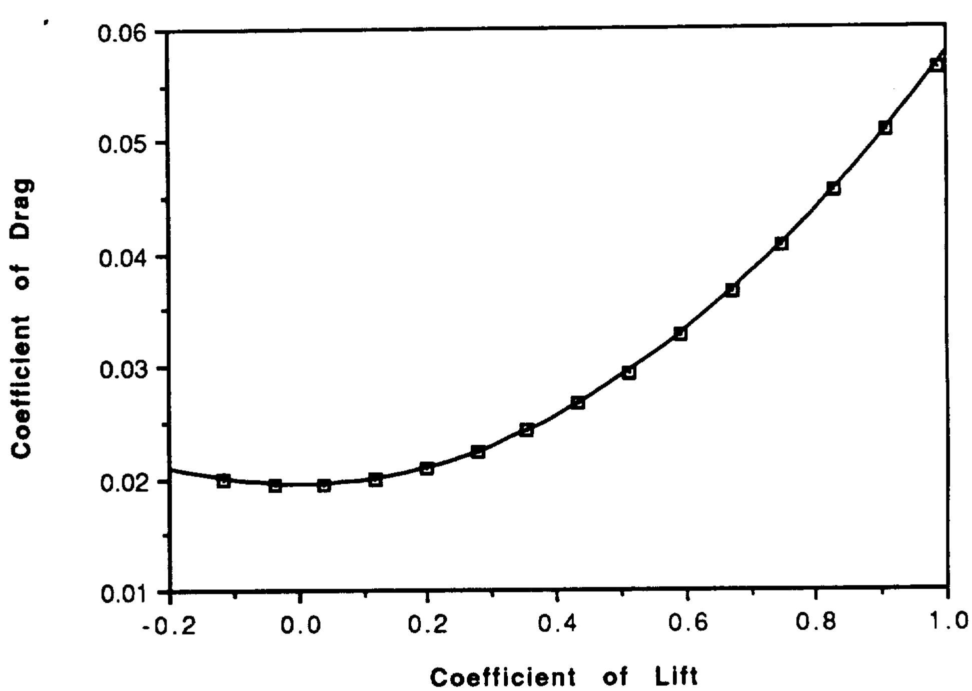

FIGURE 4.4.3: AIRCRAFT LIFT TO DRAG RATIO

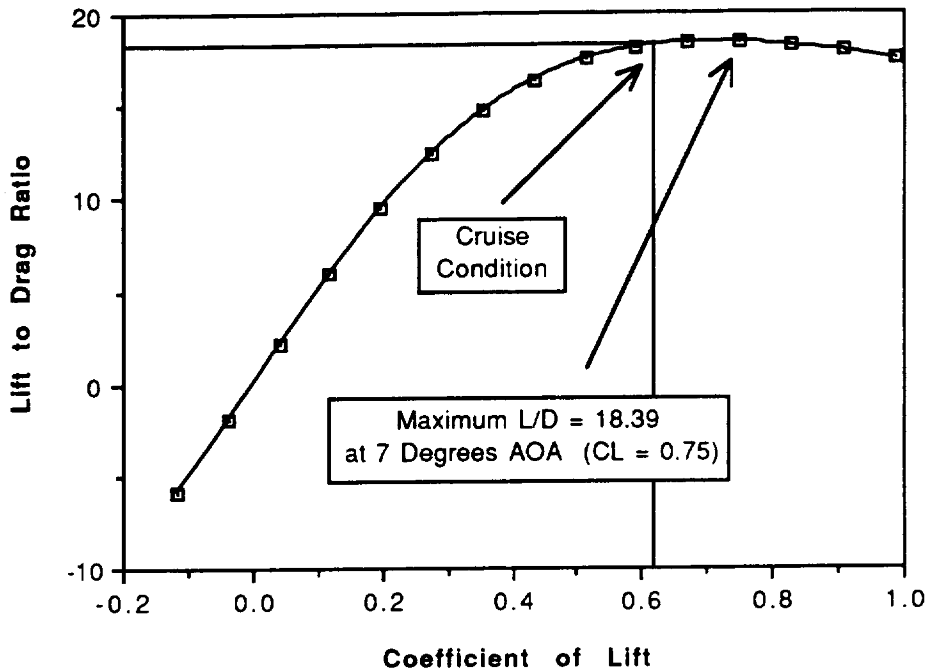

5.0 PROPULSION SYSTEM DESIGN DETAIL

The propulsion system is comprised of three main components which are all interrelated: the motor, the propeller and the batteries. The larger the motor is, the more power it will produce. With more power, it can use a smaller propeller to give it the necessary thrust for takeoff. However, the weight increases with using a larger engine because it is heavier and it requires more batteries. With the added weight, takeoff becomes more difficult. So the key point is to choose the smallest engine which will produce enough power to get the aircraft off the ground. The number of batteries are prescribed by the engine selection, but the propeller is not.

In choosing a propeller there is a tradeoff between takeoff and cruise performance. A large propeller is preferred for takeoff since it will produce large amounts of thrust. Thrust is proportional to the propeller diameter to the fifth power. So only a small increase in propeller size will produce tremendous thrust improvement. However, during cruise a large propeller will require a higher current to achieve the specified rpm. This will cause the batteries to drain more rapidly and thus reduce the range of the plane. So, the main selection criteria is to choose the smallest propeller which will give enough thrust for takeoff.

5.1 ENGINE SELECTION

In choosing the engine, a variety of sizes of Cobalt (or Astro Cobalt) electric plane engines were studied: the FAI05, 05, 15, 25, and 40. The data for their performance over a range of load torques was provided in the data bank folder. The first step in selecting an appropriate engine was to calculate the associated constants Kt and Kv. These constants were determined by graphing the torque versus the current and the output volts versus the motor rpm. The slope of these graphs were Kt and Kv, respectively (see Figures 5.1.1 and 5.1.2).

Notice that the equations of the graphs are linear. They follow the form $y = mx + b$. The m constant is the slope, and correlates to the Kt or the Kv as described above. The equations are as follows:

$$\text{Torque} = Kt * i + b$$
$$\text{Voltage} = Kv * rpm + b$$

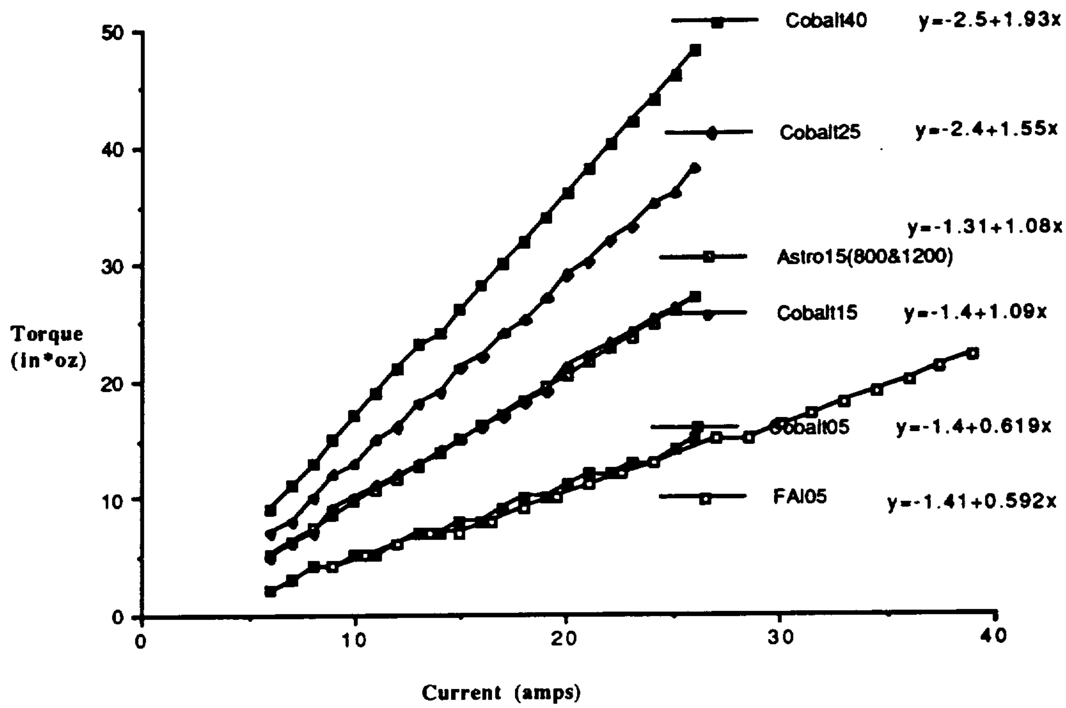

FIGURE 5.1.1 Kt FOR ALL ENGINES

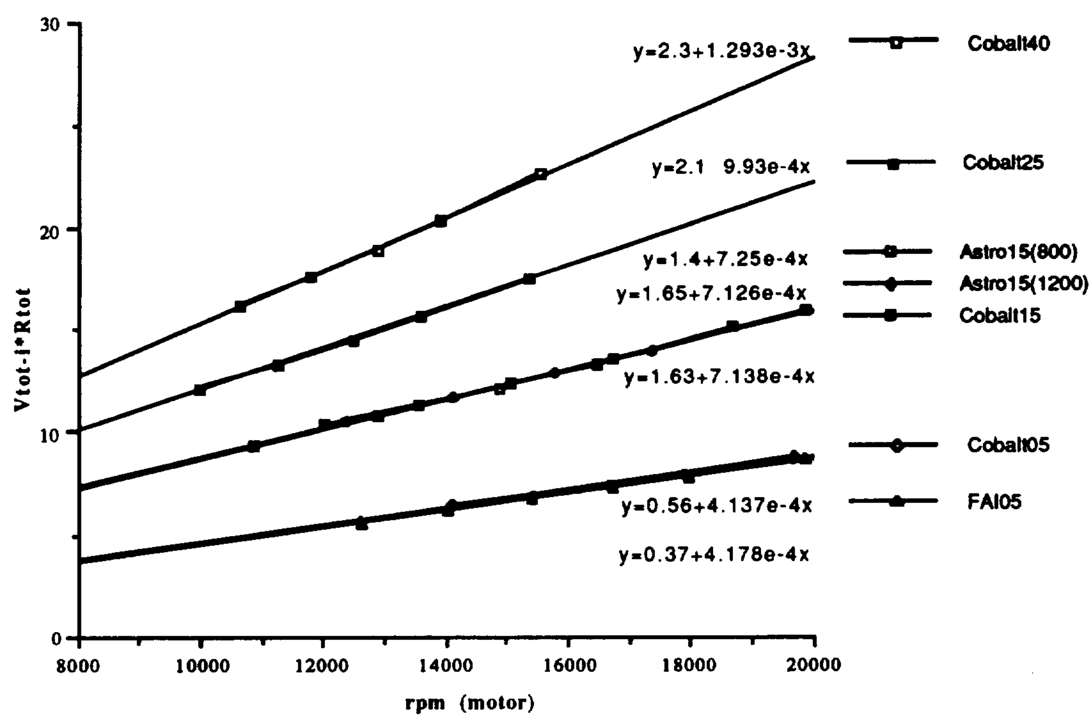

FIGURE 5.1.2 Kv FOR ALL ENGINES

Once the constants were found, they were used as input variables in the TK Solver Plus *Electric Motor Performance* Software and the *Takeoff* (Fortran) program by Dr. S. Batill. TK Solver is an iterative solving program in which all pertinent equations are entered and the computer solves them simultaneously. It was found that the Cobalt 15 would give enough power for an 8.5 pound plane to takeoff within 75 feet if full throttle voltage (14 volts) was used with a 13 inch propeller. The excess power which the Cobalt 25 engine offered was not necessary. It was heavier by 0.63 lbs and it did not offer substantial power improvement. For these reasons, the Cobalt 15 engine was selected. That means that a 13 inch propeller was needed to complete the takeoff.

5.2 PROPELLER SELECTION

As mentioned above (Section 5.0), the propeller selection is a delicate balance between takeoff and cruise performance. The only propellers selected for this study were 12, 13, and 14 inch ones. Using a blade element theory program, the values of Ct, Cp, J, and η as functions of propeller rpm were found. These values represent data from a plane travelling 26.4 ft/sec forward velocity at sea level conditions. The performance characteristics of Ct, Cp, η, were used with the *Takeoff* program and *Electric Motor Performance* to analyze takeoff and cruise performance. Figure 5.2.1 shows the relation between increased throttle and takeoff distance. As shown by the outer box labelled Minimum Requirements, this represents the window for the constraints specified by the DR&O. The engine is not allowed to use more than 14.4 volts and must takeoff within 75 feet - 51 feet with the factor of safety.

Looking at the data, it is obvious that the 12" propeller will not be able to meet the design requirements. A 13" propeller will just barely complete the task, and the 14" props have too much excess power available. This graph data is for an 8.5 pound plane, the original estimate of the plane's weight. This value is heavier than the technology demonstrator will be. But since these values were determined prior to the weight reduction in the wing structure, they were unable to reflect the new weight value of 7.5 lb. However, the trends will still be the same. The 14" prop will be too large, and the 12" will be too small. Therefore, the 13" propeller was selected. For values of current draw for takeoff and cruise, see table 8.0.1.

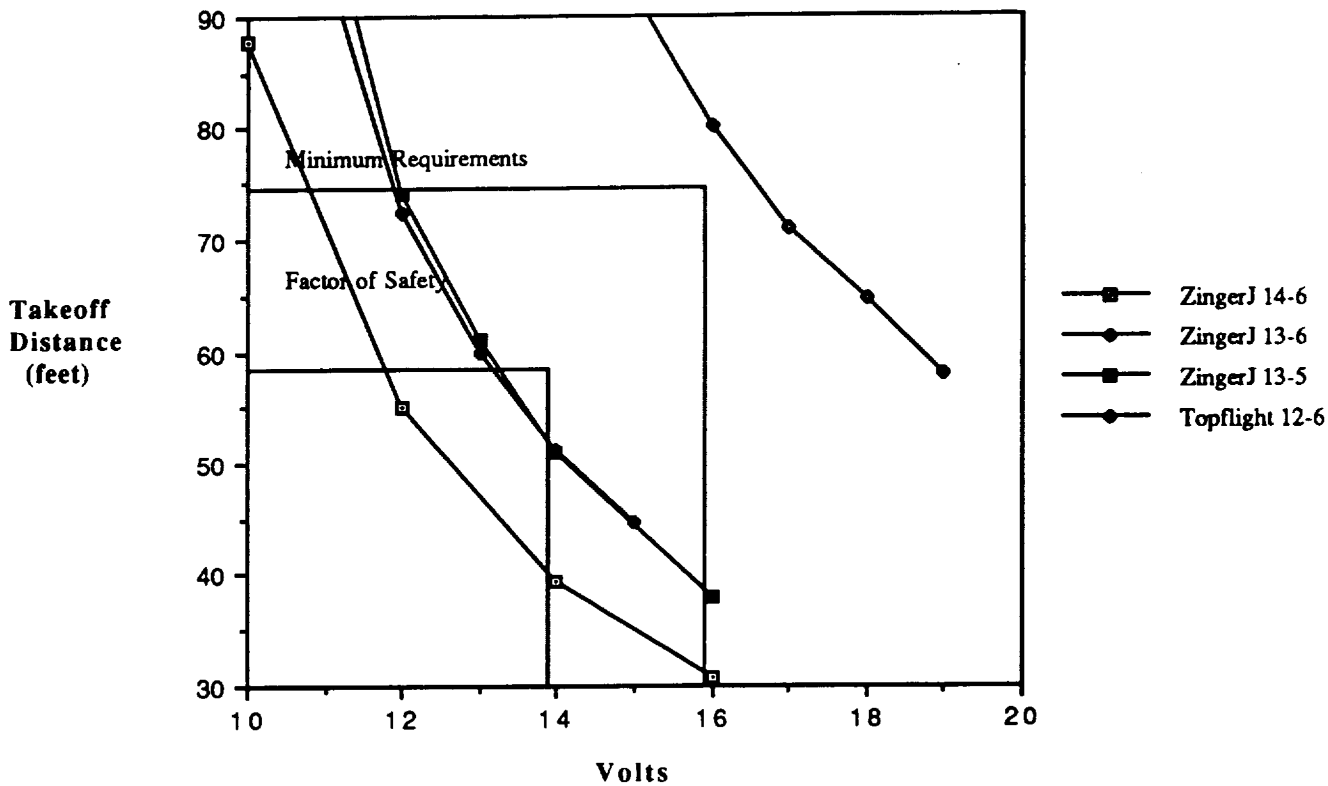

FIGURE 5.2.1 DETERMINING WHICH PROPELLERS ARE ACCEPTABLE

After choosing the propeller, the values for advance ratio and efficiency were graphed to see their relation during the different regimes during the flight. These values were obtained from the output of the propellor blade element analysis program. Within the program variables, no high Mach number corrections were assumed, but tip losses and Reynolds number adjustments were made. At takeoff, the voltage and rpms are high and thus the efficiency is low. Here, it is about 0.53. At cruise, the rpm reduces and the efficiency increases to 0.67.

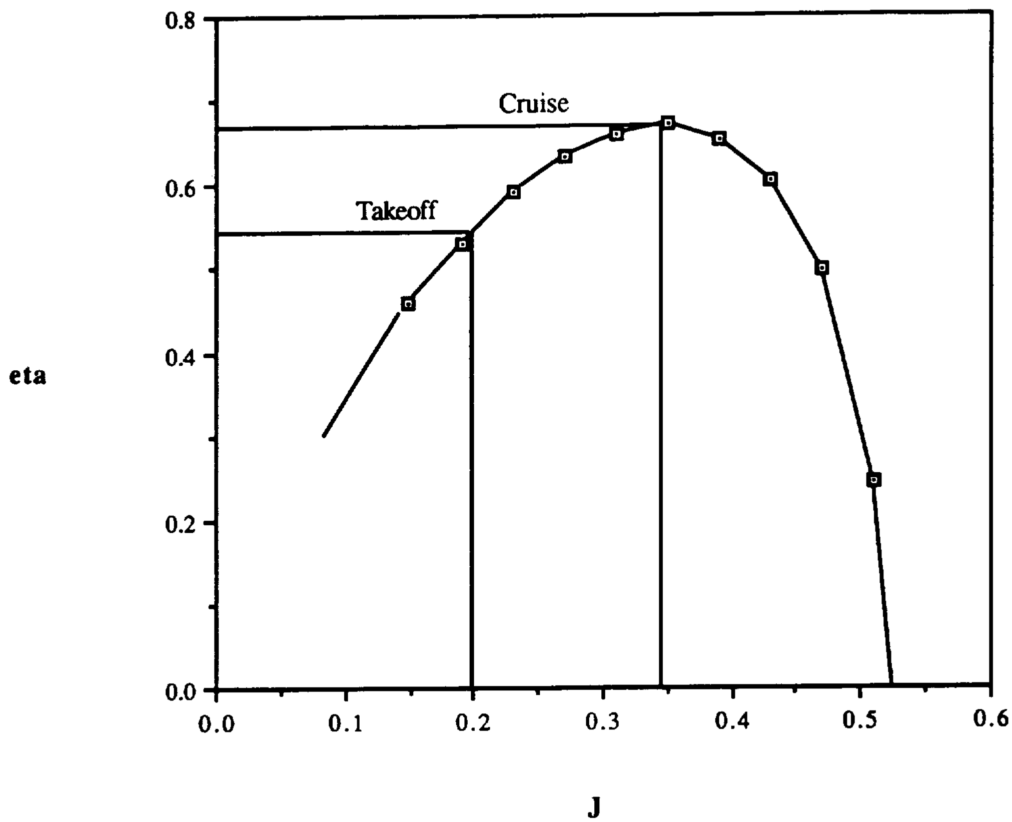

FIGURE 5.2.2 PROPELLER EFFICIENCY RANGE DURING FLIGHT CYCLE

5.3 BATTERY SELECTION

The only selection criteria in this area was to select the batteries with the most appropriate capacity. According to the DR&O, the plane needed to plan for 8100 feet of range, ground maneuvers and runway delays. Thus, the F-92 Reliant needed approximately 600 mahs of battery capacity during one flight including all these expected conditions. There was a 600 mah battery available, but that did not seem to be enough in case of some unexpected emergency. Therefore, the next step up was chosen; the 900 mah battery (More detail of this selection process is found in 8.3).

6.0 PRELIMINARY WEIGHT ESTIMATION DETAIL

This section details the weight of each component of the aircraft and its position. The aircraft center of gravity is given under various conditions. The coordinate system origin is placed at the nose, centered laterally, and on level with the cargo bay deck. The x-axis extends to the aft end of the plane; the y-axis extends out the starboard wing; and the z-axis extends vertically up. Figure 6.0 below illustrates this coordinate system.

FIGURE 6.0 AIRCRAFT COORDINATE SYSTEM

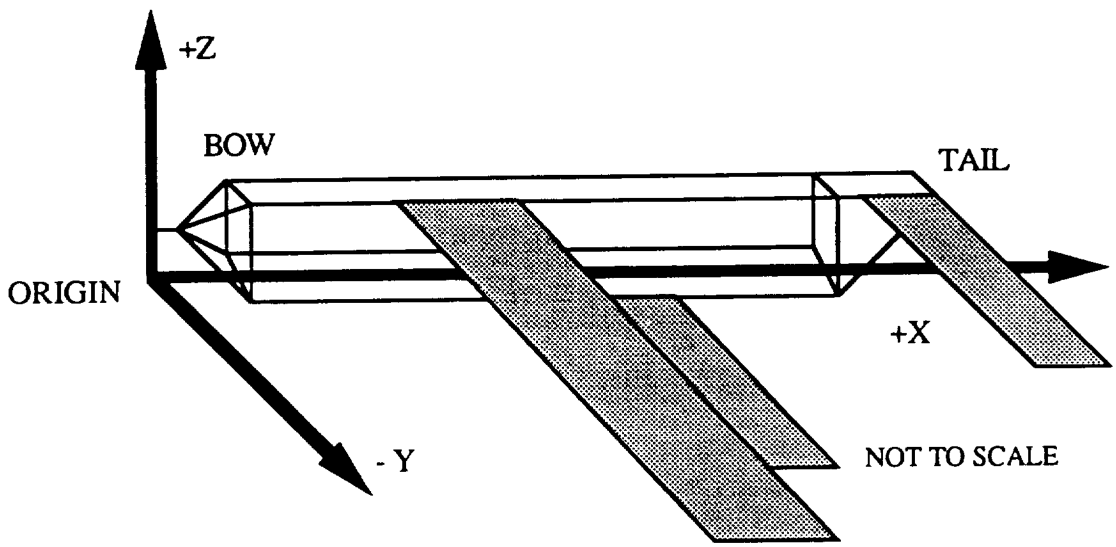

6.1 COMPONENT WEIGHTS AND CENTER OF GRAVITY

A major design variable in any aircraft is the center of gravity placement. The desired center of gravity location is achieved by altering the overall configuration and subsequent arrangement of components. The goal for this aircraft was that the center of gravity be centered at the middle of the cargo bay which ideally would also be the center of gravity of any loaded cargo. In the event that no cargo was on board, the plane would behave identically. In order to achieve this, it was necessary to place the battery packs aft. The tradeoff for the good CG behavior is the additional weight and resistance of the longer harness (power lines) from the batteries to motor.

Table 6.1 lists each component included in the weight estimation, and the component center of gravity position in the x and z axes. Figure 6.1 shows component location. As can be seen, an effort was made to place all components symmetrically in the x-y plane. This was

TABLE 6.1 **Component Weights, Positions, & Center of Gravity**

Component	Weight (lbf)	Weight (oz)	Xpos (inches)	Zpos (inches)	m*X (oz-in)	m*Z (oz-in)
---	---	---	---	---	---	---
Receiver & Antenna	0.059	0.95	10.00	4.50	9.50	4.28
Radio Battery	0.125	2.00	8.00	4.50	16.00	9.00
Servo (Elevator)	0.038	0.60	11.00	4.50	6.60	2.70
Servo (Rudder & Steering)	0.038	0.60	11.00	4.50	6.60	2.70
Pushrod (Elevator)	0.125	2.00	30.50	4.50	61.00	9.00
Pushrod (Rudder & Steering)	0.125	2.00	30.50	4.50	61.00	9.00
Main Wing - High	0.875	14.00	23.00	4.50	322.00	63.00
Fuselage	0.995	15.92	23.00	2.50	366.25	39.81
Nose Assembly	0.073	1.17	4.00	2.50	4.68	2.93
Secondary Wing - Low	0.456	7.30	30.00	-0.50	219.00	-3.65
Vertical Tail & Rudder	0.063	1.00	46.00	12.60	165.14	45.23
Horizontal Tail & Elevator	0.224	3.59	50.00	4.50	40.81	3.67
Empennage Structure	0.051	0.82	45.00	3.00	36.73	2.45
Control Mechanism	0.031	0.50	49.00	4.50	24.50	2.25
Main Gear	0.250	4.00	10.00	-3.00	40.00	-12.00
Tail Gear & Steering	0.125	2.00	39.00	-1.00	78.00	-2.00
Engine	0.656	10.50	3.00	2.00	31.50	21.00
Speed Control	0.111	1.77	6.00	2.00	10.62	3.54
Propeller	0.063	1.00	0.00	2.00	0.00	2.00
Battery (P90SCR) x 6	0.469	7.50	37.00	4.50	277.50	33.75
Battery (P90SCR) x 6	0.469	7.50	37.00	4.50	277.50	33.75
Battery Cable	0.125	2.00	21.00	4.50	42.00	9.00
Forward Payload	0.960	15.36	15.00	2.00	230.40	30.72
Aft Payload	0.960	15.36	31.00	2.00	476.16	30.72
Total Weights:						
Full Payload	7.465	119.44			2803.5	342.845
					23.47	2.87
					= CG: X	= CG: Z
No Payload	5.545	88.72			2096.9	281.4
					23.64	3.17
					= CG: X	= CG: Z

FIGURE 6.1

COMPONENT LOCATIONS

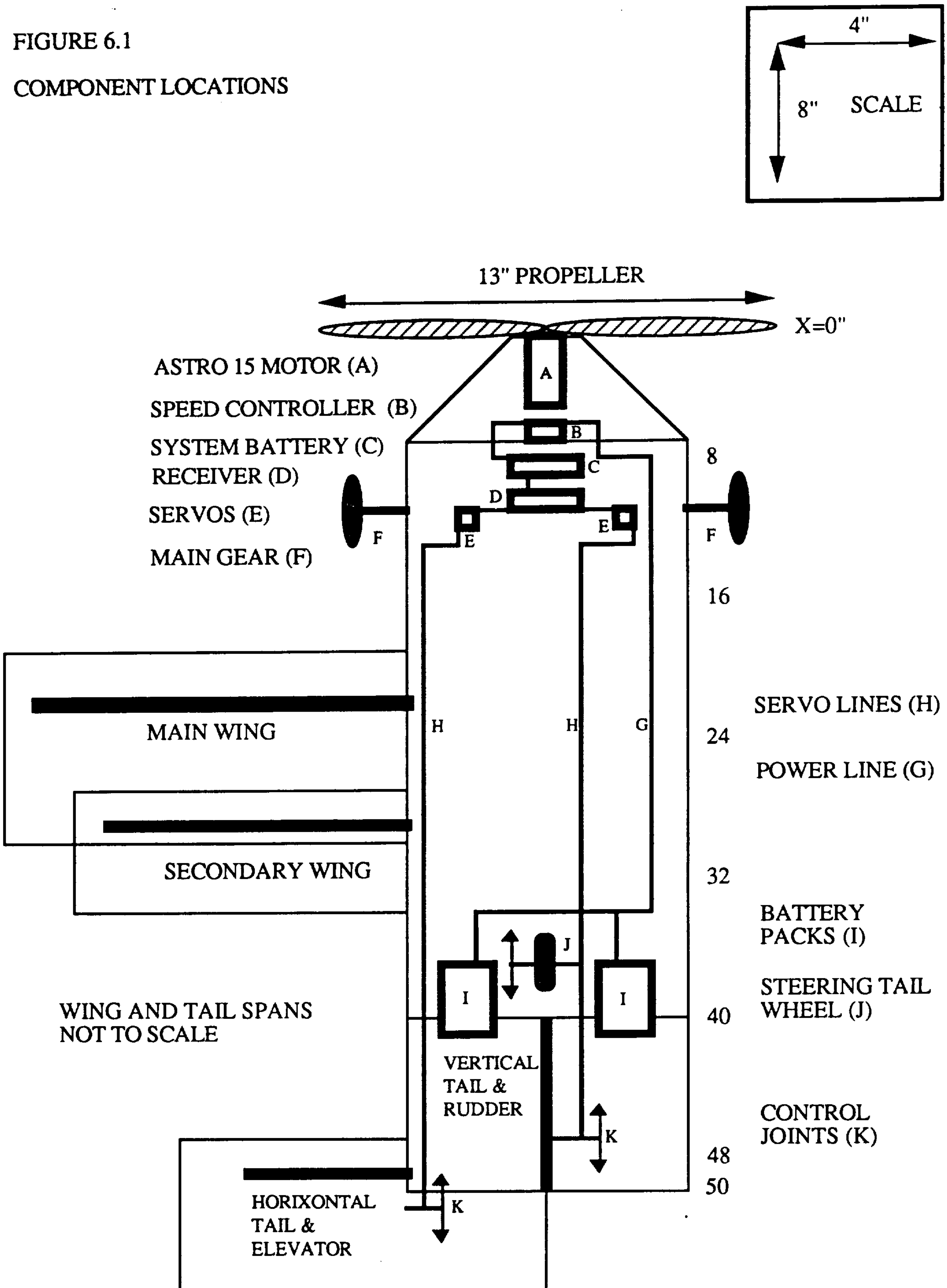

accomplished with the exception of the servolines and power lines, the effects of which were assumed to be negligible.

The total weight of the aircraft under various conditions is as follows:

DRY AIRCRAFT:	4.61 POUNDS
AIRCRAFT WITH FUEL:	5.55 POUNDS
AIRCRAFT WITH FUEL AND MAX PAYLOAD:	7.47 POUNDS

Both the X and Z coordinates of the center of gravity are calculated for two conditions:

AIRCRAFT - NO PAYLOAD	x = 23.64"	z = 3.17"
AIRCRAFT - FULL PAYLOAD	x = 23.47"	z = 2.87"

The above calculation for payload assumes an even distribution of payload weight. It is unrealistic to assume that the payload will be perfectly balanced by the loading crew, or that it is even capable of being perfectly balanced. Therefore, a limit for unbalance is set such that a maximum of 75% total weight be placed either in the forward or aft half of the bay and the remaining 25 % weight be placed in the other half. More useful calculations for unbalanced payloads result in CGs at:

75% WEIGHT FORWARD 25% WEIGHT AFT:	x = 22.44"	z = 2.87"
25% WEIGHT FORWARD 75% WEIGHT AFT:	x = 24.50"	z = 2.87"

The Weight Balance Diagram (Figure 6.2) shows the C.G. travel for an unloaded plane at 5.58 pounds, a partially loaded plane at 6.01 pounds, and a fully loaded plane at 7.45 pounds. There is clearly more allowable C.G. travel for an unloaded plane than there is for a loaded plane.

Figure 6.2 : Weight Balance Diagram

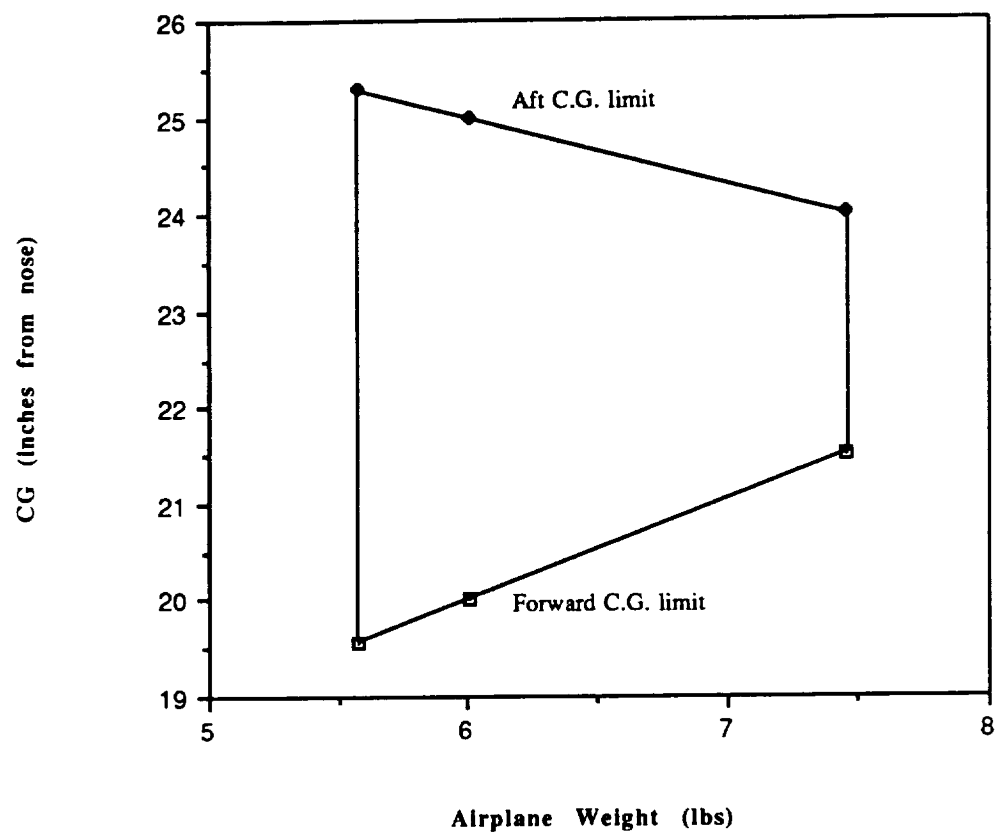

The effect of the C.G. travel on stability and control requirements is discussed in detail in chapter 7.

7.0 STABILITY AND CONTROL SYSTEM DESIGN DETAIL

This section details sizing, positioning, and orientation of horizontal tail and elevator and vertical tail and rudder. This section also details the lateral positioning of both wings. These parameters were designed to meet the requirements of stability and control, as detailed in the following sections. The final empennage design is shown below.

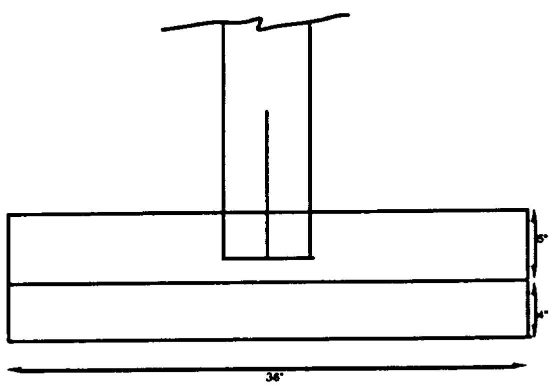

Horizontal Tail and Elevator

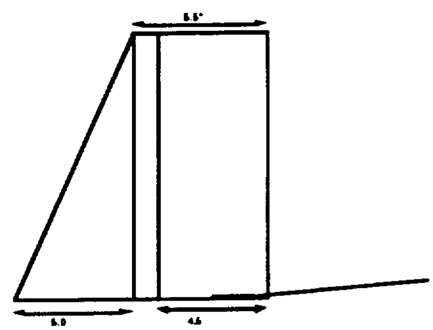

Vertical Tail and Rudder

7.1 DIRECTIONAL STABILITY

7.1.1 PITCH STABILITY AND CONTROL

The main design objective of the horizontal tail and elevator was to allow the plane fuselage reference line to trim at zero angle of attack for cg locations ranging from X_{cg}=22.4" to X_{cg}=24.3". Low angles of attack minimize fuselage drag at cruise, and the cg travel allows for versatility of cargo loading as explained in section 6.2. To maximize elevator control effectiveness, the horizontal tail plate was positioned as far back as possible on the fuselage ceiling. (X_t=49") (The fuselage ceiling was chosen for the vertical position of the horizontal tail because it provides a relatively rigid support. Although this position reduces control effectiveness of the tail since the main wing is at the same height, it avoids the structural complications of a T-tail). The tail is mounted at -4 degrees with respect to the reference line. The elevator chord is 4", and the elevator extends all the way across the tail span. The tail mounting angle combined with the elevator deflection range of -10 degrees to +15 degrees allows the plane to trim at a low angle of attack for the wide range of possible

CG locations, while providing at least +/-10 degrees of elevator deflection available for attitude control and maneuvering the aircraft.

The 1/4 chord of the main wing and the secondary wing were positioned at X_{w1}=22" and X_{w2}=29", respectively, to provide adequate static stability (negative Cm_{cg} vs. α slope) for even the most aft cg location of 24.3 inches. The 7" horizontal separation of the two wings meets the minimum acceptable separation of 6", as explained in section 4.2.2.

Figures 7.1.1 and 7.1.2 show the pitch stability characteristics of the final configuration of the F-92 Reliant aircraft for the most forward and most aft cg locations. (Xcg=22.4", and Xcg=24.3")

Figure 7.1.1 :
Cm-alpha curve for most forward CG location

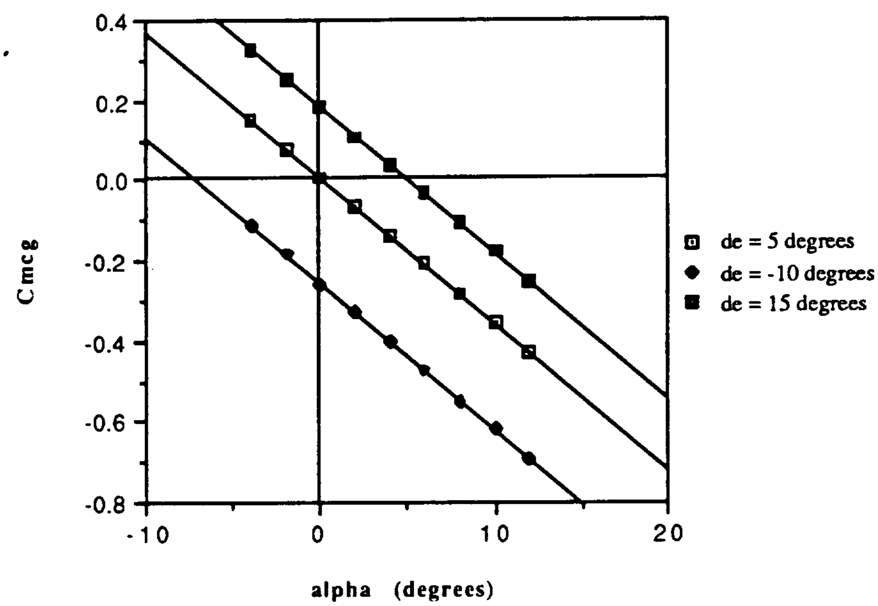

Figure 7.1.2:
Cm-alpha curve for most aft CG location

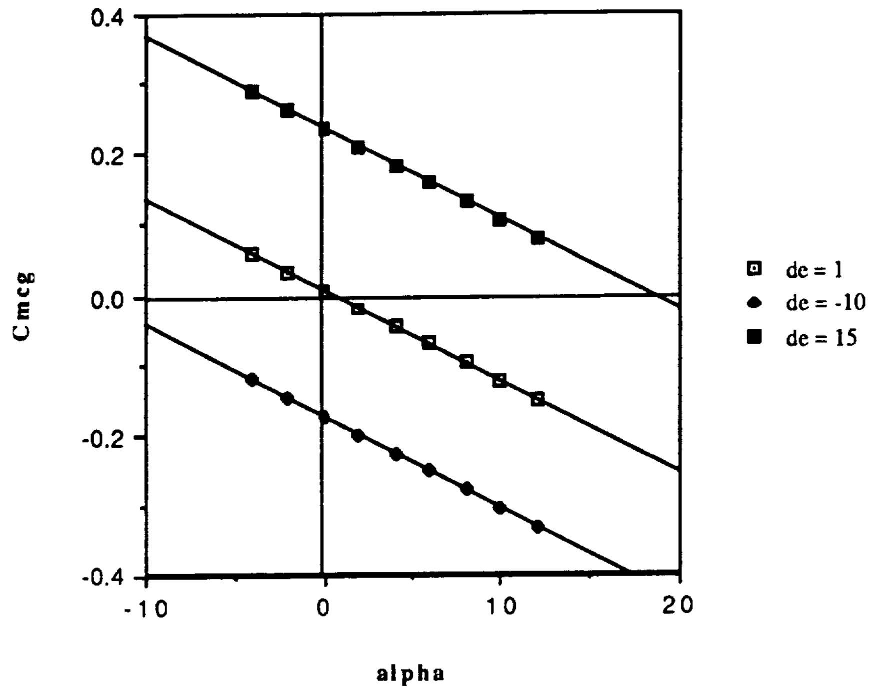

In calculating the stability curves for figures 7.1.1 and 7.1.2, equations from Reference 6, (pages 42 to 63 and figure 2.20) were used. The equations are presented in detail in Appendix B. The moment about the cg due to drag of the airplane components was neglected, and the angles of attack of each lifting surface was assumed small such that Cos(α) = 1 and Sin(α) = α. Also neglected was any moment caused by the propulsive force of the propeller, for the moment arm of the thrust vector to the cg is very small. The contribution of the fuselage to Cmcg was also neglected, and a tail efficiency factor of 0.8 was assumed. It is assumed that any deviation from the stability curves due to these approximations can be compensated for by the +/-10 degree margin of available elevator deflection.

7.1.2 YAW STABILITY AND CONTROL

Figure 7.1.3 shows the yaw stability characteristics of the aircraft.

Figure 7.1.3
Yaw Stability
Cnb vs. Beta

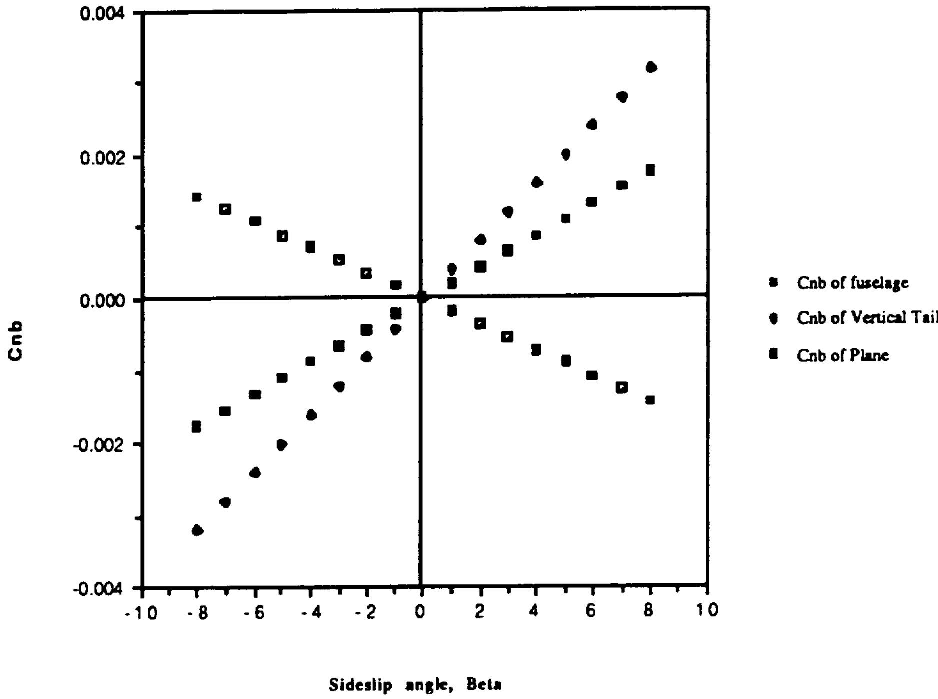

Equations and empirical expressions used to generate these slopes were obtained from Reference A, pages 67 to 72. The vertical tail area of 88 in^2 at a horizontal position of X_V=46" provides sufficient positive slope (Cn vs. β) to overcome the negative (unstable) slope due to the fuselage. To maximize rudder control effectiveness, the vertical tail was positioned as far back as possible without the rudder interfering with the tail elevator. The rudder size of 11" X 4.5", combined with the polyhedral configuration, was determined necessary to meet the requirements of roll control (section 7.1.3) This rudder size is more than adequate to maintain alignment (with a runway, for example) in a crosswind. Alignment can be maintained at a sideslip angle of up to 17 degrees (This is equivalent to a crosswind of up to 8.2 ft/s at cruise/landing conditions of 28 ft/s forward velocity.)

7.1.3 ROLL STABILITY AND CONTROL

Requirements for roll stability and control for the Reliant were met by rudder sizing and wing polyhedral design. We chose not to install ailerons onto the Reliant to save the cost and weight of an extra servo. The desired control performance required that the aircraft be capable of turning 90 degrees to the original direction of motion without exceeding a distance of 80 feet in the original direction of motion from the initiation of the maneuver at cruise conditions. (In other words, if the plane were flying toward a wall, it could avoid collision if action were taken before the plane came within 80 feet of the wall). The results were based on conservative calculations that determined the time necessary to yaw and roll for a given configuration. Given these times, the cruise velocity, and the desired radius of turn, the total distance to turn the plane was determined. For ease in manufacturing and transporting, it was determined that the center part of the wing should be 5.0 feet. This left 2.5 feet of wing on each side for polyhedral. In order to turn within a radius of 40 feet and within a straight distance of 80 feet, an effective dihedral angle of 8.5 degrees was necessary. This converted into a polyhedral angle of 16.2 degrees. With this polyhedral and a rudder deflection of 15 degrees, the plane will turn at a bank angle of approximately 30 degrees and a turn radius of 42 feet at full cargo load.

7.2 CONTROL MECHANISMS

Figure 7.2.1 shows the control mechanisms involved in moving the elevator and rudder.

Figure 7.2.1.a

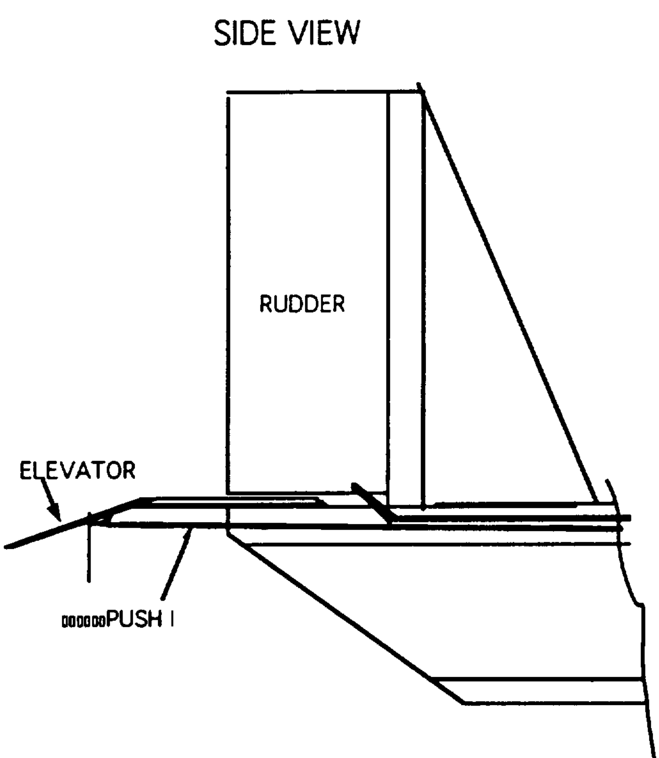

Figure 7.2.1.b

<---- Aft   Forward--->

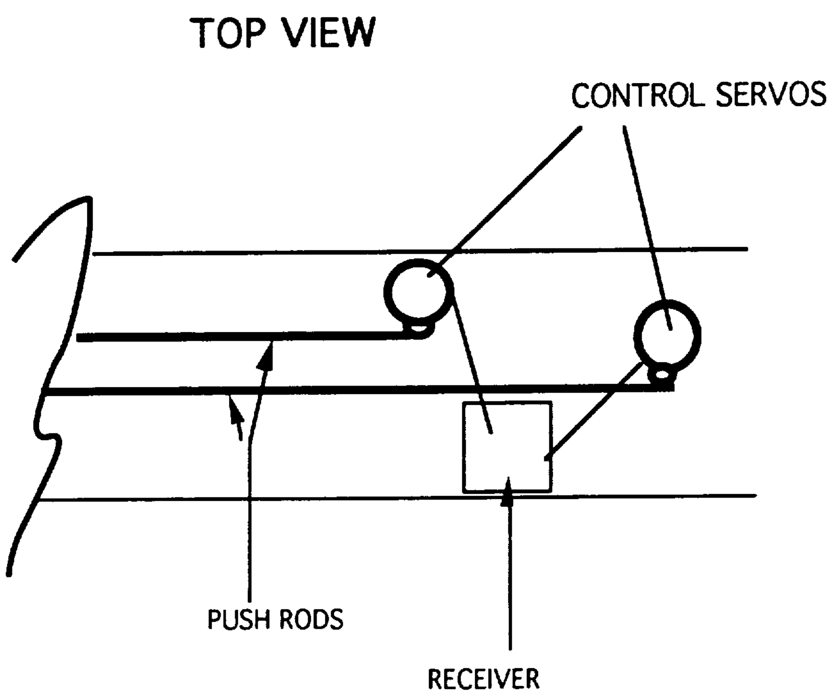

FIGURE 7.2.1

Each surface is deflected by means of a push-rod, which is moved by a control servo that is actuated by signals from a radio receiver. In this way, the ground-based pilot can adjust the surfaces as necessary to control the aircraft.

7.3 STATIC STABILITY ANALYSIS

Static stability analysis was coupled with control surface sizing and positioning in section 7.1 and is detailed in Appendix B.

8.0 PERFORMANCE ESTIMATION

Performance estimations relied heavily on the use of two computer applications: TK Solver Plus *Electric Motor Performance* Software and the *Takeoff* (Fortran) program by Dr. S. Batill. TK Solver is an iteration program which solves equations simultaneously. *Takeoff* estimates parameters such as speed, distance, current draw, thrust, and battery drain during takeoff. It is a MacFortran program which uses an iterative integration technique for time intervals of 0.05 seconds. Below in Table 8.0.1 is a summary of the performance estimates for the current configuration which is 7.5 pounds fully loaded.

	Takeoff	Climb	Cruise
Voltage (volts)	14.0	14.0	8.17
Current (amps)	11.2	13.0	5.16
Battery Drain (mahs)	9.91	12.2	400
Time (seconds)	3.85	3.37	279
Distance (feet)	50	97.8	8100

TABLE 8.0.1 PERFORMANCE ESTIMATION SUMMARY

8.1 TAKEOFF AND LANDING ESTIMATES

The takeoff performance was estimated with the help of the *Takeoff* program. The tool uses an approximation of the aircraft acceleration to find the thrust needed to achieve liftoff. The acceleration is obtained from subtracting the drag and runway friction from the thrust, then dividing the result by the plane's mass. According to the text *Aerodynamics, Aeronautics, and Flight Mechanics*, McCormick (p. 420) the friction constant ranges from 0.02 which represents a smooth dry paved runway to 0.1 for a grassy field. The particular runway for the technology demonstrator will be a dry astroturf field. This is similar to a grassy field. Therefore the runway friction was estimated to be $\mu = 0.1$. To arrive at the takeoff estimations, the plane's acceleration and velocity were monitored by the *Takeoff* program through each time step iteration until lift equaled weight; the liftoff condition.

Minimum landing distance was estimated to be 167 ft. using drag estimates as explained in section 4.3 and a conservative estimate of 0.07 for the rolling coefficient of friction. To decrease the landing distance within the allowable limit as determined by runway length, braking capability of the rear wheel was incorporated, giving a coefficient of kinetic friction of 0.9. (*Statics*, Merriam and Kreig, Appendix A) This allows for a landing distance of 59.3 ft. After taking a factor of safety into consideration, this value meets the requirement of 63 feet as established by the DR&O (section 2.2.4) except for city "B" where additional braking power must be used to meet the 51 foot requirement. The estimates of these landing distances were obtained using a spreadsheet program which increments the landing approach into small time intervals. The sum of forces was calculated in each interval, thereby enabling the velocity to be determined at each interval until motion ceased.

8.2 RANGE AND ENDURANCE

After liftoff, 880 mahs still remain in the 900 mah batteries. With the reduced current flow when airborne ($i_{takeoff}$ = 13.0 Amps; i_{cruise} = 5.2 Amps), the plane will be able to sustain flight for over nine minutes. This results in a range close to 14,500 feet. From the DR&O, a range of 8100 feet is specified. The excess battery capacity is a result of two reasons. Extra battery capacity should be planned for ground handling and taxiing could, which could use substantial energy. This means that the batteries need slightly more capacity than 600 mahs. So due to the limited battery choices available, the F-92 Reliant can fly over 1.5 times the distance for which it was designed.

Figure 8.2.1 shows that the relationship between cargo weight and range is linear. As more payload is added, the range of the plane decreases. This data shown is for the plane using the 13-5 ZingerJ propeller.

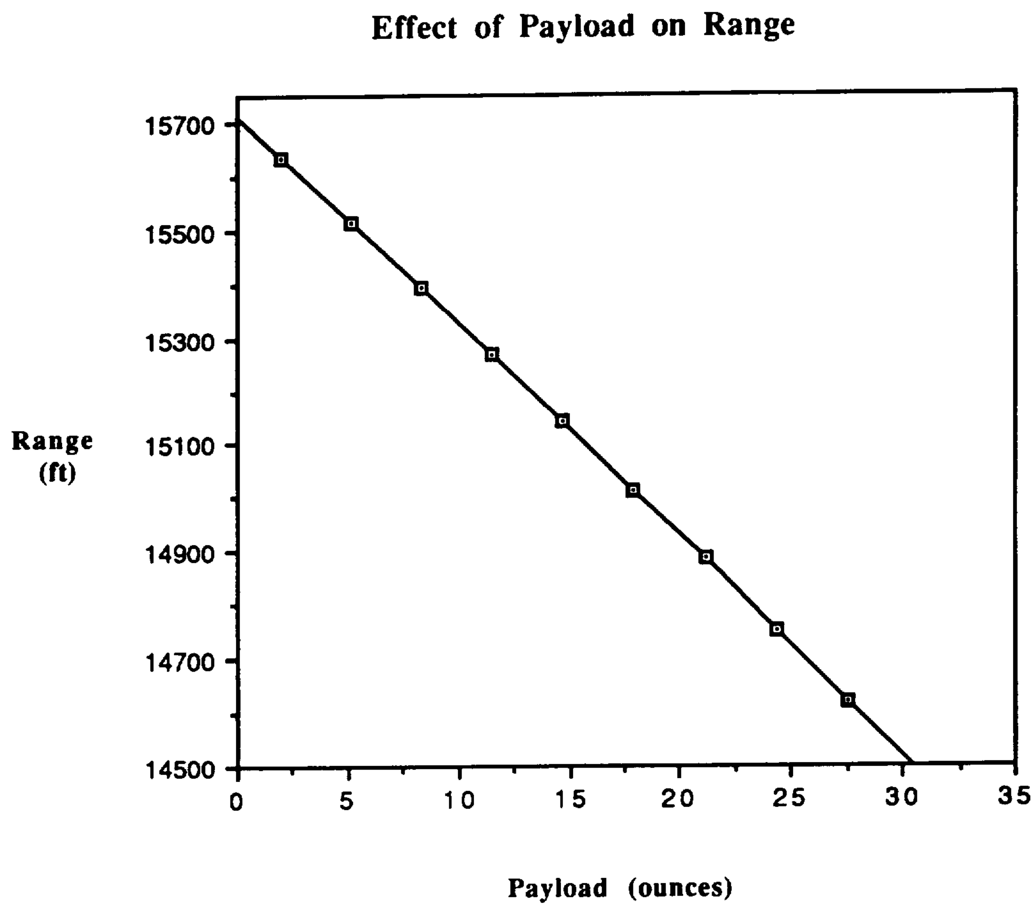

FIGURE 8.2.1 THE INVERSE RELATION BETWEEN WEIGHT AND RANGE

Figure 8.2.2 shows the aerodynamic ratios for the aircraft. For maximum endurance, the plane is to fly at the velocity where the $Cl^{1.5}/Cd$ is a maximum. This is a phenomenon which applies to propeller driven airplanes and can be found in *Introduction to Flight*, J.D. Anderson (p. 296). Page 295 of the same text explains that for maximum range, a plane is to fly at the velocity associated with L/D max. The L/D max occurs at about 25 ft/sec. This is the desired flight velocity because it will result in the largest range. (An explanation of this phenomenon can be found in *Introduction to Flight*, J.D. Anderson, p.297)

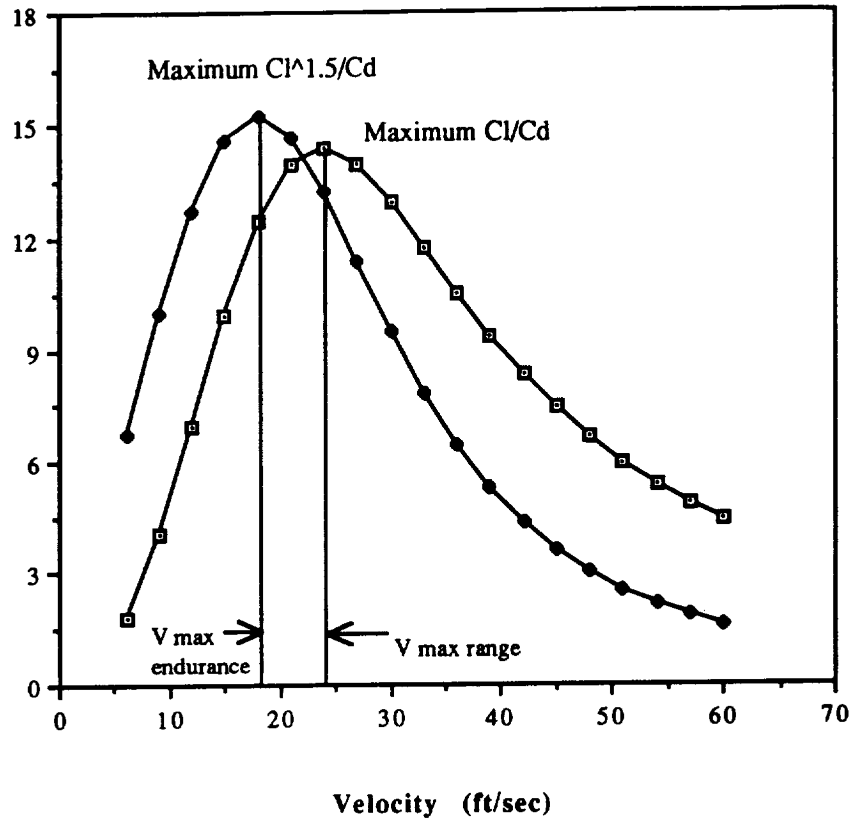

FIGURE 8.2.2 AERODYNAMIC RATIOS FOR THE F-92 RELIANT

8.3 POWER REQUIRED AND AVAILABLE

The power curve compares two performance characteristics - the power available and the power required. The power available curves are displayed on Figure 8.3.1 as a function of velocity. There are four curves, each representing a different voltage setting. They are the curves which are concave down. The second parameter is the power required. It shows the minimum possible power the plane needs to produce enough thrust to keep it in the air. It does not change with respect to voltage setting. It is determined by the plane's configuration. It does, however change due to velocity.

The two intersecting points of the power required and power available curves are the plane's minimum and maximum flight velocities. In between these velocities there is excess power available. Since the plane only needs to smaller amount of power to remain aloft (thus the power required), it can use the excess power for climbing to a higher altitude. The velocity where there is maximum excess power describes the velocity where the rate of climb reaches a maximum.

The largest velocity possible for the F-92 Reliant is just over 50 ft/sec. This exceeds the maximum velocity allowable for planes of AeroWorld. This situation can not be remedied because the maximum velocity is a result of the power available curve, which in turn is a result of the battery voltage. The 14.4 volts maximum is necessary for takeoff to occur within the design requirements. Since this cannot be altered for cruise, the plane is 'stuck' with being capable of reaching velocities it is not allowed to exceed.

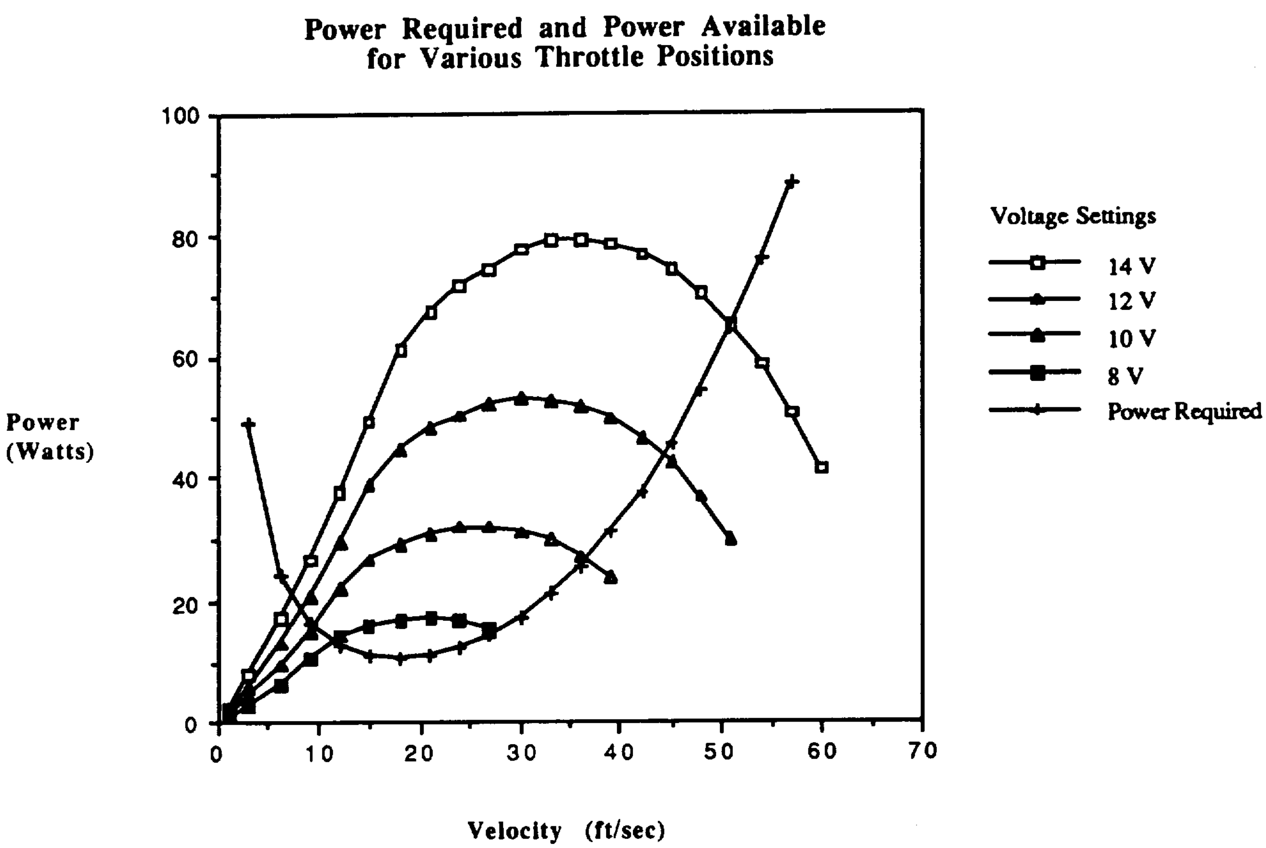

FIGURE 8.3.1 POWER CURVE

8.4 CLIMBING AND GLIDING

At liftoff, the forward velocity was nearly 26 ft/sec. At a voltage of 14.0 volts, the corresponding rate of climb is 5.22 ft/sec. As seen on Figure 8.4.1, this is close to the plane's maximum rate of climb of 5.4 ft/sec. Using a right triangle with legs of 26 and 5.22, the takeoff angle was found to be 10.9°. With this angle, the height of twenty feet (maximum cruise altitude) can be achieved in a ground distance of 97.8 feet with a time of 3.4 seconds. After this point, the plane will have used slightly over 40 mahs of its capacity. At cruise, the throttle can be reduced. That is, the voltage can be reduced from full at 14 volts, to 8.2 volts at cruise. This is done to reduce the excess power. Excess power provides the ability to climb. This is obviously not needed at cruise, so the voltage level is dropped.

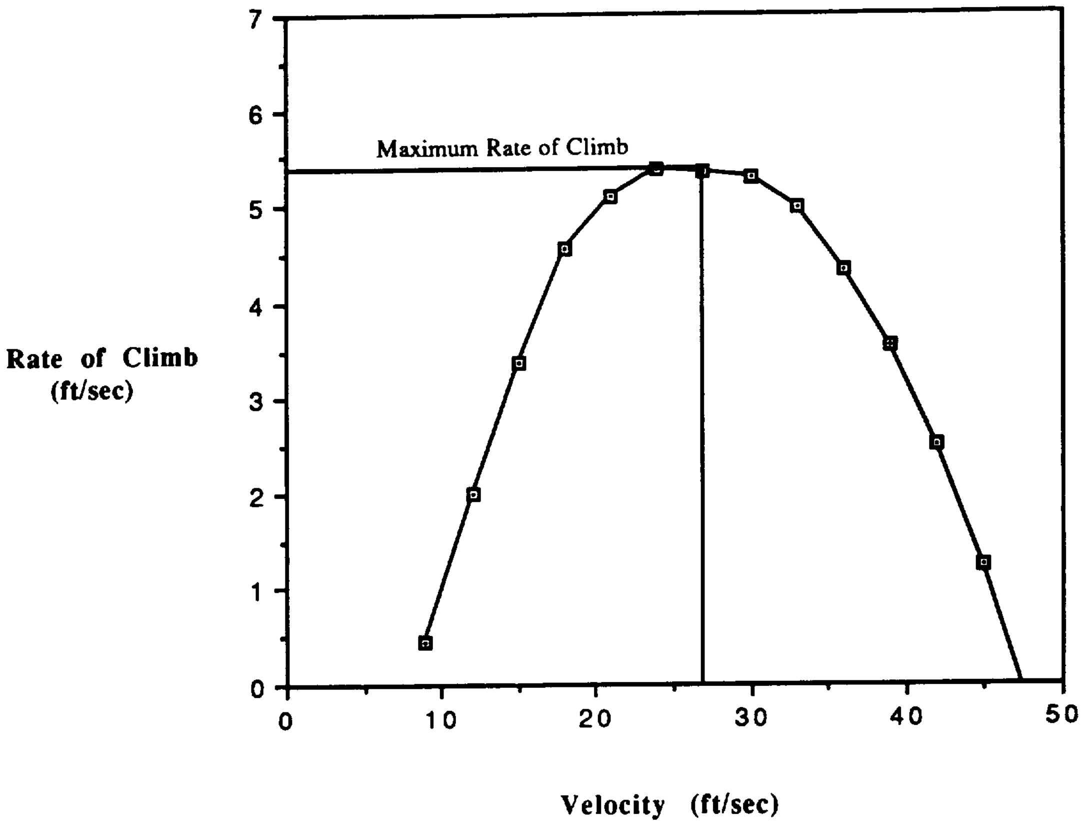

FIGURE 8.4.2 RATE OF CLIMB (at 14 Volts; W=7.5 lb)

The minimum glide angle was calculated to be 4.4 degrees, based on the maximum lift to drag ratio of 13, which includes propeller drag when windmilling. This glide ratio allows for a forward distance of 260 feet to be achieved when cruising at an altitude of 20 feet when power is cut.

8.5 CATAPULT PERFORMANCE ESTIMATE

The catapult performance analysis is included in chapter 13 under the discussion of the technology demonstrator.

9.0 STRUCTURAL DESIGN DETAIL

The major concerns in the structural design of our aircraft were the normal operating loads our aircraft will encounter in its normal operating environment and throughout its flight envelope, the material yield stresses in the primary load bearing members, and the fatigue considerations of AeroWorld materials. Presented is a discussion of the optimal fatigue "factor" for our aircraft/distribution system followed by a presentation of the load factors and the basic structural design of our aircraft.

Trade studies were conducted comparing the fleet cost per flight based on fuel costs and production costs versus the flight cycle stress reduction factor defined in the Request for Proposal (appendix A) for the *AeroWorld Transport System Design*. The fuel cost increases per flight because of the increased weight of more material to achieve a higher number of flight cycles (i.e. lower stress reduction factor). Appendix C contains the detailed procedure used to determine this variation. The production costs behave in a similar manner. The increase in the amount of material needed to achieve higher flight cycles adds cost for the purchase of more material.

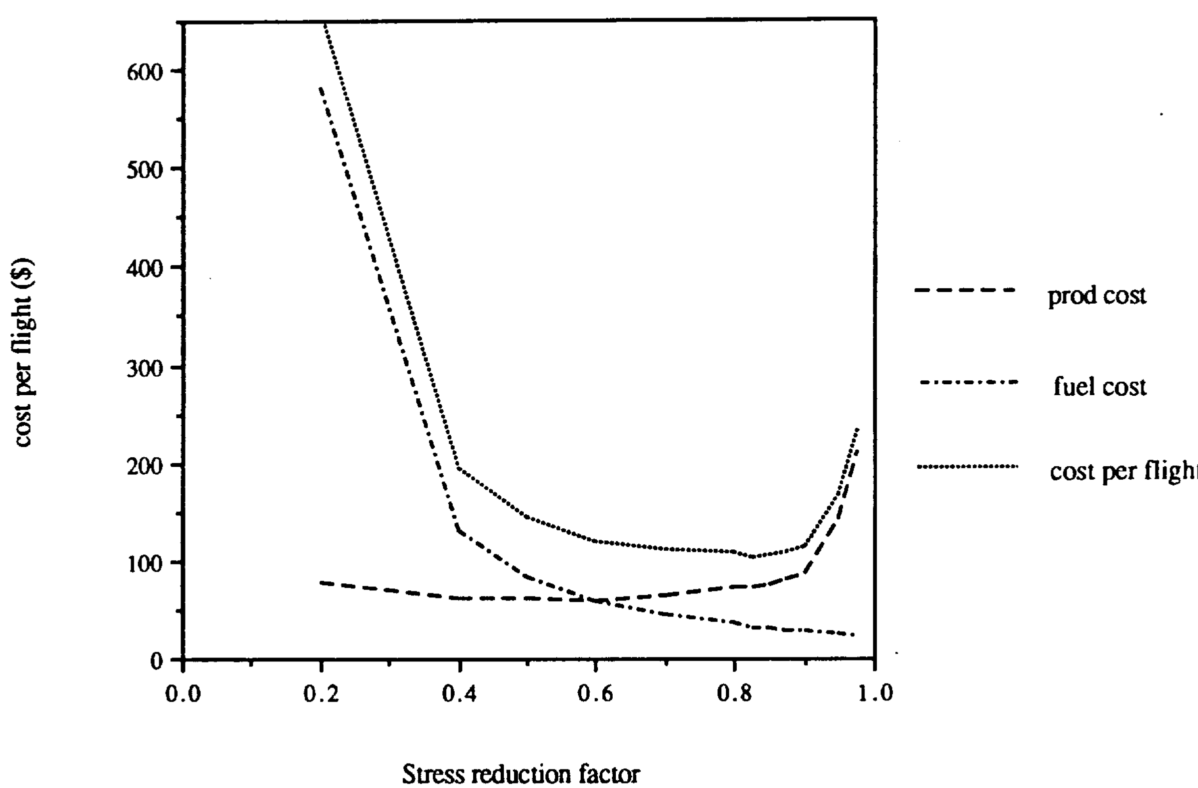

FIGURE 9.0.1 FLIGHT COSTS IN RELATION TO STRESS REDUCTION FACTOR

However, this cost increase is outweighed by the decrease in labor hours of production due to the longer unit life of the fleet. Figure 9.0.1 shows how these costs vary with respect to the stress reduction factor. It is noted that for stress reduction factors less than 0.5, a dramatic increase in costs per flight occurs. The region between 0.7 and 0.9 was deemed optimum when considered with other aspects of our design, such as the low daily flight cycles for each aircraft and the desire to minimize weight to ensure take-off performance. Thus, the final value was chosen to be 0.83, corresponding to a life of 600 flight cycles, where a cycle is defined by a take-off and landing.

9.1 V-n DIAGRAM AND FLIGHT AND GROUND LOAD ESTIMATION

9.1.1 V-n DIAGRAM

The velocity versus load factor diagrams (V-n diagram) for the maximum and minimum weight configurations are presented in Figures 9.1.1.1 a and b. The diagrams were prepared using a maximum C_l of 1.1, a minimum C_l of -.25 for the aircraft, a fully loaded weight of 7.5 pounds (120 ounces), an empty weight of 5.5 pounds (88 ounces), and a factor of safety of 1.4. The C_l values were determined from the airfoil section data, the weight estimations are from the preliminary estimation, and the factor of safety was chosen as an appropriate value for a cargo transport based on existing aircraft data. The normal operating load factors are all less than 2. The maximum normal flight load of 1.7 occurs during pull-up at takeoff. The turn radius for this load factor is 40 feet which is limited by the control surface effectiveness. While the maximum normal flight load is limited by the minimum possible turning radius and AeroWorld Mach 1 of 30 ft/s, the power available in the motor and battery combination of the aircraft will allow it to achieve speeds of over 50 ft/s. Thus, a higher load factor can be achieved as a function of C_l and V_{max}. The equation is found in Anderson (ref. 1, pg 332, eq. 6.123) as

$$n_{max} = 0.5*\rho*V^2*C_{lmax}/(W/S) \qquad (9.1.1.1)$$

A value for V_{max} of 35 ft/s was chosen with a corresponding C_l of 1.1 for the design objective. This will allow the aircraft to cruise at approximately 50 ft/s at C_l of less than 0.7, or fly at the maximum possible C_l at a speed slightly over AeroWorld Mach 1. These

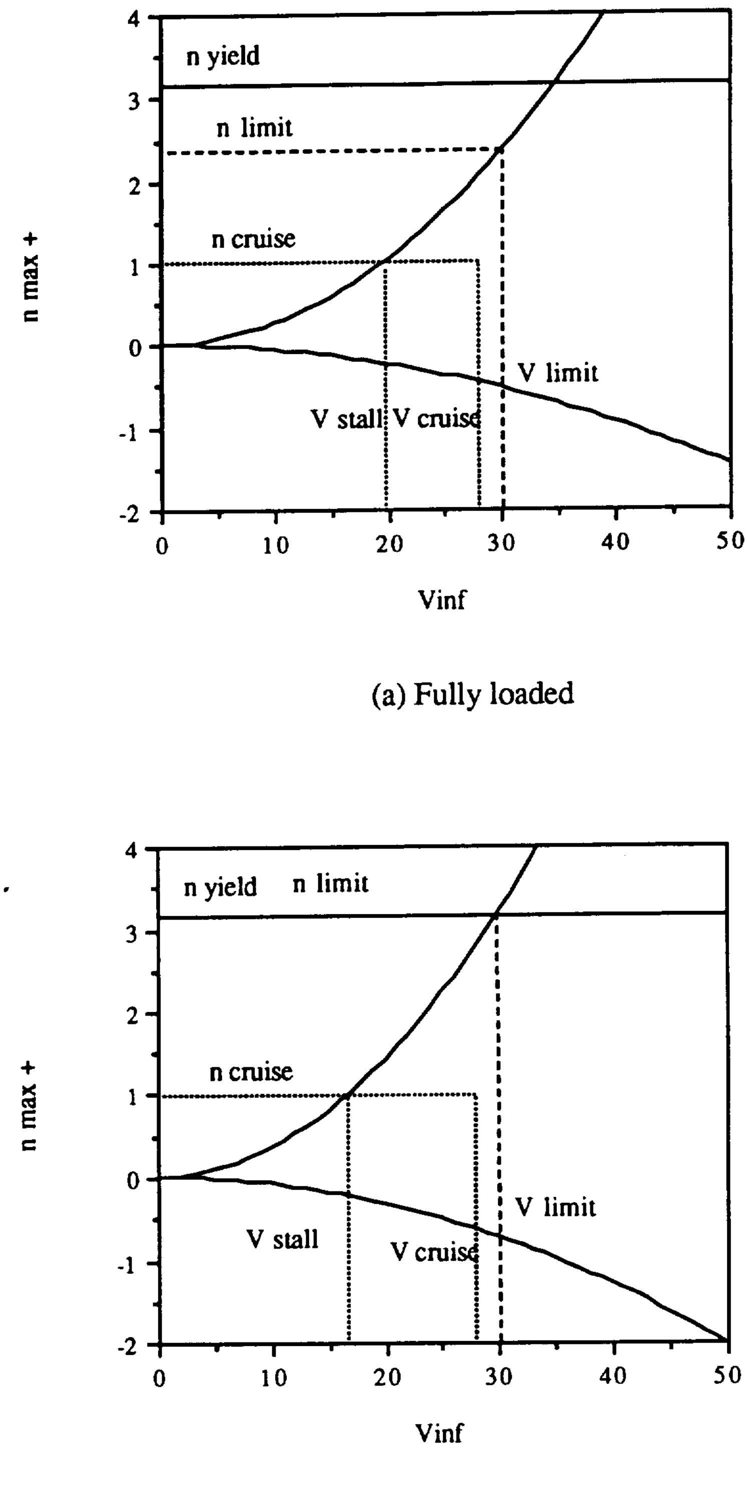

(a) Fully loaded

(b) Empty - no cargo

FIGURE 9.1.1.1 V-n DIAGRAMS FOR EXTREME WEIGHT CONDITIONS values correspond to a design load factor of 3.2. This value was chosen for three reasons.

A. While the allowable speeds in AeroWorld are limited to 30 ft/s, it might be possible that in the future this restriction would be lifted in areas where noise is not a concern. (i.e. over water)

B. It is possible that during the flight test where speed is not monitored that the aircraft might exceed its allowable operating speed of 30 ft/s.

C. The increased strength will be advantageous in ground handling where the structure will be subjected to forces much larger than normal flight loads.

In the design developments of the major structural elements, material dimensions were used for materials which are available pre-cut in an effort to limit the construction time. Material cross sections are available from 1/8 in by 1/8 in to 3/16 in by 1/2 in incremented in either dimension by 1/16 in. This discrete size variation means that our member stress factors, ($\sigma_{actual}/\sigma_{allowable}$), vary discretely and not continually. The requirement that all member stress factors be less than .83, as determined by the stress reduction factor, was surpassed. The fact that the actual stress factor was only 72% of the allowable stress factor permitted the use of a higher factor of safety than was originally intended. This improved factor of safety was found to be 1.4, which exceeded our objective of 1.2 as stated in the DR&O. The distinctions between stress factor, stress reduction factor, factor of safety and the discrete variation of material sizes will be made more apparent in the following sections.

9.1.2 FLIGHT AND GROUND LOAD ESTIMATIONS

The flight load factors of the aircraft may be determined quickly from the V-n diagrams. The load then is simply defined as

$$L = n * W \qquad (9.1.2.1)$$

(ref.1., pg 328, eq. 6.105) throughout the flight envelope. Thus, n=1 in cruise during steady level flight. The maximum load factor of 3.2 corresponds to a maximum lift of 25.5 pounds on the lifting surfaces. Divided between the surfaces, this corresponds to 16.6 pounds on the main wing and 8.9 pounds on the secondary wing. Modelling this lift as a linear distribution along the span of each wing, a root bending moment may be determined. For the main wing, the maximum root bending moment is determined to be

250 lb-in, or approximately 4000 oz-in, while the secondary wing maximum root bending moment is found to be 190 lb-in, or 3000 oz-in. A single wing of the same total area and equal to the combined aspect ratio of the current design would produce a root bending moment of over 430 lb-in, or almost 7000 oz-in. Figure 9.1.2.1 shows a comparison of the maximum member stress factor versus wing density for the tandem wing design and the single wing design. The stress factor is the same as previously defined, while the wing density is defined as the wing planform area divided by the wing weight. This produced a value which could be used to quickly compare wing designs for wings of various planforms. This quantity was derived during the initial weight estimation phase when it was desirable to predict a wing weight dependent on planform area based on available data for AeroWorld aircraft.

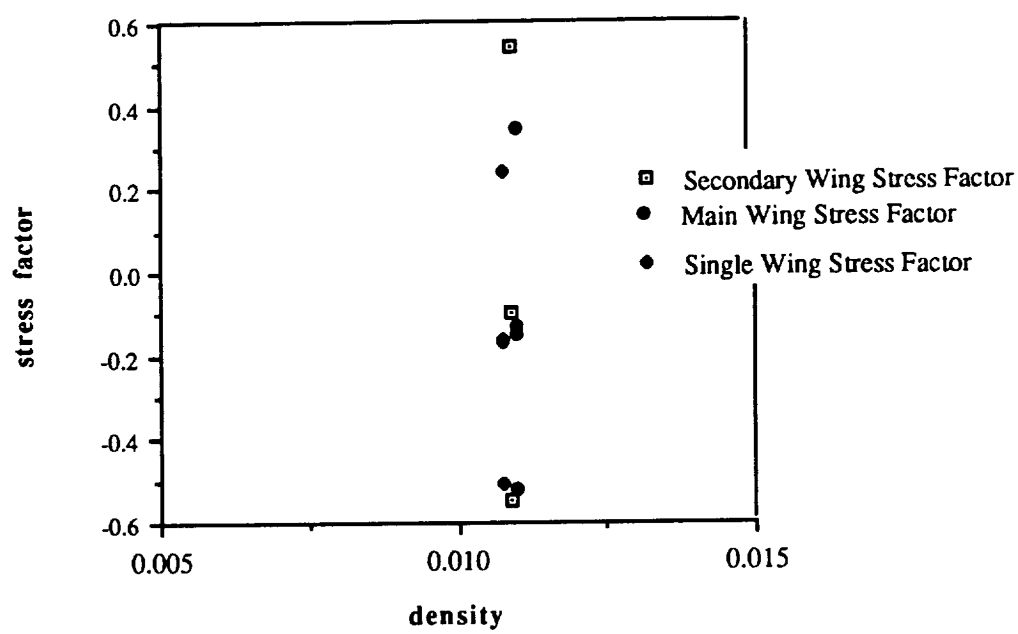

FIGURE 9.1.2.1 MEMBER STRESS FACTOR IN COMPARISON TO WING DENSITY FOR SINGLE VS. TANDEM WING DESIGN

This graph can be interpreted to mean that while the individual root bending moments of the tandem wing design are lower, the over-all wing weight will be quite similar, while the individual spar stresses are actually higher in the tandem design.

The ground load is maximum on landing. The landing load was determined by assuming a maximum rate of descent of approximately 10 ft/s. Using this value, the impact time of landing was approximately 0.1s. Therefore, using the relation found in Niu (ref 8., pg 69) the landing load was determined to be 23.3 pounds.

9.2 BASIC STRUCTURAL COMPONENTS, SUBSTRUCTURES, and ASSEMBLY

In designing the aircraft structurally, the structure was divided into three basic components each consisting of several substructures. These components consist of the lifting surface, the fuselage, and the landing gear.

9.2.1 LIFTING SURFACE

The lifting surface is comprised of the primary, or main, wing and the secondary wing. The aspect ratios of both wings, as well as their planform areas were determined by the aerodynamic considerations of the aircraft. Several structural designs were considered and analyses were performed on wing models to determine the best structural configuration which were then adapted and verified for the tandem wing structure.

The objective of the wing design was to achieve adequate strength throughout the possible flight envelope (up to a maximum load factor of 3.2) at the minimum weight possible while taking into account the factor of safety and stress reduction factor discussed previously. The wing weight goal, or limit, as specified in the DR&O was based on the weights of previous RPV wing designs for passenger transports increased by approximately 30% to account for the dramatically increased payload weight.

The wing was analyzed as a composite cantilever beam consisting of non-load bearing webs representing the spars and flanges representing the spar-caps. The primary stress was then axial stress due to bending which can be determined from the equation

$$\sigma = My / I_x \qquad (9.2.1.1)$$

found in Gere and Timoshenko (ref2., pg 214, eq. 5.10). In this analysis, the bending moment, M, was determined by the distributed lifting force being modeled as a point force acting at the midpoint of the half-span. This simplified model was used because at the time of analysis, there was still a question as to the wing locations and the effective interference in determining the actual wing lift distribution. The moment of inertia, I_x, was the composite first moment of inertia of the spar caps about the centroid

$$I_x = (1/12)\,bh^3 + (b)(h)y^2 \qquad (9.2.1.2)$$

where b is the base and h the height (ref2.,pg214, eq. 5.8). The distance y at which σ was measured was determined by the distance from the centroid to the neutral axis of the individual spar-caps. A short-coming of this analysis technique was that the load bearing characteristics of the web, or actual spar, were ignored. It was assumed that the rib-web combination would be adequate to bear the shear forces necessary to ensure that the individual spar caps act as a single composite beam. The member stress as determined from equation 9.2.1.1 was then divided by the maximum allowable material stress to produce the stress factor, which, as a dimensionless quantity, could be easily used to compare different configurations.

In an aircraft in which the skin is not stressed, the ribs bear virtually no structural loads except the load required to maintain spar position along the span and serve primarily to inhibit buckling of the spars and to maintain the airfoil shape. The number of full-chord ribs needed for structural support was determined through the use of the Euler equation for thin-column buckling (ref2., pg.557, eq.11.7)

$$P_{cr} = \pi^2 EI / L^2 \qquad (9.2.1.3)$$

In this equation, the critical load, P_{cr}, is determined by the moment of inertia of the individual member and the material modulus of elasticity divided by the length between the member supports. This equation only needs to be applied to those members which are in compression. This would correspond to any spar-caps above the centroid, in response to the lifting forces, and any spars or spar caps behind the centroid, in response to the drag forces. The member loads can be determined from the previous equation 9.2.1.1. From these loads, a critical length was determined such that

$$L_{cr} = (\pi^2 EI / P)^{1/2} \qquad (9.2.1.4)$$

Full-length ribs were implemented at increments of L_{cr} as limited by the trailing edge spar.

A simple FORTRAN program was created to determine the moment of inertia and thus the member stresses and the critical buckling length as well as to determine an approximate tip-deflection and wing density. The program used constant spar sizes at the leading and trailing edges and incremented either the top or bottom spar cap at any intermediate chord location through the allowable, or rather available, material dimensions until all member stress factors were below 0.83, which was determined by the design stress reduction factor. A listing of this program may be found in Appendix D.

Several structural configurations were analyzed in an effort to meet and exceed the set objective strength and weight. It was decided that a spar carry-through design, in which the center section of the main wing was a single unit to avoid joints in the region of the root bending moment, would produce the strongest, least weight structure. Figure 9.2.1.1 shows four different spar cap arrangements which were analyzed. From equation 9.2.1.1, it is apparent that the farther away one is from the centroid, the lower the member stress will be. (the value of I increases as distance form centroid to spar cap location squared while y increases linearly) Therefore, spar-caps were initially used at the thickest point on the airfoil, the 0.40c location. However, since the lifting force would act at the 0.25c location, large torsional moments would be created about this spar. Thus, it was decided that the main spar should be at the 0.25c location, and, henceforth, only the areas of these spar-caps were manipulated. This eliminates the lifting torsional moments while only decreasing in distance, y, from the centroid by 1%. The goal was initially to use several small, light-weight spar-caps in an attempt to minimize the number of ribs and thus reduce "dead" weight and to reduce construction time since rectangular spar members were readily available and would not have to be cut to size. But it was found that a configuration with larger spar-caps at the 0.25c with leading edge and trailing edge spars was more effective in achieving the design goals of high strength and low weight. Figure 9.2.1.2 shows the maximum stress factor as a function of wing density for the various configurations. The maximum stresses occurred in tension in the lower 0.25c spar cap. From this figure, it is noted that the chosen configuration has a ratio almost 10% lower than the other configurations.

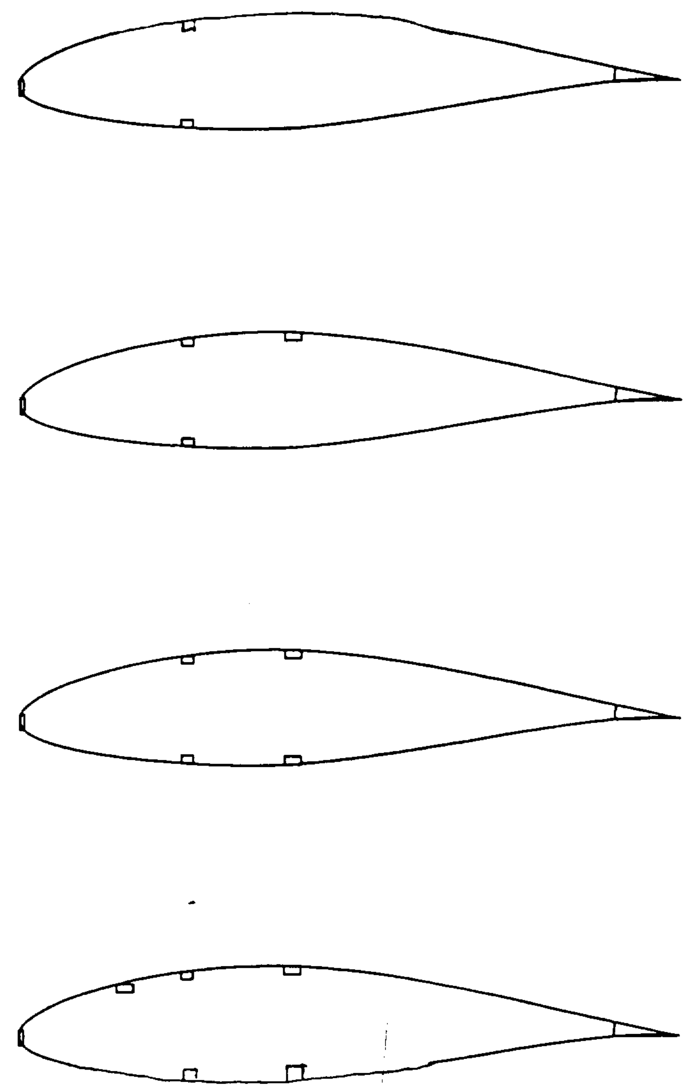

FIGURE 9.2.1.1 VARIOUS SPAR-CAP ARRANGEMENTS

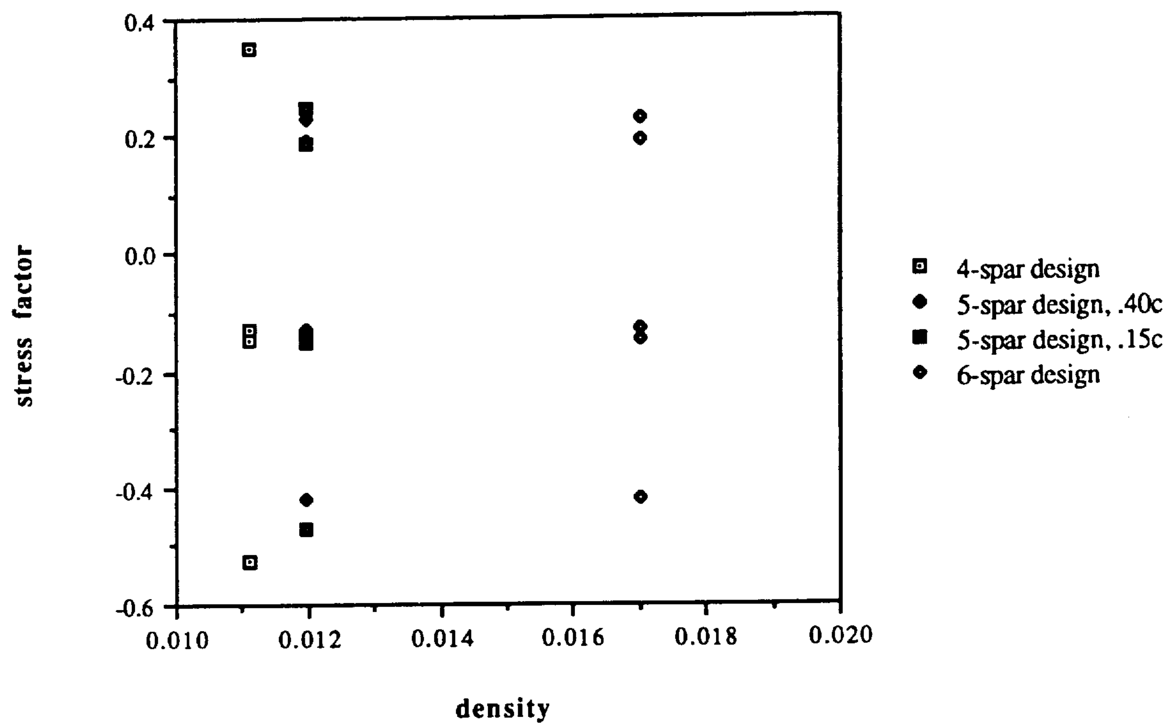

FIGURE 9.2.1.2 MEMBER STRESS FACTOR IN COMPARISON TO WING DENSITY FOR VARYING SPAR-CAP PLACEMENT

This figure shows that the 4-spar configuration produces a lighter structure which is more highly stressed. It is then apparent that the most efficient structure is that which has the most highly stressed members within the allowable limits. This final structural main wing model consists of spruce spar caps of 0.25 inches in width by 0.125 inches in height at the quarter chord with a balsa leading edge spar of 0.125 inches in height by 0.125 inches in width and a balsa trailing edge spar of 0.187 inches by 0.25 inches. For the secondary wing, the same spar-cap layout at the quarter chord was used but with the upper spar being 0.0625 inches by 0.125 inches and the lower spar being 0.187 inches by 0.187 inches, with the same dimensioned leading and trailing edge spars. In both the primary and secondary wing configurations, the maximum rib spacing was determined to be 10.5 inches. To be on the safely conservative side, and since the initial weight was so much lower than the goal set forth in the DR&O, ribs spacing was set at 9 inches. In this weight estimation, several holes were cut in each rib to reduce dead weight as much as possible.

As was stated earlier, this design analysis neglected the spar web. In the weight estimation of this configuration, a web weight was estimated. Even in using conservative estimates for rib weight and increasing the weight estimate by 4% to account for glue and possible error in the weight calculation, the weight estimation was still over 20% lighter than the conservative estimate which was derived from previous passenger RPV's designed to carry much lighter payloads. In retrospect, it was apparent that previous designs had been over designed for their flight requirements and that no increase in the average wing weight from these previous designs was necessary in the initial weight estimation of this RPV.

Therefore, in an effort to reduce the weight even more, attempts were made to produce the minimum spar webbing necessary to ensure that the spars-caps would act as a single unit. A tension field beam modeling was considered by modelling the quarter chord as a single beam with the upper and lower caps as the flanges of a beam and the ribs as rods to determine the webbing required, but it was found to be beyond the scope this analysis in that its precision exceeds the need of this analysis. There was no need to determine the web thickness to an exacting degree when material property variations are possibly quite large and when it can be seen that previous designs incorporating certain web configurations were more than adequate for the mission. Thus, a web configuration similar to previous designs was adopted using 0.0625 inch thick plywood webbing from the root to a point 9 inches from the root chord glued to both sides of the spar-caps. From there, the same thickness spruce webbing was attached from that point to a point 30 inches from the root chord on one side of the spar caps, and balsa webbing was then attached from that point until a point 18 inches from the wing tip. As with the ribs, 1 inch diameter lightening holes were cut into this webbing every 1.25 inches along the span. The secondary wing had a similar web design. Figure 9.2.1.3 on the following page represents a 2-d view of the half span of the main wing which is representative of the structural configuration of both lifting surfaces. The "riblets", or partial chord ribs seen in the drawing will be discussed in the following paragraph.

While the structural design as described in the preceding paragraphs satisfies the structural objectives of the RPV design as laid out in the DR&O, the aerodynamic requirements may not have been met. With a rib spacing of 9 inches, it is possible that the wing covering material would deform and not hold the true airfoil shape. This would result in a loss of section lift and possibly an increase in drag. For this reason, "riblets", or 0.40c ribs have been placed at intermediate positions along the span to maintain the airfoil shape from the leading edge to its thickest point, where the air-flow is most critical. This spacing of airfoil riblets at 4.5 inch increments was found to be consistent with previous designs in terms of rib spacing and was deemed adequate to achieve the proper airfoil performance. Referring to Figure 9.2.1.3 one can see the lightening holes in the ribs and the riblets and in the spar web, as well as the spar cap and rib dimensions.

The main wing consists of 3 sections and the secondary wing of two sections to meet the design requirement of storage and transportation within a 5ft x 2ft x 2ft crate. The main wing consists of a 5 foot center carry-through section which mounts to the top of the fuselage, and two 2.5 foot tip sections which are attached at an angle of 16.7° to achieve the desired polyhedral angle. The secondary wing consists of two 3.5 foot sections which mount directly to the sides of the fuselage. The methods of wing attachment will be discussed in Chapter 10, Construction Plans.

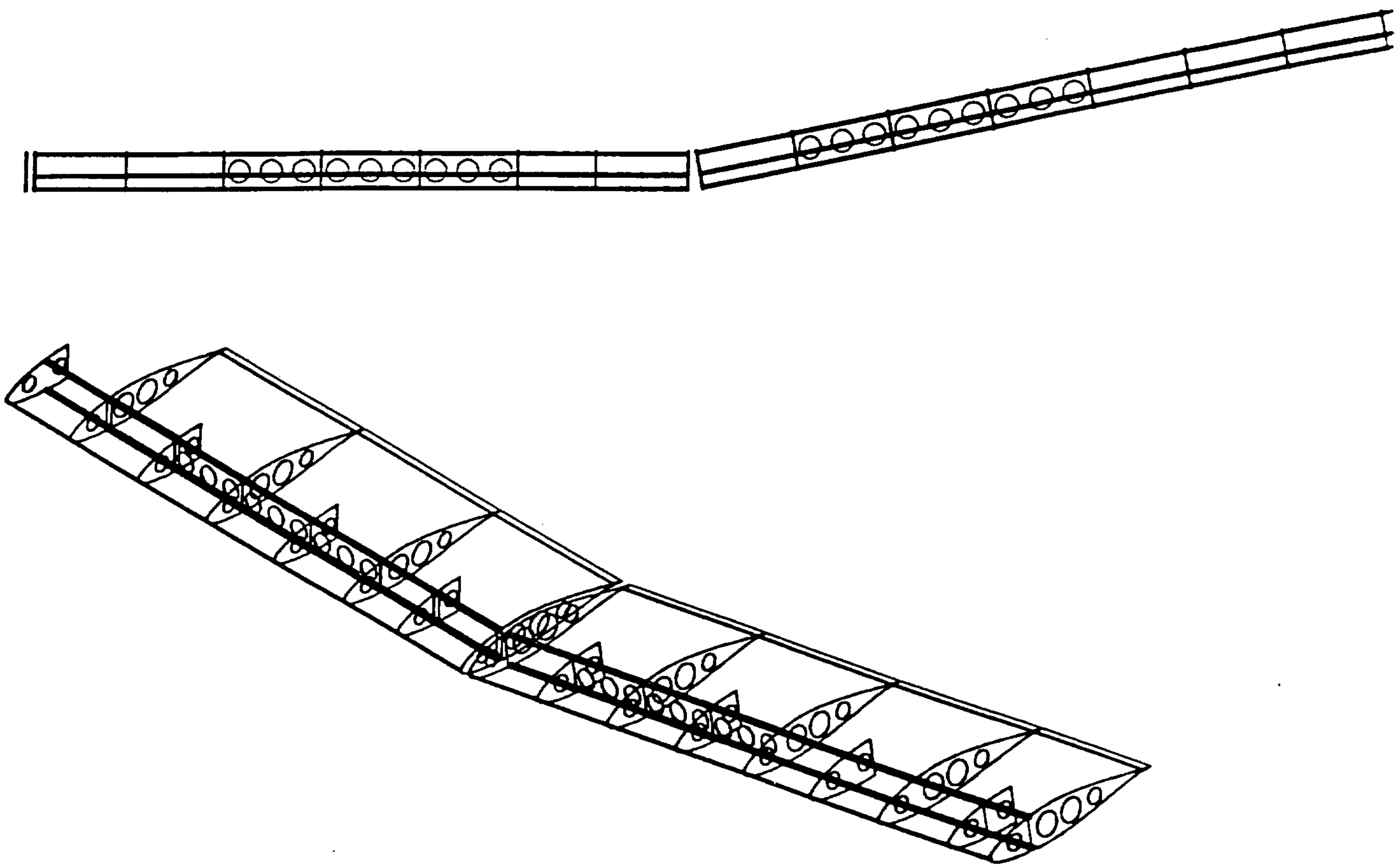

FIGURE 9.2.1.3 VIEW OF MAIN WING HALF-SPAN

9.2.2 FUSELAGE

The fuselage serves as the primary structural component which fulfills the cargo carrying mission of this aircraft. The most obvious design requirement was to meet the 1024 cubic inch payload volume requirement. Other considerations of importance were primary and secondary wing mounting, landing gear and catapult support, nose structure and engine mount support, avionics and battery storage and support, and the empennage structure, including support for horizontal and vertical tail loads.

9.2.2.1 FUSELAGE DIMENSIONS (FIGURE 9.2.2.1)

The mission of the aircraft calls for a payload volume of 1024 cubic inches weighing an average of 0.03 ounces per cubic inch, or 1.92 pounds total. The AeroWorld payload will exist in both 4" cubes and 2"cubes. For shipping, a standard pallet was chosen to carry one 4" cube or eight 2" cubes. Thus, a 4"x8" cross section by 32" length was chosen as the cargo bay geometry. This will be convenient because it allows for side by side loading of two rows of cargo. In actuality, the cargo bay will measure 4.125"x8.25"x33". This additional "safety room" allows for packaging space, slight inconsistencies in cargo size, and pallet space beneath the cargo.

A deck above the payload bay will hold avionics gear, the primary wing mount, batteries, and control devices for the tail surfaces. The space will measure 1"x8.25x43". It covers the area above the payload bay and extends 10" aft where it supports the rear access hatch and tail structure. This hatch allows for easy access to the completely unobstructed cargo bay.

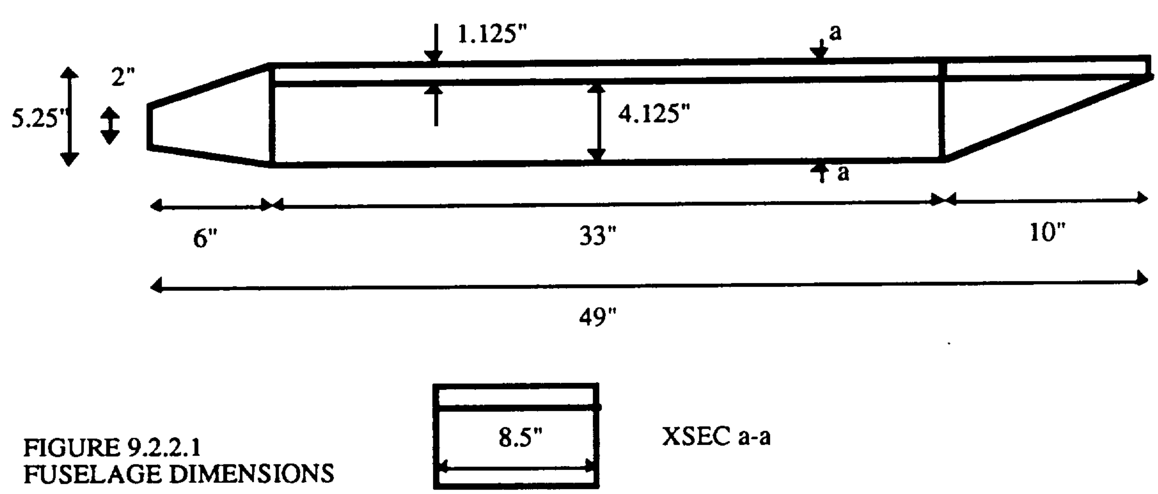

FIGURE 9.2.2.1
FUSELAGE DIMENSIONS

The nose extends six inches forward of the cargo bay. It consists of four surfaces tapered and angled together to form a pyramid. The most forward cross section is 2"x2" where the propeller shaft protrudes. The motor and speed controller are mounted in the nose section.

9.2.2.2 FUSELAGE SIDE PANELS (FIGURE 9.2.2.2)

The structure of the side panels was modelled on a truss analysis program which allowed for selection of different materials and various member cross sectional dimensions. This program and associated data file is included in appendix E. The side panels are the primary carriers of the major fuselage loads including aerodynamic lift and drag forces from the wings and tail and the weight forces of the cargo, avionics, and batteries. Three conditions were modelled at a max load factor of 3.2 (from equation 9.1.1.1): max lift and drag at max velocity with positive tail lift, max lift and drag at max velocity with negative tail lift, and a 10 foot per second vertical drop with no lift or drag acting. All of these conditions included a fully loaded but balanced payload. Each condition resulted in different critical points within the structure.

Knowing where the chord of each wing and tail would lie, the appropriate fraction of the maximum aerodynamic forces was applied at the corresponding structural nodes. This method was also used to model forces due to component weights. For example, all of the avionics gear would be attached to a floor which in turn lay over three nodes on each side panel. A value of one sixth the total avionics weight was then modelled at the corresponding nodes. The major assumption here is that the force distribution across the nodes is linear.

FIGURE 9.2.2.2
FUSELAGE SIDE PANEL

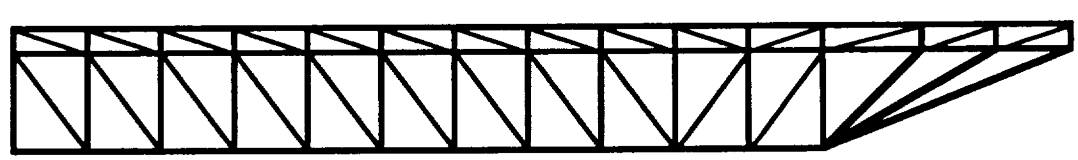

It was possible to minimize the weight of the structure to such a degree that every member would be a different cross section and material. In practice however, such a result is undesirable due to the obvious complexity in acquiring the materials and then constructing the structure. Rather, it was desired that the side panels be as easy to build as possible. Also, the minimum cross sectional dimensions of each member was set at 1/8"x1/8" for handling considerations. Each of the three main horizontal beams is one piece of uniform material and cross section. The vertical and diagonal members were kept as uniform as possible. Some variations were made in areas which required additional support. The result is that the structure is overdesigned in many areas, yet simple to build. A potential concern was additional weight, but this turned out to be negligible and worth the time saved in construction.

9.2.2.3 NOSE AND MOTOR MOUNT (FIGURE 9.2.2.3)

Two independent structures are mounted on the forward end of the fuselage main body. The first, the electric motor and speed controller mount, consists of an extended platform upon which the motor mount will be fastened. In the space between the motor mount and the main body, a platform will hold the speed controller. The harness (power and control lines) will be routed directly to the upper level of the fuselage main body for attachment to the appropriate avionics and batteries. The structure was modelled on a three dimensional truss analysis program to handle inertial loads in any direction up to four "g"s as well as the maximum thrust produced by the propeller of 3.0 pounds. Overdesign in this area was deemed conservative and proper due to failure in this area in past designs.

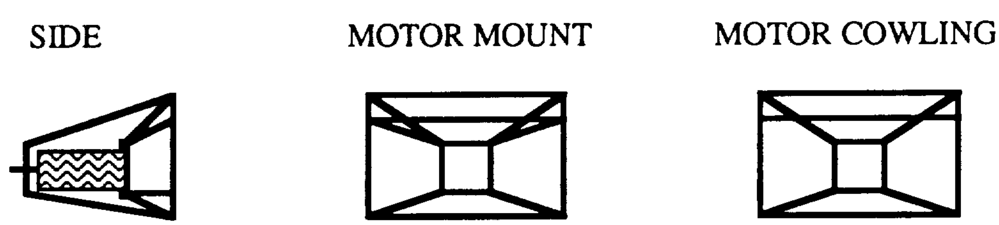

FIGURE 9.2.2.3 BOW AND MOTOR MOUNT

Second, the engine cowling will extend six inches forward of the main body in the shape of a pyramid. The effect is to taper the nose and reduce bluff body drag as well as blockage for the propeller. The loads on the cowling will be limited to aerodynamic forces during flight. These are assumed negligible. A hatch on the top surface of the cowling will allow access to the motor and speed control. Also, note that the 2"x2" forward section of access to the motor and speed control. Also, note that the 2"x2" forward section of the cowling remains open, allowing for propulsion system cooling.

9.2.2.4 LANDING GEAR SUPPORT

While the actual landing gear will be discussed in section 9.2.3, the support required by the fuselage is presented here. At a maximum 10 feet per second descent rate and impact time of 0.1 seconds, the plane will experience a 3.1 "g" deceleration. Normally it would be desired that all gear support this load equally. The worst case, for which the design accounted, is that case when only one wheel strikes first resulting in a single 23.3 pound applied force. This is handled by distributing the gear attachment to multiple cross beams on the lower fuselage deck. Analysis was done by hand modelling the combined cross beams as a single beam under a point load.

9.2.2.5 CATAPULT SUPPORT

A hook will be attached below the forward end of the fuselage main body for use in the catapult launching of the aircraft. The force expected during catapult launching is expected to be only 15 pounds, but a support structure for the hook was modelled to handle up to 25 pounds. Again, overdesign in this area was deemed conservative and proper due to uncertainty in this area and the lack of historical data to consult.

9.2.2.6 EMPENNAGE

As mentioned in section 9.2.2.1, the upper level of the main fuselage body overextends the cargo bay by ten inches. This area serves two purposes. First, it provides a structural base at a sufficient moment arm for the tail stability and control surfaces. Second, it provides the base for the rear access hatch for the cargo bay. The hatch is angled up from the cargo bay deck to the aft end of the upper deck and it opens downward providing a ramp which can be used to load cargo.

The 1/4 chord point of the horizontal tail and elevator is mounted one inch from the aft end of the upper deck. Figure 9.2.2.6.1 illustrates the rectangular planform and flat plate section. Under maximum elevator deflection at maximum speed of 50 fps, it will carry a force of 8 pounds. An appropriate sized frame was designed to handle that load which is estimated to weigh 4.0 ounces.

FIGURE 9.2.2.6.1
HORIZONTAL TAIL
AND ELEVATOR

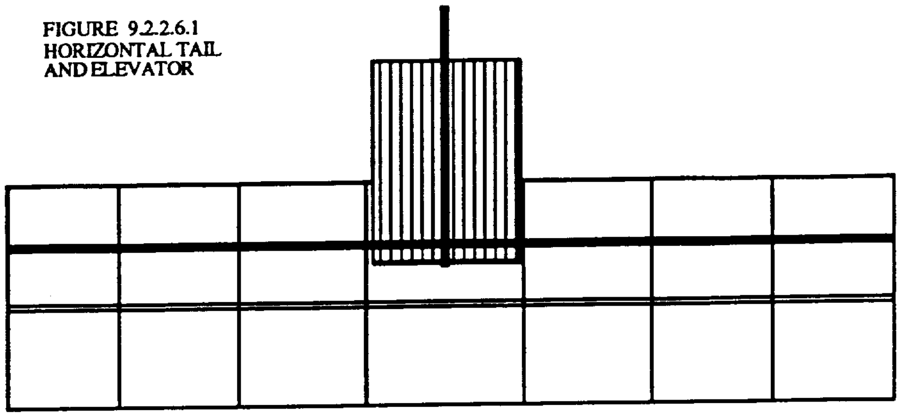

The same procedure was taken for the vertical tail and rudder. The root 1/4 chord is also attached one inch from the aft end of the upper deck. Figure 9.2.2.6.2 illustrates the combined triangle and rectangular planform and flat plate section. Under maximum elevator deflection at maximum speed of 50 fps, it will carry a side force of 2.18 pounds. An appropriate sized frame was designed to handle that load which is estimated to weigh 1.0 ounce.

FIGURE 9.2.2.6.2
VERTICAL TAIL
AND RUDDER

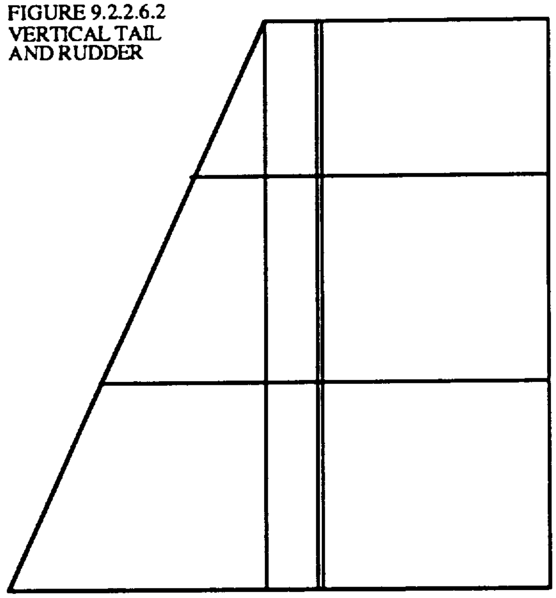

9.2.2.7 CONNECTORS, FLOORING, AND CROSS BRACING

Three tiers of connectors will join the side panels of the main fuselage body. On the lower deck, sixteen (16) connectors must support the weight of the cargo. On the upper level deck, fifteen (15) connectors must support the avionics gear and batteries. The ten (10) top surface connectors serve to add handling support and to provide frames for the access hatches to the avionics and battery areas. Figure 9.2.2.7.1 illustrates these three levels in the x-y plane. Flooring will exist in three areas and will be 1/16" thick balsa sheeting. First, the entire cargo bay must be floored. Second, on the upper deck, flooring must support the avionics gear, and third, the batteries must be supported by flooring.

Another consideration for the fuselage is resistance to torsional twisting. Ideally, no loads would be applied to cause torsion along the length of the fuselage. However, this is entirely possible in the cases of unusual flight maneuvers, asymmetric cargo loading, and general handling. The stiffness in each joint due to glueing may be sufficient, but additional cross bracing was added to ensure safety.

To prevent folding in the x-z plane, one main "X" brace exists at the front end of the cargo bay. No other main braces exist because they would interrupt the continuous cargo bay. Therefore, eight smaller "X" braces were placed in the upper deck.

FIGURE 9.2.2.7.1
TOP, MID, AND LOWER
DECKS (X-Y PLANE)

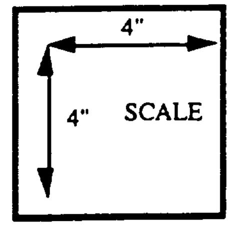

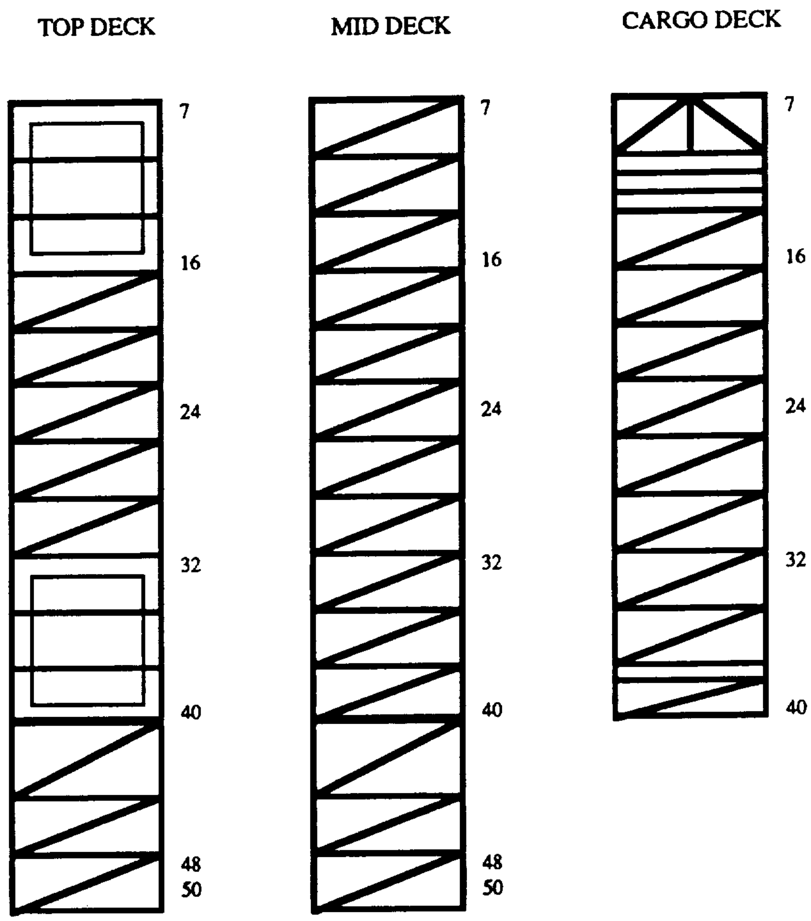

To prevent folding in the x-y plane, eleven "/" braces were placed in each deck. These will also serve to support flooring and the monokote skin of the fuselage. The "X" braces are illustrated in figure 9.2.2.7.2 and the "/" braces are included in figure 9.2.2.7.1, noted above.

FIGURE 9.2.2.7.2
BRACES (Z-Y PLANE)

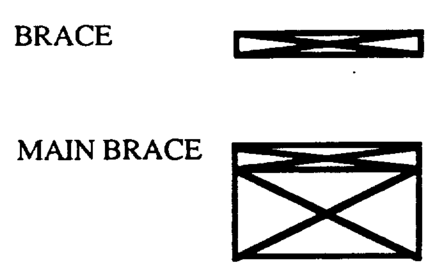

9.2.2.8 TOTAL FUSELAGE WEIGHT

Table 9.2.2.8 tabulates the estimated weight of each component in the fuselage. This estimate is based on the actual known weight of each structural member in addition to a factor of 20% which includes bonding materials and the monokote skin, where applicable. In certain cases, a 40% factor was used where heavy amounts of bonding material is expected to be used. This occurs in the engine mount and catapult support areas.

Item	Unit Weight	Quantity	Factor	Total Weight
Side Panel	2.51	2	1.2	6.03
Nose/Motor Mount	1.17	1	1.4	1.64
Catapult Support	0.114	1	1.4	0.16
Rear Cargo Bay Hatch	0.066	1	1.2	0.08
Avionics Hatch	0.073	1	1.2	0.087
Battery Hatch	0.073	1	1.2	0.087
Top Level Connectors	0.027	10	1.2	0.323
Mid Level Connectors	0.107	15	1.2	1.93
Base Level Connectors	0.107	16	1.2	2.06
Main Xsec Brace	0.24	1	1.2	0.288
Top Xsec Braces	0.144	8	1.2	1.38
Avionics Floor	0.418	1	1.2	0.501
Battery Floor	0.418	1	1.2	0.501
Cargo Bay Floor	1.53	1	1.2	1.84
Diagonal Braces	0.0255	33	1.2	1.01
Total Weight				17.91 ounces

TABLE 9.2.2.8 FUSELAGE WEIGHT BREAKDOWN (ounces)

9.2.3 LANDING GEAR

Landing gear must be designed to fulfill a number of often conflicting roles and requirements. Two of the most critical roles are to provide a stable platform for the aircraft on the ground, and to absorb and distribute ground handling and impact loads. Other factors that must be taken into consideration are propeller and fuselage clearance, ground handling behavior, and landing gear components' weight and drag penalties.

The design of the landing gear of the F-92 Reliant was driven primarily by component strength and the required fuselage ground angle. Based on a DR&O requirement that all components be able to withstand 3.5 g loadings, the landing gear was designed to undergo landing of a single side with vertical loads of up to 3.5 g without deforming, and also to withstand the forces associated with the catapult launch test. Further, this had to be done without overstressing the portion of the fuselage near the attachment point of the landing gear.

After investigating several different sizes and shapes of materials, including hollow tubing, 90° angle iron, and solid rod, it was decided to construct the landing gear from 0.25 inch aluminum rod. For the main gear, this rod would be bent into the configuration illustrated in Figure 9.2.3.1.

FIGURE 9.2.3.1
LANDING GEAR DESIGN

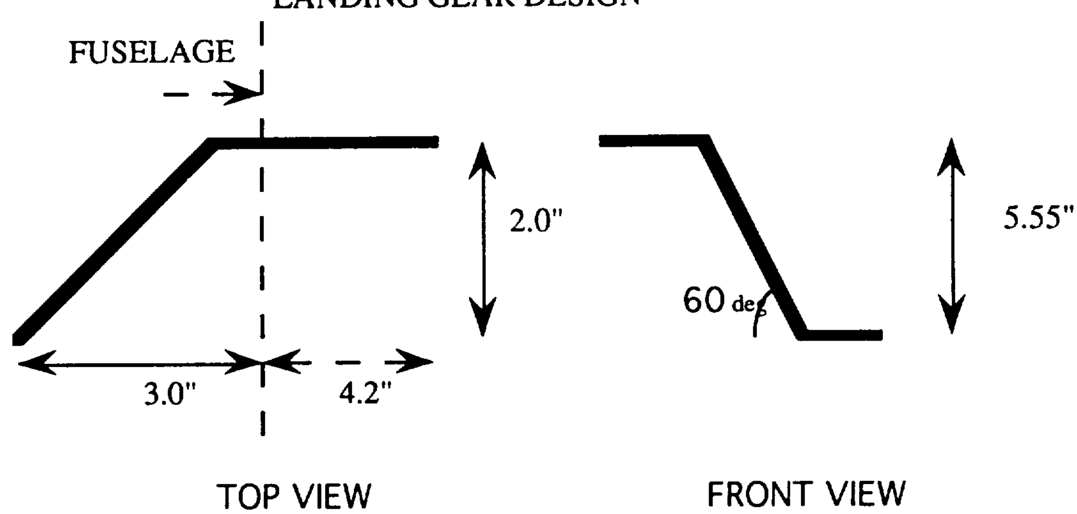

Under landings of 3.5 G, this design deflects 0.9 inches, maintaining propeller clearance of 2.0 inches in the event of a hard landing.

In addition to providing impact protection for the fuselage and propeller, the landing gear must provide a stable platform for the aircraft while it is on the ground. With this in mind, a wheel base as wide as is practical must be considered. For the F-92 Reliant, the wheel base is 14.65 inches, with the tail gear located 29 inches to the rear. For this configuration, the tip-over angle is 61.34°. This value represents an aircraft of borderline stability. However, this angle would never be reached, since the tips of the lower wing strike the ground at bank angles of slightly greater than 10°. This fact, coupled with the aircraft's lack of ailerons, makes it critical for the pilot to make a straight approach in landing. To account for any pilot error, an ablative pad will be attached to the underside of the wingtips to reduce the damage and impact to the wing in the event of an uneven landing.

The tail gear was also designed to withstand a vertical impact of 3.5 g. In order to provide steering capability, a system had to be designed to relay the actuator commands from the servos in the upper portion of the fuselage to the landing gear in the lower section. Several concepts were considered, including running connectors along the bottom floor of the cargo bay and inserting a removable column through the cargo bay. Actual selection of the method was left until construction time so that the feasibility of the systems could be thoroughly investigated. The tail gear projects 4.64 inches below the fuselage, giving the aircraft the required 4° ground angle.

TYPE: Tail-dragger	MATERIAL: 0.25" Aluminum
MAIN GEAR POSITION: 10.0"	MAIN WHEELS: 2.5" Foam
TAIL GEAR POSITION: 39.0"	TAIL WHEEL: 1.50" Foam
GROUND TRACK: 14.65"	WHEEL BASE: 28.9"
TIP-OVER ANGLE: 61°	WEIGHT: 7.0 oz.

TABLE 9.2.3.
LANDING GEAR DATA

9.3 MATERIAL SELECTION

The major factors involved in the selection of materials included strength, material availability, and the ease of workmanship. For most of the airframe, soft-woods such as spruce and balsa were found to be ideal. Spruce was chosen for the main spar caps on both wings, and for the main load bearing elements of the fuselage. Balsa was used for the noncritical parts of the fuselage and empennage structures, and the leading and trailing edge spars of the wings. These materials are readily available through many sources in a wide variety of pre-cut dimensions, provide very good strength to weight characteristics, and are easily cut, shaped, and joined with the use of the proper adhesives into the desired structural configuration. For areas of high loads, such as the engine mount, the landing gear mount, and the webbing near the root chord of the main wing, birch plywood was selected. This plywood offers a much higher modulus of elasticity and isotropic in-plane characteristics which are desirable for these areas. For the RPV skin, Monokote was selected. Monokote was selected due to its availability, its ease of application, and the fact that previous available data and models give a good representation of its expected characteristics. The following Table 9.3.1 lists the selected materials and their characteristics.

Material	ρ(lb/in^3)	σ_{com}(psi)	σ_{ten}(psi)	σ_{xy}(psi)	E(psi)
Balsa	0.0058	600	400	200	65000
Spruce	0.016	9000	6200	750	1.3e6
Plywood	0.0231	2500	2500	2500	2.01e6
Monokote	0.125e-6	N.A.	25000	25000	??

TABLE 9.3.1 MATERIAL PROPERTIES

The material properties of wood as opposed to those of isotropic materials such as aluminum presented several problems in the preliminary analysis. For an isotropic material, the failure mechanism is primarily shear. When an element is axially loaded, the shear force on a plane which is 45 degrees from the loaded axis will typically exceed the material shear stress before the compressive or tensile stress is exceeded. The primary consideration of cut wood which must be taken into account is that the material values are in relation to the grain orientation.

While a planar isotropic material such as plywood will have a σ_{xx}, σ_{yy}, and σ_{xy}, which are related to the various surfaces of an element rotated in the xy plane, the values of compression or tension for spruce or plywood are relative only to the grain. If shear were caused along the grain boundaries, the given value of σ_{xy} would be the value for failure. If the grain were axially loaded in compression or tension, the values given would be the proper failure values. If the forces are applied perpendicularly to the grain boundaries, the allowable stress values would be smaller. Therefore, it is critical that the grain be oriented in the proper direction in the construction. The maximum tensile or compressive values used in analysis are those listed in the table. The maximum tensile values were used as the maximum allowable stresses in tension or compression such that the smaller of the two allowable stress values were used so that in the event that the RPV were loaded in a negative sense, it would be as strong as it would be during normal flight loadings.

10.0 CONSTRUCTION PLANS

The construction of the F-92 Reliant will begin with the simultaneous construction of several of the major assemblies. The major assemblies are divided into the three major components discussed in the previous section, the lifting surfaces, the fuselage, and the landing gear. These groups can then be further divided into subgroups. The lifting surfaces include the main wing, consisting of the carry-through section and the wing tips, and the secondary wing, consisting of two half-span sections. The fuselage can be divided into three sections : the nose, including the motor mount and cowling; the main body; and the empennage, including the vertical and horizontal stabilizers and control surfaces. After the structure is complete, the landing gear, propulsion components, and avionics gear will be attached.

10.1 MAJOR ASSEMBLIES

10.1.1 LIFTING SURFACES

10.1.1.1 MAIN WING

The main wing consists of a center, 5-foot carry-through section which mounts to the top of the fuselage and two 2.5 foot tip sections which will be attached to the carry-through section at the desired angle required for stability, thus producing a wing with polyhedral. The carry-through section will be attached to the fuselage by means of 5/16 inch diameter dowel rods mounted in a bracket coming out of the top of the fuselage near the proper location of the wing quarter chord, with nylon screws with a variable number of spacers securing the trailing edge. The spacers will be used such that the angle of incidence of the wing will be easily changeable to adapt to the conditions and to optimize the actual design configuration in the event that modification is necessary. The carry-through section will be constructed with spruce spar caps of 0.25 inches in width by 0.125 inches in height at the quarter chord with a balsa leading edge spar of 0.125 inches in height by 0.125 inches in width and a balsa trailing edge spar of 0.187 inches by 0.25 inches. The main wing carry-through will contain 7 full chord ribs and 7 riblets alternating every 4.5 inches made out of 0.0625 inch balsa. 0.0625 inch Plywood webbing will be integrated over the center 2 feet of the carry-through section to ensure adequate support. Spruce webbing will then be employed for 9 inches on either side of the center section. Then balsa will be used from those points to points 9 inches from the end of the center section where plywood will again be employed to support the tip mount.

The tips of the main wing will be constructed using similar spar dimensions. The tips will employ 0.0625 inch plywood webbing over the first 4.5 inches, with balsa through the next 9 inches, and no webbing over the last foot and a half. The tips will be mounted through the use of a 0.125 inch thick spruce beam of approximately 3 inches in length which will extend from the tip section and insert into the carry through section and be held between the spars and webbing. For the secondary wing, the same spar-cap layout will be used. In both the primary and secondary wing configurations, the maximum rib spacing was determined to be 10.5 inches. To be on the conservative side, and since the initial weight was so much lower than the goal set forth in the DR&O, ribs spacing was set at 9 inches. In this weight estimation, several holes were cut in each rib to reduce dead weight as much as possible.

With a rib spacing of 9 inches, it is possible that the wing covering material would deform and not hold the true airfoil shape. This would result in a loss of section lift and possibly an increase in drag. For this reason, "riblets", or 0.40c ribs have been placed at intermediate positions along the span to maintain the airfoil shape from the leading edge to its thickest point, where the air-flow is most critical. This spacing of airfoil riblets at 4.5 inch increments was found to be consistent with previous designs in terms of rib spacing and was deemed adequate to achieve the proper airfoil performance. Figure 10.1.1.1 shows a 3-view of the root and carry through section of the main wing. One can see the lightening holes in the ribs and the riblets, as well as in the spar web, as well as the spar cap and rib dimensions.

FIGURE 10.1.1.1 THREE-DIMENSIONAL VIEW OF
MAIN WING CARRY-THROUGH

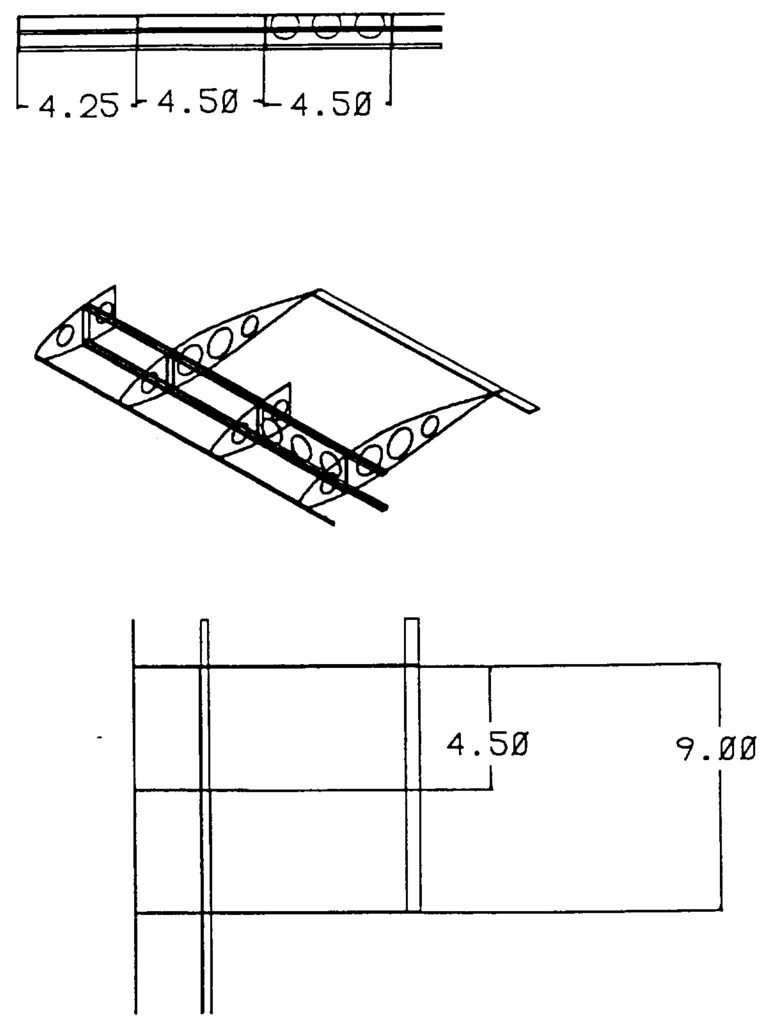

10.1.2 FUSELAGE

The fuselage construction team will first build the main body which will serve as the base to which all other components will be attached. These components include wings, tails, nose, engine mount, and landing gear.

10.1.2.1 MAIN BODY

The first task in constructing the main body is to fabricate the port and starboard side panels. These are illustrated in figure 9.2.2 (see section 9). For simplicity in construction, the side panel was designed with 3 main horizontal beams. These are connected vertically by members of the same material and cross section every 3 inches. The exception is at the forward end and the aft end of the cargo bay where heavier beams are used. Next, the angled support pieces for the rear access hatch will be attached. Finally, the cross beams will be added in each mesh.

With the side panels completed, they will be joined on each of the three levels by connecting beams which were described in section 9.2.2.7. The cross bracing will also be added at this time. On the lower deck, the additional beams for landing gear support and catapult support will also be added. Flooring will not be added at this time in order to allow for maximum access during subsequent construction and attachment of other components.

10.1.2.2 NOSE AND ENGINE MOUNT

With the main body structure complete, the nose cowling and engine mount will be attached. Achieving high sturdiness and bonding will be critical to the stability of the engine mount. The actual engine mount hardware should be secured at this time. Then the cowling may be attached.

10.1.2.3 EMPENNAGE

The angled support pieces for the rear access hatch were attached when constructing the side panel, but the actual hatch door must be built now. The door is hinged on the cargo bay floor and opens downward to provide a ramp for loading cargo.

The vertical tail and rudder will be attached at this time. The components should be fabricated prior to attachment. Excess length should remain at the base of the vertical posts in the vertical tail structure for bonding to the main body.

The horizontal tail and elevator will also be fabricated as separate components. This is for construction simplicity as well as for meeting specifications ; the tail span is 36 inches which will not meet packaging constraints unless it is removable. Therefore, the horizontal tail will be laid out similarly to the fuselage side panel. Note that it is a flat plate and does not require airfoil cross sections. It will be bonded and coated with Monokote. Then it may be secured to the main body with appropriate hardware .

10.1.3 LANDING GEAR ASSEMBLY

The landing gear is bent to meet the specifications shown in Figure 9.2.3.1. It is then attached to the base of the fuselage using epoxy to form a solid joint. The tail gear is inserted, leaving space above it to attach it to the control rods that serve the rudder. The final method for allowing steering capability is to be decided once the space available has been finally and physically determined.

10.2 COMPLETE PARTS COUNT

The values given in this section correspond to the quantities of raw materials purchased to construct a given component or group of components.

10.2.1 LIFTING SURFACE

The lifting surface is comprised of the wing carry through section, the wing tips, and the secondary wing. These are grouped in a single section to reflect how the raw materials will be used. For example, in the carry through section 10 feet of 1/4 x 1/8 spruce were needed, but these can only be purchased in 36 inch lengths, resulting in the need for 3 1/3 pieces. The extra 2/3 of a piece could then be used in the secondary wing to lengthen the 36 inch pieces to the required 42 inches. This raw material listing reflects an effort to minimize scrap in the actual construction of the wings.

(12) 36" x 1/4" x 1/8" spruce

(6) 36" x 1/8" x 1/8" balsa

(6) 36" x 1/4" x 1/8" balsa

(3) 36" x 4" x 1/16" balsa sheet

(1) 24" x 8" x 1/16" plywood sheet

(1) 12" x 4" x 1/16" plywood sheet

(1) 24" x 3" x 1/4" spruce

10.2.2 FUSELAGE

SIDE PANELS:

(4) 36" x 1/8" x 3/16" balsa

(14) 36" x 1/8" x 3/16" spruce

(1) 12" x 3/16" x 3/16" balsa

(2) 12" x 3/16" x 3/16" spruce

CONNECTING BEAMS AND BRACES

(6) 36" x 1/8" x 1/8" balsa

(3) 36" x 1/8" x 3/16" spruce

(1) 36" x 3/16" x 3/16" balsa

(5) 36" x 3/16" x 3/16" spruce

BOW AND ENGINE MOUNT

(1) 36" x 1/4" x 3/16" Spruce

(1) 36" x 3/16" x 1/8" Spruce

(1) 36" x 1/8" x 3/16" Balsa

(1) 36" x 1/8" x 1/8" Balsa

VERTICAL TAIL

(2) 36" x 1/4" x 3/16" Spruce

(2) 36" x 1/4" x 1/8" Balsa

HORIZONTAL TAIL

(4) 36" x 1/4" x 3/16" Spruce

(2) 36" x 1/4" x 1/8" Balsa

(1) 36" x 1/4" x 1/8" Spruce

CATAPULT & LANDING GEAR SUPPORT

(2) 36" x 1/4" x 1/4" Spruce

(1) 24" x 3/16" x 2" Bass

(1) 6" x 1/8" Diameter Brass Rod

10.2.3 LANDING GEAR

0.25" Diam. Aluminum Rod	2
1.25" Diam. Foam Wheels	2
0.75" Diam Rubber Wheel	1
Lock Washers	4

10.2.4 AVIONICS

(1) Radio Transmitter / Receiver Pair

(1) Receiver Battery

(2) Servos

(2) Pushrods

10.2.5 PROPULSION SYSTEM

(1) Astro 15 Electric Motor

(1) Speed Controller

(1) Fuse

(2) Six Packs of P-90-SCR Panasonic Batteries

(1) 30" 2-Conductor cable to connect battery packs to speed controller

10.3 ASSEMBLY SEQUENCE

Once again, the aircraft will be divided into its major components and substructures. These major components will be constructed simultaneously by small teams of 2 or 3 people in an effort to bring all elements to completion at the same time, thus employing all members of the group as efficiently as possible.

10.3.1 MAIN WING

The main wing will be the most challenging to construct and requires the most precision in that slight variations in the lift distribution over the primary lifting surface can cause drastic effects in the predicted flight performance. The primary show stopper in this, as in all areas, is weight. Every effort must be made to keep the weight to its predicted values.

The spar-caps will be purchased pre-cut and consist of solid shafts through each of the 3 sections of the main wing. The airfoils shapes, ribs and riblets, will be produced simultaneously in bulk to achieve a uniform shape and close tolerances. The creation of lightening holes in both the ribs and riblets represents a time consuming process, but one which will be necessary to achieve the desired performance. The ribs and riblets will be attached simultaneously to both the leading edge and lower quarter chord spars. Then the upper quarter chord spar and trailing edge spar can be added. The webbing can then be attached to the spars. Next, the structural attachment points must be assembled or machined. And finally, the sections can be coated with the aircraft skin, monokote.

10.3.2 SECONDARY WING

The secondary wing is almost identical to the first in its actual construction, except that the chord is shorter, and thus the ribs are smaller. The two sections will be constructed out of single piece spruce and balsa spars, with the construction occurring in the same fashion as above.

10.3.3 FUSELAGE

As noted in section 10.1.2, the critical component to fabricate is the main body of the fuselage. Once this is complete, all other components may be fitted for accurate dimensions and tolerances, then attached.

11.0 ENVIRONMENTAL IMPACT

The F-92 Reliant and the distribution system it serves does not operate in a vacuum. Just as the environment in which the aircraft operates impacts the design of the craft, the aircraft also can have significant, and often detrimental effects on its surroundings. It is the responsibility of the designers and operators to ensure that these effects are avoided or minimized to the greatest possible extent.

11.1 DISPOSAL COSTS

The actual disposal of each F-92 RELIANT aircraft after its useful life has expired is a difficult issue, considering the wide variety of components included in the construction. While certain components will have reached or in fact exceeded their safe operation limits, others will experience little if any wear detrimental to their performance. In light of that, the salvage of these usable parts is of great economic and environmental importance. Reducing the amount of waste material per aircraft reduces the volume of material actually being disposed. This reduction in disposal volume in turn reduces the expenditures necessary to find final resting places for the materials.

11.2 NOISE CHARACTERISTICS

Since the F-92 RELIANT is a part of a system that's designed operating environment includes night flights around populated areas, it is critical to the success of the overnight delivery system that the aircraft produce as little noise pollution as possible. There are two avenues by which this noise can be reduced : design and operations.

From the design standpoint, the propeller is the primary source of noise, with the power plant being the distant secondary source. As a system, however, these two account for approximately 80% of the total noise generation of the aircraft system. Since the greatest noise will be generated at takeoff and landing, which coincidentally occur in the greatest proximity to population centers, care must be taken to optimize the noise characteristics for these environments. Fortunately this can be done without any harm to the performance of the aircraft. The most effective way of reducing noise is to increase the number of blades on the propeller. Other techniques include choosing a larger engine to reduce the percentage of maximum power used at takeoff. The lower the ratio of power used to power available, the lower the noise production.

From the operations standpoint, the operators of the F-92 RELIANT should work in co-operation with the appropriate civil authorities to minimize the impact of Reliant operations on the public. This should include the establishment of noise abatement flight profiles, possible flight blackout hours, and airport load limits. Public acceptance is critical to the success of the package delivery system. If the negative impact of the noise of the system is greater than the service performed by the aircraft, the network is certain to lose business and eventually fail. It is therefore not only socially but economically imperative that the aircraft impact as little as possible on the acoustic environment of the citizens of AeroWorld.

11.3 WASTE AND TOXIC MATERIALS

Although the majority of the structure of the F-92 RELIANT is biodegradable, certain components of the power system pose a threat to the environment, particularly during production or in the event of a crash.

While the engine itself is a non-polluting electric system, the Nickel Cadmium batteries are a source of possible heavy metal contamination of the environment. Special care should be taken during the production of the batteries to minimize the chance of leakage. Since the batteries are supplied by a sub-contractor, care should be taken to insure that the sub-contractor follows all required as well as prudent measures to prevent contamination.

The inclusion of these batteries in the aircraft also poses a problem in the event of an aircraft accident. Careful location and padding of the batteries would reduce the chances of battery rupture. Also important are the flammability characteristics of the batteries.

Finally, disposal of the batteries poses a long term problem. Although with careful use, the batteries can be used for several generations of aircraft, eventually it will become necessary to dispose of the materials. Every effort should be made to recycle as many of the components as possible, with the remainder of the components being prudently disposed of to the best of the ability of available technology.

Although primarily an aircraft corporation, AE 441 should foster the development of cleaner power sources of power as well as improved handling techniques for the current technologies. Examples include the acceleration of the zinc-air battery system, which not only offers improved materials characteristics but also offers the prospect of greatly reduced fuel costs to the operator.

12.0 ECONOMIC ANALYSIS

The primary consideration in creating the transportation system is profit making both for the designer and the user. Instrumental to this is an accurate assessment of both the marketing strategies and the costs incurred in building and using the aircraft. This includes the cost of the materials and components used in building the aircraft, the labor necessary to carry out the construction, and the fuel and operations costs of daily use of the aircraft.

12.1 PRODUCTION COSTS

12.1.1 COST ESTIMATES

The cost of construction of the technology demonstrator is broken up into two primary areas--materials and labor. The materials costs are further subdivided into avionics, power supply, engine, and actual construction materials.

The early estimation of production costs and times was complicated by the fact that the design configuration was not solid. However, as aircraft configuration and performance became more concrete and more accurately estimated, a production cost breakdown was made, the results of which are displayed in Figure 12.1.1. Table 12.1.1 itemizes the actual cost estimates made.

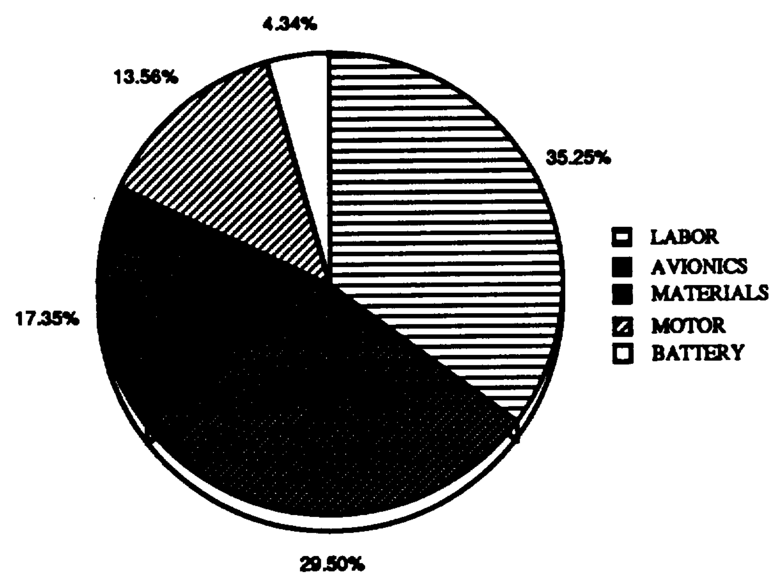

Estimation of the Breakdown of Production Costs

FIGURE 12.1.1

ITEM	VALUE	COST ($ AeroWorld)
MATERIALS	$160	64,000
AVIONICS	$272	108,800
MOTOR	$125	50,000
BATTERY	$40	16,000
CONSTRUCTION	130 hours	130,000

TABLE 12.1.1

Some of these factors, namely the motor and battery costs, were known precisely for the aircraft since the propulsion and fuels systems were set early in the design project. The figure for the avionics too is a set figure since the equipment is standard to all AE 441 aircraft. The cost of other construction materials, as well as the estimate of labor required is based on an analysis of historical data compiled from previous construction efforts undertaken in previous AE 441 projects.

Production costs shown here are based on the construction of a single prototype vehicle. The costs are not representative of the costs incurred in manufacturing the fleet of aircraft required to provide G-Dome with the level of service they desire. The implementation of a mass production system, rather than the hand-crafted nature of the original prototype would reduce both the labor and materials costs. A further reduction in costs could be achieved by maximizing the interchangeability among the Reliant variants within the fleet.

Possibly the most important method of reducing the cost to the user, and increasing AE 441's profits is the buy back program proposed for the F-92 Reliant. With AE 441 buying each aircraft back from its user at the end of its useful life (600 flights), the costs to both parties are reduced. The user no longer has to worry about disposal costs, and the relative price of the aircraft for the user drops significantly. This buy back program is advantageous for AE 441 in that it allows the salvage and reuse of non-stressed parts of the Reliant. For example, engines, batteries, speed controllers, and certain low load structural parts do not experience the same service loading as the wing, and may possibly be rated for re-use in other aircraft. This "cannibalism" of parts has been successfully practiced in military and other organization for years, and instituting it from the start of the F-92 Reliant program has benefits to all involved. The environmental advantages of the buy-back program are discussed in sections 11.1 and 11.3.

12.2 MAINTENANCE COSTS

The estimated maintenance costs of the F-92 Reliant is $25 per flight. This is based on a battery change time of 30 seconds. This is accomplished by the simplification of the battery access and distribution within the aircraft. Further reduction in fleet maintenance could be achieved by making a modular power system, allowing all aircraft in the fleet to use the same basic power supply system.

12.3 OPERATIONS COSTS

The estimation of the operational costs of the F-92 Reliant is complicated by the fact that the distribution system uses a fleet of several different sizes of aircraft, each with their own performance and cargo characteristics. Estimations that involve a single aircraft will therefore result in less efficient, more costly operations than will be found in actual operations. Further, each route represents a different flying range and time of travel, and scheduling would place the appropriate aircraft on each route. Cost estimation, however, assumes that each route is flown by the same aircraft, at a given cargo loading and fuel consumption per foot flown. This too leads to greater error between the actual operational costs and those predicted here. These values, however, offer a worst case scenario for costs, and actual operations will provide information to more accurately predict future costs.

There are two primary drivers of operations costs--fuel and servos. Of these, fuel is by far the greater, representing more than 95% of the cost of each flight. Based on a maximum fuel cost, and on two servos per aircraft, the cost per flight of each aircraft would be approximately $5500 to the AeroWorld operator. This does not represent the cost per flight that is necessary to recoup the capital investment in the aircraft.

13.0 THE TECHNOLOGY DEMONSTRATOR

Initial testing of the technology demonstrator has proved unsuccessful. Details of the tests, as well as planned modifications and future tests, are explained in section 13.3. Sections 13.1 and 13.2 describe the outcome of the technology demonstrator before any flight testing. Section 13.4 presents cost and labor data for construction of the technology demonstrator.

13.1 CONFIGURATIONAL DATA AND GEOMETRY

Every effort was made to strictly adhere to the design specifications for weight, dimensions and placement of components. (One exception to this was the orientation of the horizontal lifting surfaces, as explained in section 13.3.1) During the design phase it was expected that there would be variations in material weight, dimensions, and performance as well as unforeseeable problems by the inexperienced team members. Therefore consideration was given toward adding flexibility to the design configuration. Examples of this flexibility include:

1 - Sufficient room was given for variable longitudinal and lateral placement of the batteries. This allowed for fine tuning of the center of gravity once the technology demonstrator was complete.

2 - The main wing could be secured at variable angles of attack. This allowed for adjustment after other lifting surfaces had been fixed at incorrect angles of attack.

3 - The variable height tail gear was added to compensate for errors made when setting angles on the lifting surfaces. This allowed for varying the angle of attack of the fuselage during ground roll in order to avoid stalling during takeoff.

4 - A slot was built for placing the vertical tail rather than a fixed joint. This allowed for varying the placement of the vertical tail in order to make attachment of the horizontal tail and elevator less difficult.

5 - A dual catapult hook was attached due to uncertainty with the requirements and operation of that test. With two points of attachment, the more favorable one may be utilized for better performance.

6 - Plenty of hatches were provided for excellent access to all gear which might need attention as well as reduce AeroWorld maintenance time. These include the nose hatch for motor, fuse and speed control access; the avionics hatch for avionics access, servo adjustments, system battery charging, and access to the main gear attachments; the main wing hatch for access to the main wing mount; the battery hatch for battery charging, steering access, and pushrod adjustments; and finally the main cargo bay hatch which in addition to use for cargo, gave additional access to the tail gear and pushrods.

7 - Use of variable sensitivity control horns and pushrods allowed for calibration and sensitivity adjustment of control surfaces and the steerable tail wheel. It was expected that adjustment would be necessary after taxi and flight tests.

Overall dimensions of the technology demonstrator matched those of the design specification with the exceptions of slight variations (+/- 1/8 inch) in few areas. Difficulties which contributed to these variations included warping of the wood under glue and monokote loads as well as the lack of high accuracy jigs. Tolerances in cutting and sanding pieces to the specified shapes were also a factor.

The dimensions of the Technology Demonstrator are as follows:

Overall Length	55.75 inches
Overall Height	21.75 inches
Fuselage Length	50.1 inches
Fuselage Max Width	8.56 inches
Fuselage Max Height	8.56 inches
Primary Wing Span	9.86 feet
Primary Wing Chord	10.25 inches
Secondary Wing Span	7.69 feet
Secondary Wing Chord	7.75 inches
Horizontal Tail / Elevator Span	3.0 feet

Horizontal Tail / Elevator Chord	8.94 inches
Vertical Tail / Rudder Height	11.0 inches
Vertical Tail / Rudder Tip Chord	5.56 inches
Vertical Tail / Rudder Root Chord	10.63 inches

The angles of the Technology Demonstrator are as follows:

Component	Mounted Angle of Attack Relative to Fuselage
Main Wing	8 degrees
Secondary Wing	14 degrees
Horizontal Tail	4 degrees

13.2 WEIGHT DATA AND CENTER OF GRAVITY

For the most part, weight predictions were very accurate and slight additions in some components were negated by lighter-than-expected components. When completed, however, the aircraft was 0.5 pounds overweight. This is primarily due to two components which were underestimated: the main and secondary wing mounts. Another culprit was the batteries which weighed 0.2 pounds more than expected. This added weight would result in 25% less payload capacity. However, no payload was loaded for the technology demonstrator tests.

Values which are presented below in table 13.2 may be compared with the design values given in table 6.1. Due to problems which arose during the flight tests (discussed in section 13.3), weight data will be presented for two cases. Table 13.2 contains the breakdown by component of the total aircraft weight. The initial results corresponding to the design configuration are first given. These indicate a center of gravity at 23.75 inches and total weight of 6.0 pounds (no payload). As will be discussed in 13.3, a second configuration was used in which the secondary wings were removed and ballast was placed in the nose. The ballast consisted of 10.0 ounces of lead secured above the motor mount. The total weight for this second case was 6.14 pounds and the center of gravity was at 21.5 inches.

TABLE 13.2

Component Weights, Positions, & Center of Gravity For Technology Demonstrator

Component	Weight (lbf)	Weight (oz)	Xpos (inches)	Zpos (inches)	m*X (oz-in)	m*Z (oz-in)
---	---	---	---	---	---	---
Receiver & Antenna	0.061	0.98	10.00	5.00	9.80	4.90
Radio Battery	0.132	2.11	8.00	5.00	16.88	10.55
Servo (Elevator)	0.041	0.65	11.00	5.00	7.15	3.25
Servo (Rudder&Steering)	0.041	0.65	11.00	5.00	7.15	3.25
Pushrod (Elevator)	0.047	0.75	30.50	5.00	22.88	3.75
Pushrod (Rudder&Steering)	0.047	0.75	30.50	5.00	22.88	3.75
Fuselage & Motor Mount	1.094	17.50	23.00	2.50	402.50	43.75
Main Wing - High	0.813	13.00	22.00	6.00	286.00	78.00
Main Wing Mount	0.266	4.25	23.00	6.00	97.75	25.50
Secondary Wing - Low	0.419	6.70	29.00	-0.75	194.30	-5.03
Secondary Wing Mount	0.125	2.00	29.00	-0.75	58.00	-1.50
Vertical Tail & Rudder	0.088	1.40	46.00	12.60	64.40	17.64
Horizontal Tail & Elevator	0.253	4.05	50.00	5.75	202.50	23.29
Main Gear	0.394	6.30	11.00	-4.00	69.30	-25.20
Tail Gear & Steering	0.175	2.80	38.00	-2.00	106.40	-5.60
Engine & Clamp	0.563	9.00	3.00	2.00	27.00	18.00
Speed Control	0.110	1.76	6.50	3.00	11.44	5.28
Propeller	0.057	0.91	0.50	1.75	0.46	1.59
Battery (P90SCR) x 6	0.567	9.07	34.50	4.75	312.92	43.08
Battery (P90SCR) x 6	0.567	9.07	34.50	4.75	312.92	43.08
Battery Cable	0.144	2.30	20.75	4.50	47.73	10.35
Ballast	0.563	9.00	3.00	3.25	27.00	29.25
	Total Weights:				Centers of Gravity:	
Design Configuration: (Both Wings/No Ballast)	6.000 Pounds	96.00 Ounces			23.75 = CG: X	3.14 = CG: Z
Altered Configuration: (Main Wing Only/Ballast)	6.144 Pounds	98.30 Ounces			21.50 = CG: X	3.42 = CG: Z

13.3 TECHNOLOGY DEMONSTRATOR TESTS

After completing the construction of the technology demonstrator, several tests were planned to compare its performance with the predicted design values. Because of several difficulties with getting the technology demonstrator to fly properly, we were unable to use these tests for that purpose. Instead, the tests provided a means of finding the source of the problems associated with the technology demonstrator-- whether it be a design problem or a construction problem, or a combination of the two. Section 13.3 describes the discrepancies between the aircraft design and the actual construction of the technology demonstrator. This section also describes the safety considerations taken and the results of the tests, as well as future test plans and planned construction modifications.

13.3.1 TECHNOLOGY DEMONSTRATOR DISCREPANCIES

Before constructing the technology demonstrator, it was decided to modify the design slightly. For the design configuration, the fuselage was expected to fly at a 6-degree angle of attack under full cargo load. To decrease drag at cruise, it was desired to bring this fuselage angle as close to zero as possible. To accomplish this, the incident angles of the two wings and horizontal tail could all be increased 6 degrees with respect to the fuselage. The restriction against this plan was the possibility of stall at takeoff. It was thus decided to shift the horizontal surfaces by an intermediate value of 4 degrees, allowing the fuselage to be orientated at 2 degrees instead of 6 degrees during cruise.

For the most part, the construction of the technology demonstrator went smoothly and did not deviate from the intended design until the very end. The construction of the lower, secondary wing mount was intended to be secured at an angle of 8 degrees with respect to the fuselage. The actual angle turned out to be 14 degrees, and was not able to be adjusted without completely re-doing the lower wing mount. This angle, plus the 4 degree angle of inclination of the fuselage due to landing gear configuration, means that on takeoff the lower wing would be inclined 18 degrees relative to free-stream. This was definitely unacceptable because the secondary wing is expected to stall at 15 degrees relative to freestream.(Stall characteristics are explained in section 4.3)

To correct this problem in the short amount of time available, it was decided to reduce the angle of the fuselage by 6 degrees. This was accomplished by raising the tail gear from 4.875 inches to 7.8 inches, which caused the fuselage to rest at an angle of -2 degrees with respect to the runway. The secondary wing was now orientated 12 degrees with respect to the runway. In order that the main wing and the tail maintain the same orientation with respect to the secondary wing, and with respect to freestream, they were inclined an additional 6 degrees with respect to the fuselage. The end result was that the all angles with respect to freestream were as intended, with the exception of the fuselage, which was at -2 degrees. These changes are summarized in table 13.3.1.

Table 13.3.1 Technology Demonstrator Modifications

	Angle of Attack Relative to the Runway (degrees)			
Configuration	Main Wing	Secondary Wing	Horizontal Tail	Fuselage
Initial Design	2	8	0	4
Intended TechDemo	6	12	4	4
Actual TechDemo	6	18	4	4
Adjusted TechDemo	6	12	4	-2

13.3.2 SAFETY CONSIDERATIONS

Human safety was a major concern during the taxi and flight tests. All of the spectators were required to stay behind a viewing net. The members of each design team were expected to keep an eye on their plane at all times to avoid any accidents. Whenever the propeller was being handled, both of the switches were turned off, and the batteries were disconnected.

Safety of the plane was also a consideration. A "shake" test was done before the flight test to ensure that there were no loose parts in the plane that might damage the plane in flight. This test was also to ensure that nothing flew off during the flight test and hurt someone watching the flight test. The landing gear was tested by dropping the plane from approximately eight inches to make sure that the landing gear could handle the force of a landing and to see whether or not the plane could land without hitting the secondary wing on the ground. The secondary wing did not touch the ground in this test, but it did come fairly close to the ground. The strength of the wing was tested by two people supporting the plane by holding onto it at the 70% span point on either side of the wing. The wing held up the plane and therefore the wings were judged strong enough to lift the plane.

13.3.3 TAXI TEST

To ensure the plane did not attempt to leave the ground during the taxi tests, a maximum of 1/3 throttle was used. Although the plane tended to veer to the right slightly, it was easily controlled to move along a straight line, and turned without difficulty.

13.3.4 FLIGHT TESTS

At the time of this writing, 3 flight tests have been performed. Several more are intended. This section explains the results of the flight tests performed to date and planned future tests.

Flight Test 1

Plan: Bring the technology demonstrator up to takeoff speed, raise it from the ground about 5 feet, and then land it.

Result : The technology demonstrator had difficulty performing this task. The plane had difficulty maintaining alignment with the runway. When the plane did get off the ground, it exhibited what appeared to be a severe type of dutch-roll motion before impacting with the ground. This test was repeated several times with the same result.

Analysis : It was concluded that possible causes of the problems were as follows:

1) Over-sensitivity of the landing gear. This would explain difficulty in maintaining runway alignment.

2) Stalling of the lower wing. Uneven stalling might explain the difficulty in maintaining runway alignment at high speed, as well as the radical motion which took place immediately after takeoff. Stalling of the lower wing would also cause the center of pressure to move forward, causing the plane to be unstable in pitch. This could further account for the bizarre motion after takeoff.

Solution : It was decided to remove the lower wing and repeat the test. Even with the removal of the lower wing, takeoff was possible because the plane was carrying no cargo. To compensate for the resulting forward movement of the center of pressure due to the removal of the rearward wing, ballast was secured in the nose of the plane such that the center of gravity was now slightly forward of the main spar of the main wing. Furthermore, the tail gear was lowered back to the original 4.875 inches, raising the fuselage to the original 4-degree angle of inclination relative to the runway. Finally, the tail gear motion was desensitized by increasing the moment arm on the gear's control horn.

Flight Test 2

Plan: Bring the technology demonstrator up to takeoff speed, raise it from the ground, and keep in the air as long as possible.

Result : The technology demonstrator still had difficulty taking off; it still had difficulty maintaining alignment with the runway and it still exhibited unstable motion for the few seconds that the plane was in the air before impacting with the ground. This test was repeated several times with the same result.

Analysis : It was concluded that possible causes of the problems were as follows:

1) Roll instability due to asymmetric stalling of the outboard sections of the main wing.

2) Directional instability due to fuselage blockage of the vertical tail.

Solution : It was decided to lower the angle of attack of the outboard sections of the main wing and to repeat the test. This was accomplished by twisting the outboard sections and then tightening the monokote. The test was repeated, but the results remained unchanged. The next step consisted of attaching a make-shift sheet of thin plywood to the vertical tail, increasing its area by about 20%, and increasing its directional instability.

Flight Test 3

Plan: Bring the technology demonstrator up to takeoff speed, raise it from the ground, and keep in the air as long as possible.

Result : The technology demonstrator still had difficulty maintaining alignment with the runway and still it exhibited unstable motion in the air, although to a lesser degree. The pilot was able to hold the plane in the air for approximately 8 seconds and perform a 180-degree turn.

Analysis : Directional instability appears to be difficult to achieve with the design configuration. This is likely due to blockage or disruption of the airflow to the vertical tail, caused by the large fuselage.

Solution : For future tests, additional vertical surface area will be included on the underside of the fuselage near the tail gear. It is hoped that this vertical surface, by being placed underneath, will not be blocked by the fuselage. Furthermore, the ballast will be removed to decrease the overall weight. To compensate for the removal of ballast and keep the plane stable in pitch, the batteries will be moved forward.

Planned Flight Tests

It is expected that the next flight test will prove successful and directional stability achieved. Future tests will involve reconstructing the lower wing mount so that the lower wing can be easily adjusted to the desired 8-degree angle of inclination relative to the fuselage. The center of gravity will be move aft to correlate with the original design configuration.

13.3.5 CATAPULT TEST

The data required for the catapult characteristics prediction program is included in appendix F. It was decided that, given the difficulties with the Reliant's secondary wing, the catapult test would be performed using only the main wing. This will also increase the accuracy of the program's predictions since the program was not designed to analyze the catapult performance of biplanes.

13.4 MANUFACTURING COSTS

The following is a review of the actual expenditures of capital and labor on the construction of the technology demonstrator, and compares actual expenditures with those predicted.

In the estimation of the construction costs, historical data was used to try to assess what the cost of the materials required would be for the technology demonstrator. In making this assessment, the greater size of the F-92 Reliant was taken into account. The original estimate of the materials cost of the aircraft was $160, excluding avionics and propulsion. The final cost of the materials for the technology demonstrator, again excluding propulsion and avionics, was $220. The difference can be attributed in part to the fact that no aircraft prior to this had approached the scale of the F-92 Reliant, and in part to materials wasted due to inexperienced workmanship. Figure 13.4.1 breaks down the material's expenditure for each major subcomponent of the structure. Table 13.4.1 provides the detailed costs of each component. The costs as computed here were derived from an analysis of the parts count for the technology demonstrator.

FIGURE 13.4.1
MATERIALS COSTS

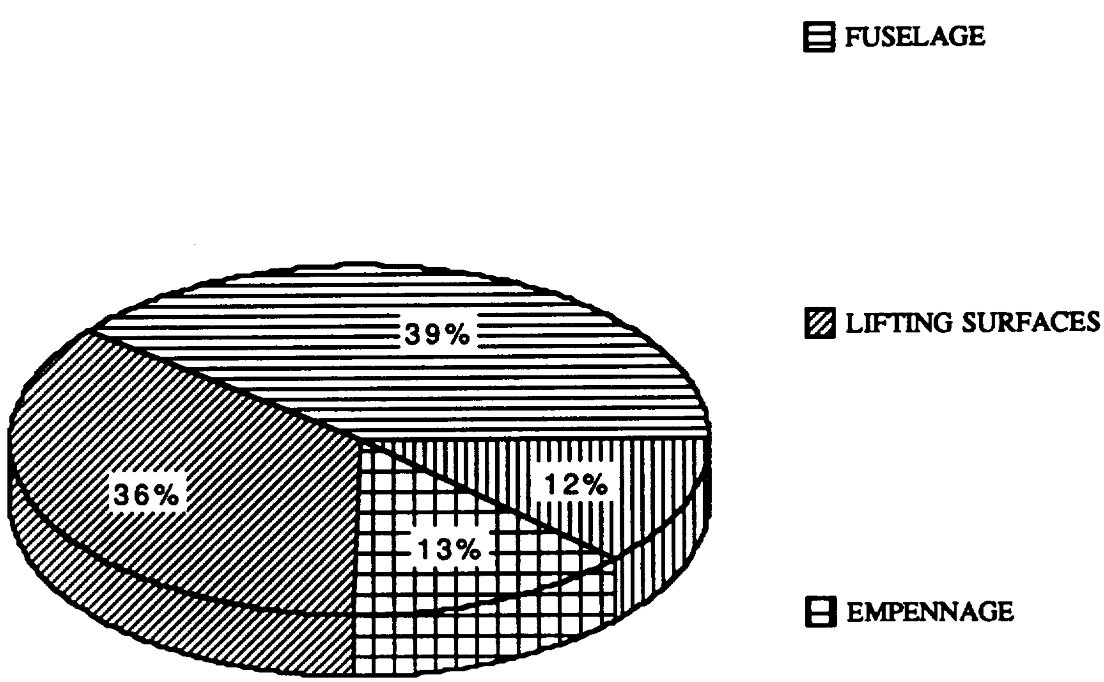

TABLE 13.4.1
COMPONENT COSTS

COMPONENT	COST
FUSELAGE	$32.46
LIFTING SURFACES	$31.50
EMPENNAGE	$11.71
LANDING GEAR	$10.51

The total materials costs of all the components of the technology demonstrator was $657.00. This figure was again broken down by major sub-systems, as illustrated in Figure 13.4.2.

FIGURE 13.4.2
TECHNOLOGY DEMONSTRATOR COSTS

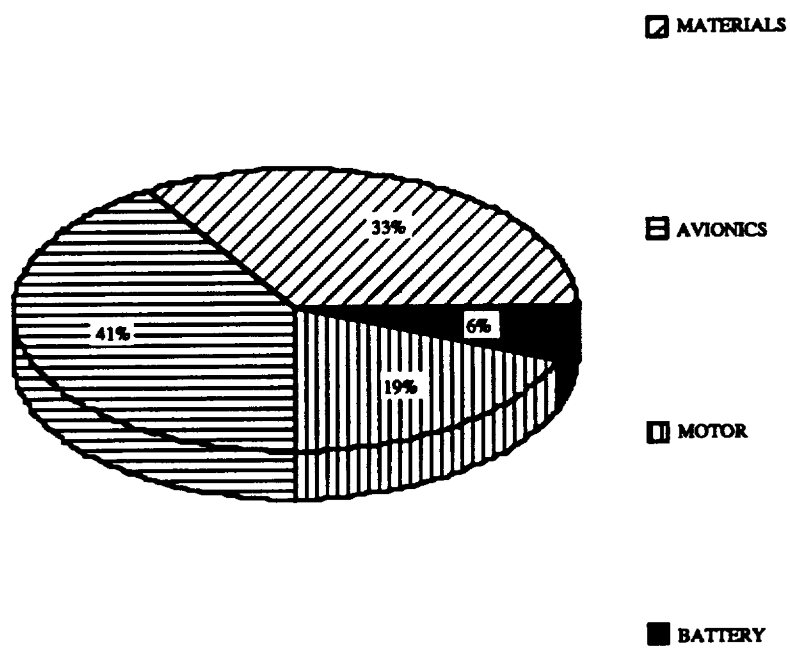

TABLE 13.4.2
PRIMARY DEMONSTRATOR COMPONENT COSTS

COMPONENT	COST
MATERIALS	$220.00
AVIONICS	$272.00
MOTOR	$125.00
BATTERY	$40.00

Finally, the estimation of the time required to construct the technology demonstrator was 140 hours. In actuality, this figure was 130. This includes time spent in assembling the prototype the first time. Figure 13.4.3 breaks the time spent on the construction down for the major component systems of the demonstrator.

FIGURE 13.4.3
TECHNOLOGY DEMONSTRATOR
LABOR

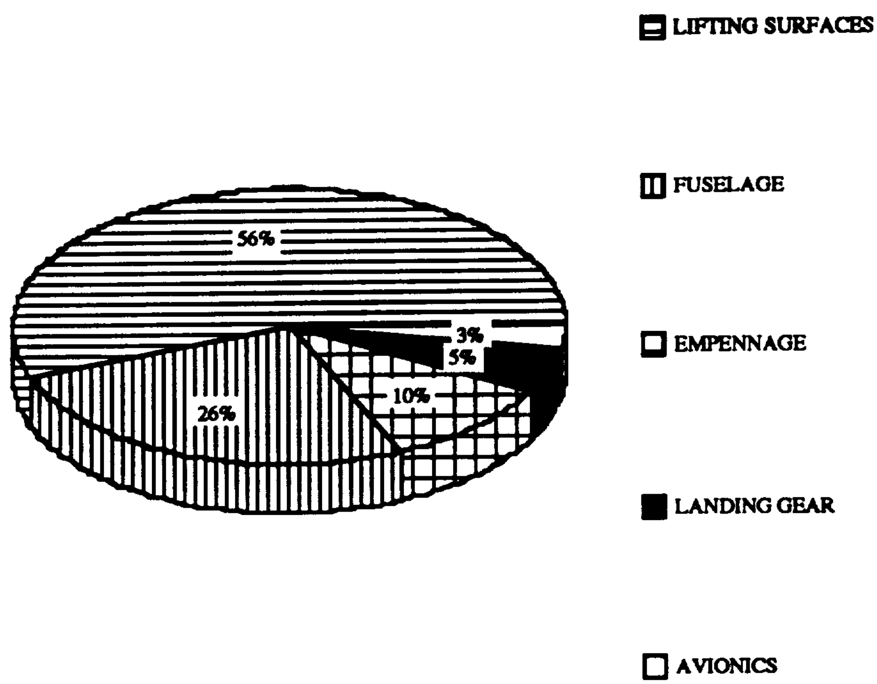

TABLE 13.4.3
MAJOR SUBSYSTEMS CONSTRUCTION TIMES

COMPONENT	CONSTRUCTION HOURS
LIFTING SURFACES	72.50
FUSELAGE	33.50
EMPENNAGE	13.50
LANDING GEAR	6.75
AVIONICS	3.75

Appendix A

Request For Proposal

UNIVERSITY OF NOTRE DAME
DEPARTMENT OF AEROSPACE AND MECHANICAL ENGINEERING

AE441: Aerospace Design; Request for Proposals - RFP Spring 1992

Air Transport System Design

The successful development of an air transportation system depends upon a sound understanding of the market and efficient development of an aircraft system which can operate effectively in that market. Since a particular aircraft cannot satisfy every possible user need, it must be evaluated on how well it meets it own design objectives.

In order to be considered as a reasonable aircraft system for a commercial venture, it must be able to operate at a profit which requires compromises between technology and economics. The objective of this project will be to gain some insight into the problems and trade-offs involved in the design of a commercial transport system. This project will simulate numerous aspects of the overall systems design process so that you will be exposed to many of the conflicting requirements encountered in a systems design. In order to do so in the limited time allowed for this single course a "hypothetical world" has been developed and you will be provided with information on geography, demographics and economic factors. The project is formulated in such a fashion that you will be asked to design a basic aircraft configuration which will have the greatest impact on a particular market. The project will not only allow you to perform a systems design study but will provide an opportunity to <u>identify those factors which have the most significant influence on the system design and design process</u>. Formulating the project in this manner will also allow you the opportunity to fabricate the prototype for your aircraft and develop the experience of transitioning ideas to "hardware" and then validate the hardware with prototype flight testing.

An aircraft which is simply the fastest or "looks neat" will not be considered a marketable product. Economic feasibility and, in particular, compliance with <u>your</u> design objectives will provide the primary means for evaluating your system design.

OPPORTUNITY

The project goal will be to design a commercial transport which will provide the greatest potential return on investment. Maximizing the profit that your airplane will make for an "overnight" package delivery network can be accomplished by minimizing the cost per "package". G-Dome Enterprises has conducted an extensive market survey for an airborne package delivery service and is now in the market for an aircraft which will allow them to operate at a maximum profit. AE441, INC. has agreed to work with them to establish a delivery system. This includes a market analysis, the establishment of a distribution concept and the development of a number of aircraft concepts to help met this market need. This will be done by careful consideration and balancing of the variables such as the payload, range, fuel efficiency, production costs, as well as maintenance, operation and disposal costs. Appropriate data for each is included later in the project description.

The "world" market in which the airline will operate is shown in Figure 1. Table 1 gives the parcel volume between each possible pair of cities each day. Table 2 gives other useful information regarding each city including details on location and available runway length. The service may operate in any number of markets provided that they use only one airplane design and any potential derivatives (your company does not have the engineering manpower to develop two different designs). Consider derivative aircraft as a possible cost-effective way of expanding the market.

REQUIREMENTS

1. Develop a proposal for an aircraft and any appropriate derivative aircraft which will maximize the return on investment gained by the airline through careful consideration and balance of the payload/volume, the distance traveled, the fuel burned, and the production cost of each plane. The greatest measure of merit will be associated with obtaining the highest possible return on investment. You will be expected to determine the freight cost for all markets in which you intend to compete. The proposal should not only detail the design of the aircraft but must identify the most critical technical and economic factors associated with the design.

2. Develop a flying prototype for the system defined above. The prototype must be capable of demonstrating the flight worthiness of the basic vehicle and flight control system and be capable of verifying the feasibility and profitability of the proposed airplane. The aerodynamic performance of the prototype will be evaluated using a "stick-fixed" catapult launch of the aircraft carrying a specialized instrument package and where the range of the aircraft under specified launch conditions will be the primary measure of aerodynamic efficiency. Flightworthiness and handling qualities of the prototype will be demonstrated by flying a closed figure "8" course within a highly constrained envelope.

BASIC INFORMATION FOR "AEROWORLD"

The following information is to be used to define special technical and economic factors for this project. Some are specific information others are ranges which are projected to exist during the development of this airplane.

1. Payload: There are two standard parcel packing containers, a 2"cube and a 4"cube. Remember these are cargo, therefore items like access and ease in loading are important. Since various types of cargo can be considered, cargo weight/volume requirements are also important. Cargo weights can vary from 0.01 to 0.04 oz/cubic inch.
2. Range: distance traveled in feet
3. Fuel: battery charge measured in milli-amp hours
4. Production cost = 400 x (total cost of prototype in dollars) $ + 1000 x (prototype construction man-hours) $.
5. Operation costs = (number of servos in the aircraft) x flight time in minutes - this is a cost per flight
6. Maintenance costs = $50 per man-minute for a complete "battery" exchange - this is a cost per flight
7. Fuel costs = $5.00 to $20.00 per milli-amp hour
8. Regulations will not allow your plane to produce excessive "noise" from sonic-booms; consider the speed of sound in this "world" to be 30 ft/s.
9. The typical runway length at the city airports is 75 ft, this length is scaled by a runway factor in certain cities.
10. Time scale: "AeroWorld day" is 30 minutes
11. Propulsion systems: The design, and derivatives, should use one or a number of electric propulsion systems from a family of motors currently available.
12. Handling qualities - To be able to perform a sustained, level 60' radius turn.
13. Loiter capabilities - The aircraft must be able to fly to the closest alternate airport and maintain a loiter for one minute.
14. Aircraft Life - Is based upon the fatigue life of the materials used in AeroWorld. Figure 2 provides a chart used to estimate the reduction in working stress based upon the number of take-off/landing cycles the aircraft experiences.

SPECIAL CONSIDERATIONS FOR THE TECHNOLOGY DEMONSTRATOR

The prototype system will be an RPV and shall satisfy the following:

1. All basic operation will be line-of-sight with a fixed ground based pilot, although automatic control or other systems can be considered.
2. The aircraft must be able to take-off from the ground and land on the ground under its own power.
3. The prototype flight tests for the Technology Demonstrator will be conducted in the Loftus Center (Figure 3) on a closed course. The altitude must not exceed 25' at any point on the course.
4. Catapult launch tests will be conducted in the Loftus center. Details on the catapult and instrument package will be provided.
5. The complete aircraft must be able to be disassembled for transportation and storage and must fit within a storage container no larger than 2'x2'x5'.
6. Safety considerations for systems operations are critical. A complete safety assessment for the system is required.
7. The Technology Demonstrator will be a full sized prototype of the actual design and must be used to validate the most critical range/payload condition for the aircraft.
8. Takeoff must be accomplished within the takeoff region shown on Figure 3.
9. A complete record of prototype production cost (materials and manhours) is required.
10. The radio control system and the instrumentation package must be removable and a complete system installation should be able to be accomplished in 30 min.
11. System control for the flight demonstrator will be a Futaba 6FG radio system with up to 4 S28 servos or a system of comparable weight and size.
12. All FAA and FCC regulations for operation of remotely piloted vehicles and others imposed by the course instructor must be complied with.

CITY	A	B	C	D	E	F	G	H	I	J	K	L	M	N	O
A	0	300	100	20	20	200	450	40	100	300	350	80	60	80	10
B	500	0	100	40	30	450	300	60	150	400	300	400	100	100	20
C	200	100	0	30	20	120	90	30	30	30	50	300	30	40	30
D	20	20	30	0	100	50	20	20	90	60	80	30	20	20	20
E	20	20	20	150	0	100	30	20	100	100	200	60	30	30	10
F	200	350	120	60	100	0	250	60	250	400	500	350	300	250	20
G	350	400	90	40	30	350	0	300	300	300	250	200	150	120	20
H	40	60	30	30	20	60	300	0	200	350	250	100	100	100	30
I	100	150	30	90	200	250	300	200	0	350	450	250	200	200	20
J	300	400	30	60	100	400	300	250	350	0	500	300	250	400	20
K	350	400	60	80	200	500	250	250	450	500	0	400	450	500	10
L	80	400	300	30	60	250	200	100	250	300	400	0	350	400	20
M	60	100	30	20	30	200	150	100	200	250	450	350	0	350	30
N	80	200	20	20	30	250	120	200	200	300	500	400	350	0	20
O	20	20	20	20	20	20	20	20	20	20	20	20	20	20	0

Origination city - columns
Destination city - rows

TABLE 1. DAILY CARGO LOAD FROM CITY TO CITY - (CUBIC INCHES)

CITY	LONG.	LAT.	Runway Length factor
A	-21	6	1
B	-15	12	0.8
C	-10	-5	0.6
D	-1	-10	1
E	9	-1	1
F	-4	10	1
G	-5	17	1
H	-1	12	1
I	8	7	1
J	5	15	1
K	9	17	1
L	20	15	1
M	20	5	1
N	24	10	1
O	20	-9	0.75

TABLE 2. CITY INFORMATION (Each Longitude and Latitude increment is 200 ft.)

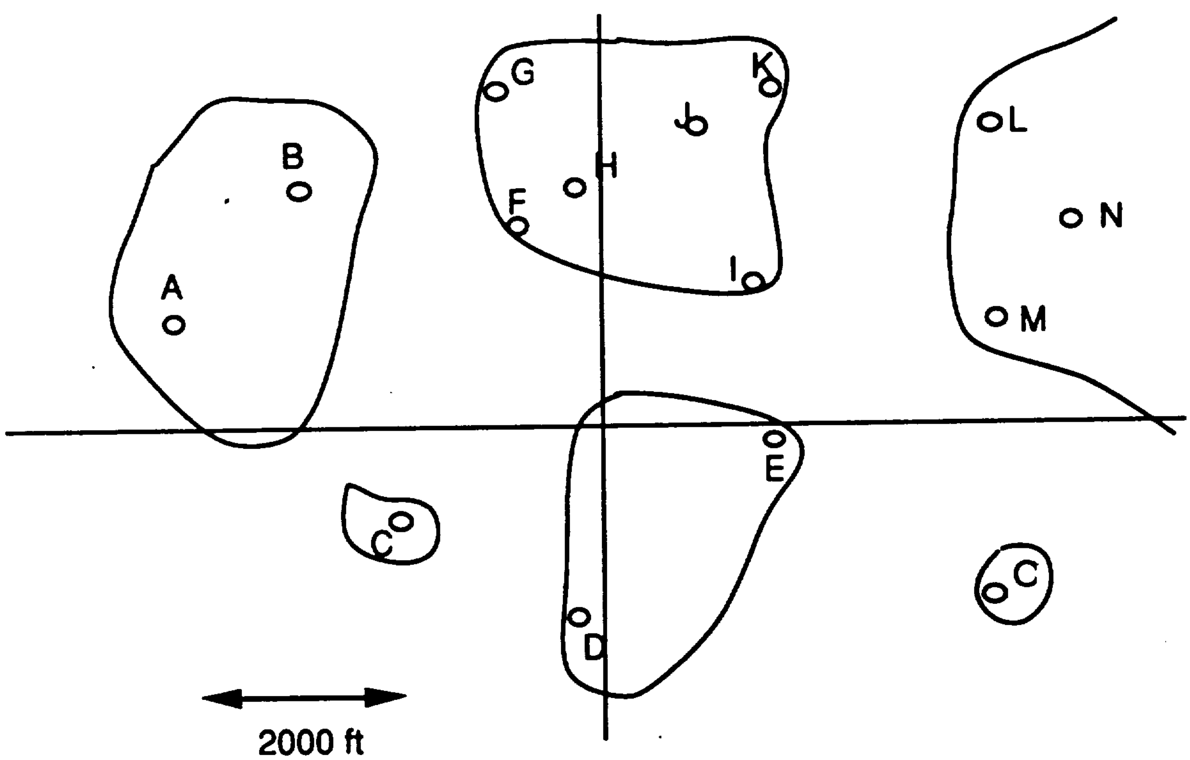

Figure 1. AeroWorld Geography

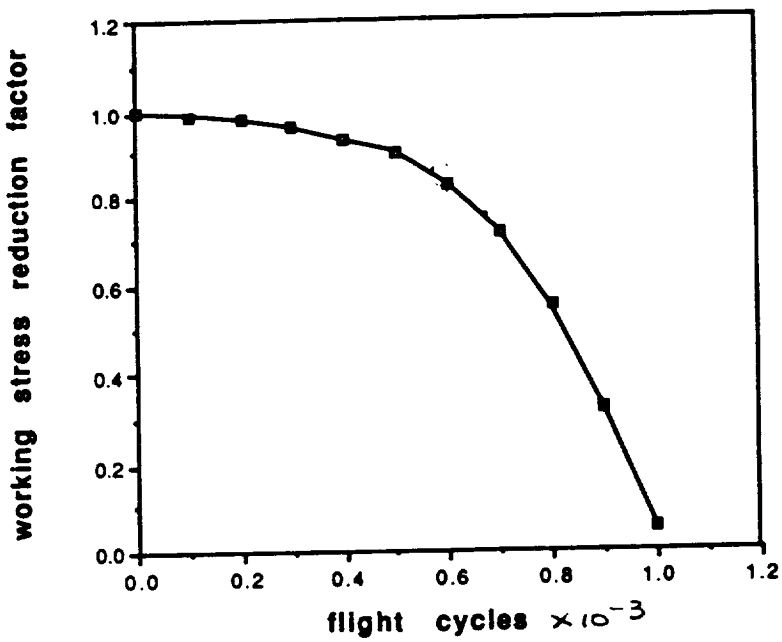

Figure 2. Working stress reduction factor for fatigue life calculation

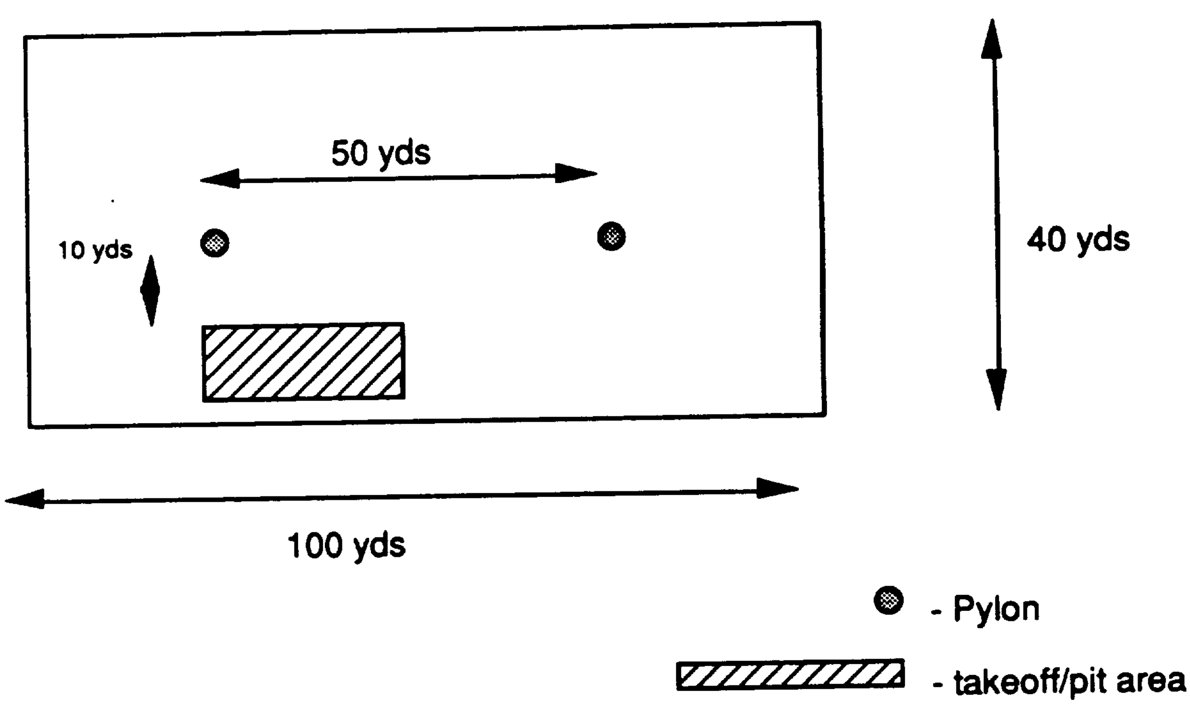

Figure 3: Prototype Flight Test Arena

Appendix B

Stability and Control Analysis

Appendix B

Stability and Control Analysis

B.1 PITCH STABILITY

We determined the stability characteristics of the Reliant aircraft by making up a spread sheet to determine the Cm-α curve. We first inputted the geometry of the configuration along with the necessary airfoil characteristics. These are as follows :

Notation is as follows:

Main variables	Subscript Variables
S=surface area	w=main wing
b=span	c=secondary wing
c=chord	t=tail
X=X-position	e=elevator
τ = flap effectiveness parameter	

wing	secondary wing	tail	elevator
Sw = 8.45 ft**2	Sc = 4.55 ft**2	St = 2.25 ft**2	Se = 1 ft**2
bw = 10 ft	bc = 7 ft	bt = 3 ft	be = 3 ft
cw = 0.845 ft	cc = .65 ft	ct = 0.75 ft	ce = 0.33 ft
Xw = 1.833 ft	Xc = 2.416 ft	Xt = 4.083 ft	Xe = 4.583 ft
lw = .075 ft	lc = -.5083 ft	lt = -2.175 ft	τ = 0.64
		η = 0.9	

airfoil (NACA 63-418)	flat plate
Cmo = -.06	Clo = 0
Clo = 0.35	Clα = 0.109654/rad
Clα = 0.10367/rad	
e = 0.8	

Both the main wing and the secondary wing are built airfoils and the tail is a flat plate. Assuming these values to be relatively set, there were five remaining variables : incidence angles of the wing, canard, and tail (iw,ic,it), CG location, and elevator deflection angle (∂e)

. The following equations from Ref. 6 were used to determine the $Cmcg_{total}$:

$$Clw = Clo_{airfoil} + Cl\alpha_{airfoil} \div (1+57.3*Cl\alpha_{airfoil} / (\pi*e*ARw)) * (\alpha+iw)$$

$$Cmcgw = (Clw * lw/cw + Cmo_{airfoil})* Sw / (Sw + Sc)$$

$$Clc = Clo_{airfoil} + Cl\alpha_{airfoil} \div (1+57.3*Cl\alpha_{airfoil} / (\pi*e*ARc)) * (\alpha+ic)$$

$$Cmcgc = (Clc*lc/cc+Cmo_{airfoil}*cc/cw) * Sc/(Sw+Sc)$$

$$\varepsilon = 2 * Clw / (\pi * ARw) * 57.3$$

$$Cl\alpha t = Clo_{flat\ plate} + Cl\alpha_{flat\ plate} \div (1+57.3*Cl\alpha_{flat\ plate} / (\pi*e*ARt))$$

$$Clt = Cl\alpha t * (\alpha - \varepsilon + it)$$

$$Cmcgt = Clt *lt/cw*St/(Sc+Sw)*\eta$$

$$Cmcge = -St *lt / (Sw+Sc) / cw * \eta * \tau * Cl\alpha t * \partial e$$

$$Cmcg_{total} = Cmcgw + Cmcgc + Cmcgt + Cmcge$$

The Cm - α curve was determined by plotting $Cmcg_{total}$ vs α. This curve must have a negative slope for the plane to be stable. By adjusting the incidence angles of the wing, canard, and tail, and using the elevator to ensure reasonable trim angles, stability was achieved for a range of CG locations.

B.2 ROLL AND YAW STABILITY

The vertical tail, rudder, and polyhedral were used to give the plane roll stability and control. The following values were assumed :

∂r = 15 degrees	vt height = 11"	tau = 0.72	$Cl\alpha$ = 0.0864
r width = 4.5"	vt length = 8"	Ix = 0.24 slug ft**2	e = 0.8
r length = 11"	ARvt = 1.375	Iz = 1.39 slug ft**2	V = 28 ft/s
Sr = 49.5 in**2	Sv = 88 in**2	β = 3 degrees	Cm_{rest} = .0035
	Xv = 23 "	ρ = 0.002377 slug/ft**3	

The variable values were the polyhedral angle, the length of wing to be deflected in the polyhedral, and the radius of turn. The time it takes to yaw three degrees was determined by first determining the force of the rudder when it is deflected 15 degrees, and then the yawing moment provided by the rudder. These values were determined using the following formulas obtained from Ref. 6 :

$$Cl_{rudder} = 2 * \pi / 57.3 / (1+2/ (e * ARvt)) * \tau * \partial r$$

$$Mcg_{rudder} = (Cl_{rudder} * Sv * Xv/12 - Cm_{rest} * \beta/2 * (Sc+Sw)*cw)* 0.5 * \rho * V**2$$

The yaw rate and time to yaw was determined from the following formulas from Ref. 6 :

$$\beta = Mcg_{rudder} / Iz$$
$$\text{time to yaw} = \text{sqrt}\ (2 * \beta / \beta)$$

The change in angle of attack and the resulting change in lift and roll due to yawing were determined by the formulas from Ref. 6:

$$\Delta\alpha = \beta * \Gamma$$
$$\Delta Cl = Cl\alpha * \Delta\alpha$$
$$\Delta L = \Delta Cl * 0.5 * \rho * V{**}2 * (5 - Xk)*2$$
$$\Delta Roll = \Delta L * ((5-Xk)/2+Xk)/2$$

where Xk is the distance from the CG to where the polyhedral begins. Next, the time to roll was determined by determining the roll rate and roll angle :

$$\phi = \Delta Roll / Ix$$
$$\phi = \arctan\ (V{**}2 / gR)$$
$$\text{time to roll} = \text{sqrt}\ (2 * \phi / \phi)$$

The total distance required to make a turn can then be determined by using the following formula :

$$Dtotal = V*(\text{time to yaw} + \text{time to roll}) + R$$

where R is the radius of turn. R is required by the mission to be at most 60 feet; we determined that for flying in Loftus, it would be most desirable to turn within a radius of 40 feet. We varied Γ, Xk and vertical tail and rudder size until we reached a configuration that allowed us to turn within a radius of 40 feet and within a total distance of 80 feet .This turn requires a banking angle of 30 degrees, which is reasonable.

Appendix C

Stress Reduction Factor / Life Span Tradeoff Study Procedure

The following is extracted from a tradeoff study performed by Mike Nosek to determine the optimum stress reduction factor for the main wing of the F-92 Reliant aircraft. It is included to show the procedure that was used in developing figure 9.0.1

Procedure:

Table C-1 is composed of 6 columns used to generate figures 1,2, and 3:

Column 1,2

To find optimum stress reduction factors of the spars, I swept the reduction factors over the range from .2 to .975, as displayed in Table C-1, column 1. The working stress reduction factor determines the lifetime of the structure, as determined from figure 4. Figure 4 is a reproduction of the fatigue life curve given in AE 441 course handout. This fatigue-life information is tabulated in column 2.

Column 3

Knowing the maximum bending moment at the root chord, and the allowable stresses in each material, the cross-sectional areas of the spars could be adjusted to increase or decrease the stress reduction factor at the base of each spar. This is where I used a nifty computer program that Dr. Batill made us write last semester in AE 446. (HS#9, problem 2.) (The program code is in the appendix.) For each stress reduction factor, the areas were minimized such that the maximum stress divided by the stress reduction factor did not exceed the allowable stress. In each case Spruce was used for spars 1,2, and 4; balsa was used for spar # 3. This was because the trailing-edge spar (#3), even at the minimum area of .0156 in^2 always remained well below the allowable stress. As such, the weaker Balsa was used to reduce weight. After minimizing area (hence weight) of each spar, the corresponding weight was then calculated knowing the density,ρ, and wing span,b.

Assumptions: Rectangular lift,drag distribution
Weight forces of wing negligible compared to aerodynamic forces
Pitch moment of wing negligible compare to bending moment
∴ Mohr's circle intersects origin and $\tau max=\sigma max/2$

Calculations: Mz|max root =(Clmax*Q*S*n|max)*(b/2)
My|max root= Mz root/ (L/D)|max

σ allowable = σlyield/ factor of safety

τ allowable=τlyield/f.s.=.5*σ allowable

$\therefore$ σ allowable = τlyield*2/factor of safety

Weight of spars = $\Sigma(\rho i*Ai)*b$

Column 4

Fuel cost per flight due to the wing was calculated as a function of weight. The lower the stress reduction factor, the higher the weight of the wing spars, the higher L/D, the more power (thus current draw) needed at Vcruise, the more fuel (mahr's) expended.

Assumptions: average flight = 2300 ft

Vcruise = 28 fps

time= 2300ft/28fps

volt∞=9V

Calculations:

Power = i∞Volt∞=D*v∞

=Q∞S*v∞*(Cdo+Cl^2/(πeAR))

=Const + W^2/(.5*ρ*v∞*S)/(πeAR)

=A + B

Const A will be unaffected by wing weight, so can be ignored for purpose of tradeoff study

i=B/Volt∞

Fuel=i*time

Fuel cost=f(weight) = i(weight)*time*$13/mahr

Column 5

Production cost per flight was calculated as follows:

Assume cost of ribs, monocot,etc = $22

cpv = cost/ volume of spar = $.30/in^3 (spruce)

=$.15/in^3 (balsa)

cost of spars = Σ(cpv*Ai)*b

man-hrs to build wing ~ 30 hrs
Production Cost=400*(cost of wing) + 1000*(# man hrs to build wing)
=400*($20+Σ(cpv*Ai)*b)+1000*(30)
Production cost per flight = Production cost / # flight cycles (column 2)

Column 6

Total cost per flight is merely sum of fuel costs and production costs

total cost per flight = fuel cost/flight + production cost/flight
column 6 = column 4 + column 5

Thus after minimizing the cross-sectional areas of the wing spars, the computer code could generate columns 3 through 6 in table C-1, and graph them as a function of stress reduction factor as in figure 9.0.1.for the purpose of selecting an optimal stress reduction factor.

TABLE C-1

1	2	3	4	5	6
Stress reduction factor	#flight cycles	weight of the 4 wing spars	fuel costs per flight	production costs per flight	total costs per flight
	(#)	(lbs)	($)	($)	($)
0.2	940	2.1	580.26	78.31	658.56
0.4	860	1.126	130.95	61.48	192.43
0.5	810	0.893	82.31	60.48	142.78
0.6	790	0.8926	59.12	59.14	118.26
0.7	700	0.659	44.91	64.42	109.33
0.8	620	0.601	37.31	71.17	108.48
0.825	600	0.5524	31.52	72.19	103.72
0.85	570	0.5427	30.42	75.71	106.13
0.875	535	0.5135	27.24	79.75	106.99
0.9	500	0.5135	27.24	85.33	112.58
0.95	300	0.4843	24.24	140.60	164.84
0.975	200	0.4746	23.27	210.10	233.37

Stress Reduction Factor vs. Costs Due to Fuselage Structure

Summary:
This section details the procedure used to determine the optimum SRF for the fuselage structure of the aircraft. The fuselage side panel was modelled in 2-dimensions and maximum loads (aerodynamic and cargo) were applied at a load factor of 3.2. Fuel cost per flight and production costs per flight were estimated. Results indicated that the optimum SRF was 0.85, corresponding to 570 flight cycles. However, SRF = 0.825 was selected in order to increase flight cycles as well as to be compatible with the wing SRF value.

Discussion:
With regard to a structural component, such as the fuselage in this case, the primary variables are as follows:

- Factor of Safety: the ratio of yield stress to stress in a material. Usually 1.1 - 1.5 in aircraft. The minimum factor of safety was set at 1.2 for our aircraft.

- Stress Reduction Factor: The loads an aircraft will experience are set. But the structural factor of safety under such loads is not. The longer a life span, the higher the original factor of safety must be in order to allow for more deterioration in the structure and still remain above the desired minimum factor of safety. Therefore, the SRF value is the percentage of stress bearing effectiveness of a material corresponding to a number of flight cycles.

- Dimensions of Structural Members: The base and height of each member in the structure may be varied to provide the desired moment of inertia, stress, and buckling characteristics.

- Material of Structural Members: The material of each member may be varied as well. Spruce and balsa are the two options considered in this design.

The stress reduction will be varied and in each case will correspond to a maximum factor of safety (FOS Maximum = FOS Minimum / SRF). Due to the fatigue rules in AeroWorld, the plane will only fly once at this max FOS, its first flight. With each additional flight cycle, the FOS will approach the minimum FOS. The fuselage must therefore be designed for the max FOS, and so in effect, a certain weight and volume of materials will correspond to each SRF.

The goal was to find a trend between the SRF and the life span costs incurred by the weight and volume of structural materials. The following figures of merit are determined:

- Weight of Structural Materials: A summation of the weight of each member in the structure.

- Production Costs Due to Structural Materials: Based on the formula
  $ Prod = 400*(cost of materials) + 1000*(construction man hours). Cost of materials was estimated by multiplying a cost per volume of each material by the

volume of that material used. CPV for spruce: \$0.30; for balsa: \$0.10. Construction time was estimated as 25 man hours.

- Production Costs Due to Structural Materials per Flight: The above value divided by the number of flight cycles allowed by the SRF.

- Fuel Costs per Flight Due to Structural Materials: The power required for cruise equals a current * voltage which also equals a drag * cruise speed: $P = I \cdot V_{olt} = D \cdot V_{cruise}$. Drag is a function of weight and only the component due to weight of the structure is considered. V_{olt} and V_{cruise} are constant. Therefore current is a function of weight. Current * Flight Time equal the fuel used where flight time is estimated by:

  $$= \text{avg range} / V_{cruise} / 3600 \text{ sph}$$
  $$= 2300 \text{ ft} / 28 \text{ fps} / 3600 \text{ sph}$$
  $$= 0.0228 \text{ hours}$$

  The current*flight time multiplied by an average expected fuel cost of \$ 13 / milliamp hour yield the fuel cost per average flight. This procedure was detailed above for the wing.

- Total Cost Per Flight Due to Structural Materials: is the sum of the above costs per flight.

The procedure of this trade off study was as follows:

[1] Select a SRF with corresponding # Flight Cycles.
[2] Optimize fuselage model for corresponding max FOS.
[3] Use weight and volume values from optimized structure to compute costs.
[4] Repeat [1 - 3] for desired range of SRF.
[5] Plot SRF vs. Total Costs Per Flight. Locate optimum point.

The results are presented in Table C-2 and plotted in Figure C-1. The total cost reaches a minimum at a SRF of 0.85. Examining Figure 2, SRF vs. # Flight Cycles, it may be seen that this corresponds to 570 flight cycles.

It should be noted that the curve has little slope in the area of the minimum, allowing for variance with little effect on total cost. This condition proved valuable in our case. As detailed above, SRF value for the wing was 0.825 which corresponds to 600 flight cycles. It will be advantageous to squeeze 30 more flight cycles out of the fuselage to get full life out of the wing. Also, 600 is the value which was specified in the DR&O. In actuality the strength will be greater due to the desire to make the components of a similar member cross section for reduced confusion (time) during purchasing and construction. The lower SRF serves to justify this.

FUSELAGE STRESS REDUCTION FACTOR VERSUS COSTS

STRESS REDUCTION FACTOR	# FLIGHT CYCLES	WEIGHT OF FUSELAGE SIDES (LBS)	FUSELAGE FUEL COST PER FLIGHT ($)	PRODUCTION COST PER FUSELAGE ($)	PRODUCTION COST PER FLIGHT ($)	TOTAL COST PER FLIGHT ($)
0.900	500	0.287	26.48	25787.75	51.58	78.06
0.875	535	0.299	28.68	25819.26	48.26	76.94
0.850	570	0.310	30.93	25842.89	45.34	76.27
0.825	600	0.324	33.68	25885.03	43.14	76.83
0.800	620	0.337	36.58	25926.97	41.82	78.40
0.750	670	0.380	46.48	26019.67	38.84	85.31
0.700	700	0.417	56.01	26152.93	37.36	93.37
0.650	710	0.450	65.18	26245.17	36.97	102.14
0.600	790	0.497	79.43	26379.81	33.39	112.82
0.550	800	0.580	108.28	26586.78	33.23	141.51
0.500	810	0.671	144.81	26866.56	33.17	177.98

TABLE C-2

Optimum Stress Reduction Factor: Fuselage Side Panels

Figure C-1

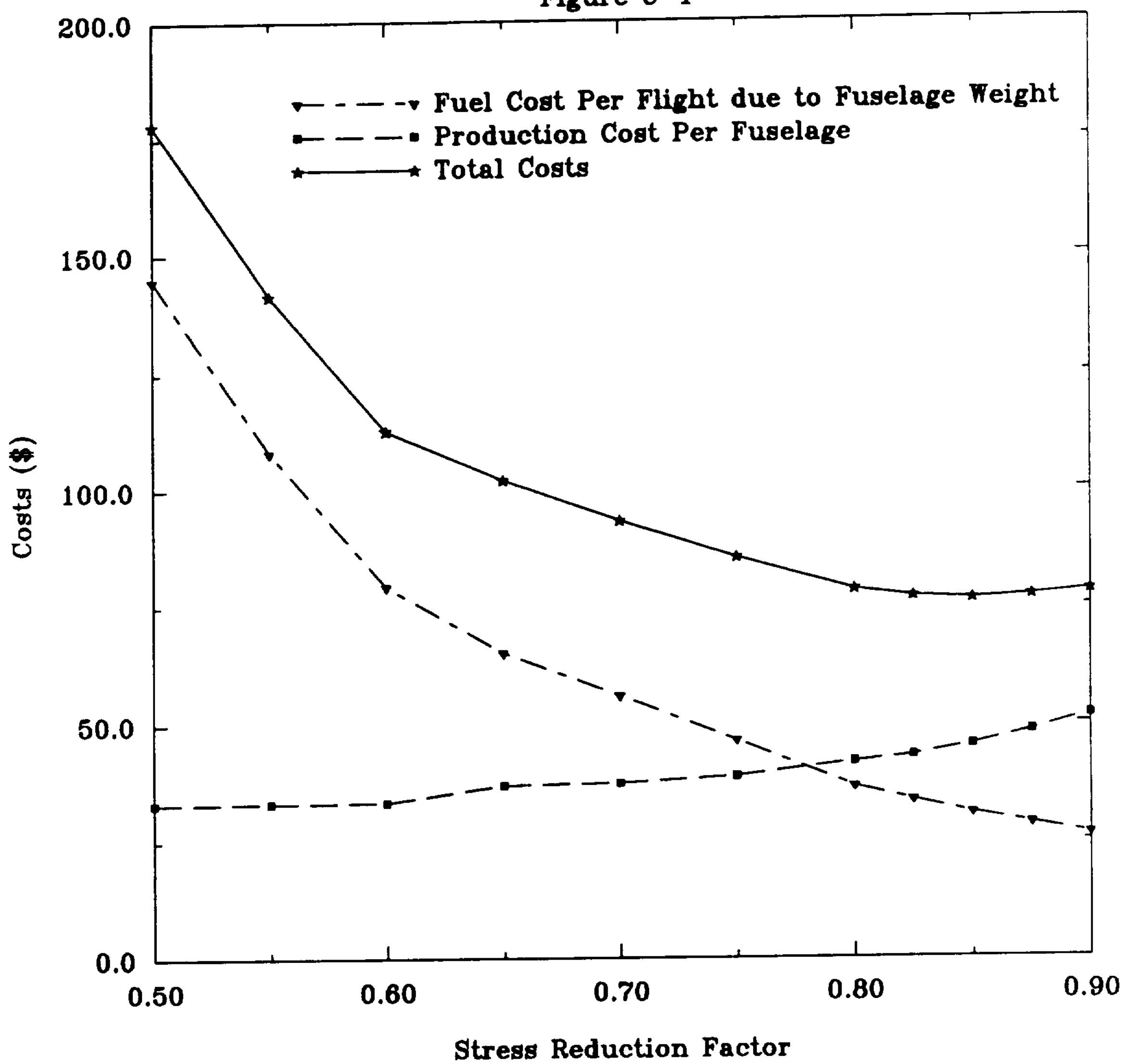

Appendix D

Spar Location Analysis Program

tradeprog.f

```
*       Program for bending
*       and buckling analysis of
*       wing modelled as compound beam

*       define variables

        real sigxx(6),sigalxx(6),a(6),dx(6),dy(6),rho(6),E(6),b(6),h(6),ixx(6) iy
(6),strfac(6),lbuck(6),buckfac(6),Pcr(6),sigyy(6)
        real ybar,xbar,Qx,Qy,AR,S,c,q,F,M,sparar,adx,ady,tipdef,sumeix,sumeiy, spa
rs,wribs,bb,lmin,Fd
        integer ribno

*       Open data output files


*       graphical output file
        open (12,file='stone')
*       tabular output file
        open (13,file='defone')
*       dimensional output file
        open (14,file='demone')
*       dimensional output file
        open (16,file='bucone')
*       dimensional output file
        open (17,file='bucyone')
*       dimensional output file
*


*       Enter number of spars (sparnum), wing AR, wing S,
*       and the predicted forces(F=lift, Fd=drag)
*       Forces should be entered and will be displayed in psi
*       Densities should be entered and will be displayed in lb/in^3
*


        sparnum=4.
        AR=10
        S=13
        F=12.3
        Fd=.5

*       Determination of span length (bb), chord (c),
*       and the root-chord bending moments

        bb=sqrt(AR*S)
        M=F*(bb/4.)
        Md=Fd*(bb/4.)
        c=(S/bb)


*       Initialize output files with proper column headings

        write (13,*) 'wingden lmin tipdef  ribno  E1,E2,E3,E4,E5,E6'
        write (12,*) 'wingden,strfac(1),strfac(2),strfac(3),strfac(4),strfac(5 ,st
rfac(6)'
        write (16,*) 'wingden,buckfac(1),buckfac(2),buckfac(3),buckfac(4),buck ac
5),buckfac(6)'
        write (14,*) 'b(1),h(1),b(2),h(2),b(3),h(3),b(4),h(4),b(5),h(5),b(6),h 5)'

*       Spar dimensions (b=base, h=height),
*       locations (dx=distance from x axis,dy=distance from y axis),
*       material properties (E=modulus of elasticity, rho=density,
*       sigalxx=maximum tensile/compressive stress)
*       are defined internal to a loop which
```

```
*        will increment the size of one spar throughout a given
*        range in eight steps
*

         do 75 mm=1,8,1
         lmin=100.
         zz=real(mm)/16.

*        #1 spar
         b(1)= .25 /12.
         h(1)=.125 /12.
         dx(1)=1.39 /12.
         dy(1)=0. /12.
         rho(1)=.016 *(12.**3)
         E(1)=1.3e6 *144.
         sigalxx(1)=6200. *144.

*        #2 spar
         b(2)=zz /12.
         h(2)=.25 /12.
         dx(2)=-.89 /12.
         dy(2)=0. /12.
         rho(2)=.016 *(12.**3)
         E(2)=1.3e6 *144.
         sigalxx(2)=6200. *144.
*
*        #3 spar
         b(3)=.125 /12
         h(3)=.125 /12
         dx(3)=0. /12
         dy(3)=-3.42 /12
         rho(3)=.0058 *(12.**3)
         E(3)=65000 *144.
         sigalxx(3)=400. *144.


*        #4 spar
         b(4)=.25 /12.
         h(4)=.187 /12.
         dx(4)=0. /12.
         dy(4)=10. /12.
         rho(4)=.0058 *(12.**3)
         E(4)=65000 *144.
         sigalxx(4)=400. *144.
*
*

*        Loop to determine centroid, spar volume and wight, and
*        to determine the first moments of inertia

         do 10 ii=1,sparnum
                 a(ii)=b(ii)*h(ii)
                 sparar=sparar+a(ii)
                 wspars=wspars+a(ii)*(rho(ii))*(bb/2.)
                 adx=a(ii)*abs(dx(ii)*c)
                 ady=a(ii)*abs(dy(ii)*c)
                 Qx=Qx+adx
                 Qy=Qy+ady
*        write (*,*) a(ii),sparar,wspars,adx,ady,Qx,Qy
 10      continue

         ybar=Qx/sparar
         xbar=Qy/sparar
.
```

```
*       Loop to determine the compound moment of inertia

        do 15 j=1,sparnum
                ixx(j)=(b(j)*h(j)*h(j)*h(j))/12. + a(j)*((dx(j))-ybar)**2.
                iyy(j)=(h(j)*(b(j)*b(j)*b(j)))/12. + a(j)*((dy(j))-xbar)**2.
                sumeix=E(j)*ixx(j) + sumeix
                sumeiy=E(j)*iyy(j) + sumeiy
*       write (*,*) ixx(j),iyy(j),sumeix,sumeiy
 15     continue

*       Loop to determine the individual member stresses, the stress
*       factor (stress/stress allowable), and the euler buckling length
*       to determine the maximum rib spacing

        do 20 jj=1,sparnum
                sigxx(jj)=(M*((dx(jj))-ybar)*E(jj))/sumeix
                sigyy(jj)=(Md*((dy(jj))-xbar)*E(jj))/sumeiy
                strfac(jj)=(sigxx(jj)+sigyy(jj))/sigalxx(jj)
                lbuck(jj)=sqrt(((3.14159265359**2)*E(jj)*ixx(jj))/(abs(sigalx  jj)
)*a(jj)))
                        if (lbuck(jj) .lt. lmin) then
                        lmin=lbuck(jj)
                else
                continue
                endif

  20    continue

*       determination of the euler buckling load and the
*       buckling factor (stress/critical buckling stress)

        do 25 l=1,sparnum
        Pcr(l)=((3.14159265359**2)*E(l)*ixx(l))/(lmin**2.*a(l))
        buckfac(l)=sigxx(l)/Pcr(l)

  25    continue

*       Final determination of wing tip deflection, minimum
*       number of ribs required, and an overall
*       wing weight and wing density (wing weight/wing planform)

        q=F/(bb/2)
        tipdef=(q*(bb/2.)**4.)/(8.*sumeix)
        if (lmin .lt. .833) then
                lmin=.83
        else
        continue
        endif
        ribno=(bb/2)/lmin
        wribs=ribno*(c*.065)*0.0625*(.0058*1728.)
        wtot=wribs+wspars+S*.0162
        wingden=2.*wtot/S
        write (*,*) lmin,wribs*16,ribno,wtot*16

*       Data output

        write (*,*) wingden*.111,strfac(1),strfac(2),strfac(3),strfac(4),strfa (5)
,strfac(6)
        write (16,*) wingden*.111,buckfac(1),buckfac(2),buckfac(3),buckfac(4),  ck
fac(5),buckfac(6)
        write (12,*) wingden*.111,strfac(1),strfac(2),strfac(3),strfac(4),stri  (5
),strfac(6)
        write (13,*) wingden*.111,lmin*12.,tipdef*12,ribno
        write (14,*) b(1)*12.,h(1)*12.,b(2)*12.,h(2)*12.,b(3)*12.,h(3)*12.,b(4  *12
```

```
.,h(4)*12.,b(5)*12.,h(5)*12.,b(6)*12.,h(6)*12.
   75      continue
           write (13,*) E(1)/144.,E(2)/144.,E(3)/144.,E(4)/144.,E(5)/144.,E(6)/1


           close (16)
           close (14)
           close (13)
           close (12)



           stop
           end
```

Appendix E

Fuselage Truss Analysis Program

And Data File

RMC-TRUSS.f

```
      PROGRAM MAIN
C
C     STATIC ANALYSIS OF A 3-D SPACE TRUSS
C     REF: MODIFICATION OF A PROGRAM DEVELOPED IN
C     FINITE ELEMENT STRUCTURAL ANALYSIS BY T.Y.YANG
C     DEVELOPED BY S.M. BATILL - 3/17/87
C     converted to MPW/LS fortran 8.27.90
C
C     MODIFIED BY RYAN M. COLLINS 22 MARCH 1992
C             TO CALC WEIGHT, BUCKLING, AND FOS
C
C     ND= DIMENSION OF MAIN ARRAYS, MAX NO OF NODES OR ELEMENTS
C     NELE = NUMBER OF AXIAL FORCE ELEMENTS
C     NNOD = TOTAL NUMBER OF NODES
C     ESTFT = ELEMENTAL STIFFNESS MATRIX IN GLOBAL SYSTEM
C     LAMX,LAMY,LAMZ = ELEMENT DIRECTION COSINES
C     XNOD,YNOD,ZNOD = COORDINATES OF NODES IN GLOBAL SYSTEM
C     FORC = APPLIED LOAD ARRAY
C     NODIS = NODAL DISPLACEMENT ARRAY
C     AREA =  ELEMENT CROSS SECTIONAL AREA ARRAY
C     EMOD = ELEMENT MODULUS ARRAY
C     SYTF = CONSTRAINED GLOBAL STIFFNESS MATRIX [K]
C     SLOD = LOAD VECTOR {F}
C     SOLU = STIFFNESS FORMULATION SOLUTION VECTOR {X}
C     IBOU = BOUNDARY CONDITIONS ARRAY
C     NODN = ELEMENT NODAL CONNECTIVITY DATA ARRAY
C     ICOR = DEGREE OF FREEDOM TABLE
C     FILENM = FILE NAME FOR INPUT DATA FILE
C     IPR1 = PRINT OPTION - ELEMENTAL STIFFNESS MATRICIES
C     IPR2 = PRINT OPTION - GLOBAL STIFFNESS MATRIX
C     SRF = STRESS REDUCTION FACTOR
C
C     ALL INPUT IS INCLUDED IN USER GENERATED DATA FILE
C

      PARAMETER (ND=100)
      real*8 ESTFT(6,6),LAMX,LAMY,LAMZ, LN(ND), WD(ND), DENS(ND),
     $ XNOD(ND),YNOD(ND),ZNOD(ND),FORC(ND,3),NODIS(ND,3),
     $ AREA(ND),EMOD(ND),SYTF(ND,ND),SLOD(ND),SOLU(ND),
     $ MOI(ND), WGT(ND), SMAX(ND)
      DIMENSION IBOU(ND,3),NODN(ND,2),ICOR(ND,6)
      CHARACTER *15 , TITLE,FILENM
      IRD=2
      IWR=6
      IPT=9
      IKY=5
C
C     DATA INPUT SECTION
C
2000  FORMAT(/)
2001  FORMAT("1")
      write(iwr,*)'    3-d space truss program'
      write(iwr,*)'    developed at the university of notre dame'
      write(iwr,*)'    by prof. s. batill, aerospace and mechanical enginee: ng'
      write(iwr,*)'    last modified 11.21.90'
      write(iwr,*)'    '
      write(iwr,*)'     based upon a code presented in FINITE ELEMENT STRUC: RA
'
      write(iwr,*)'     ANALYSIS by T.Y.Yang - Prentice-Hall publisher'
      write(iwr,*)'    '
      write(iwr,*)'    MODIFIED BY RYAN M. COLLINS 24 MARCH 1992'
      write(iwr,*)'         TO CALCULATE WEIGHT, BUCKLING, AND FOS'
      write(iwr,*)'   '
      write(iwr,*)'    fem model input from data file'
```

```
      write(iwr,*)'    '
      write(iwr,*)'    compiled using Language Systems Fortran'
      write(iwr,*)'    '
      WRITE(IWR,1000)
 1000 FORMAT(" INPUT DATA FILE NAME",/)
C     FILENM = 'test.dat'
      READ(IKY,*) FILENM
      WRITE(IWR,1001) FILENM
      WRITE(IPT,1001) FILENM
      WRITE(IPT,2000)
 1001 FORMAT(/," DATA INPUT FILE - ",A10,/)
      OPEN(UNIT=2,FILE=FILENM,STATUS='OLD')
      READ(IRD,*) TITLE
      READ(IRD,*) NNOD,NELE,IPR1,IPR2, SRF
      WRITE(IWR,22) NNOD,NELE
      WRITE(IPT,22) NNOD,NELE
      WRITE(IPT,2000)
 22   FORMAT(5X,"NUMBER OF NODES = ",I5,
     $ /,5X,"NUMBER OF ELEMENTS = ",I5)
      IF(IPR1.EQ.1) WRITE(IWR,31)
 31   FORMAT(//,10X," ELEMENT STIFFNESS MATRIX WILL BE PRINTED",/)
      IF(IPR2.EQ.1) WRITE(IWR,32)
 32   FORMAT(//,10X," GLOBAL STIFFNESS MATRIX WILL BE PRINTED",/)
C
C     NODAL DATA INPUT FROM DATA FILE
C
      WRITE(IPT,2000)
      WRITE(IPT,92)
 92   FORMAT("  BOUNDARY CONDITIONS AND NODAL COORDINATES",/)
      DO 50 I=1,NNOD
      READ(IRD,*)N,(IBOU(I,J),J=1,3),XNOD(I),YNOD(I),ZNOD(I),
     $       (FORC(I,J),J=1,3)

C     WRITE(IWR,42)N,(IBOU(I,J),J=1,3),XNOD(I),YNOD(I),ZNOD(I)
      WRITE(IPT,42)N,(IBOU(I,J),J=1,3),XNOD(I),YNOD(I),ZNOD(I)
 50   CONTINUE
 42   FORMAT(1X,4I5,3E16.5)
      WRITE(IPT,91)
 91   FORMAT(/,"  APPLIED LOAD DATA - NODE ,FX, FY, FZ",/)
      DO 51 I=1,NNOD
C     WRITE(IWR,43)I,(FORC(I,J),J=1,3)
      WRITE(IPT,43)I,(FORC(I,J),J=1,3)
 51   CONTINUE
 43   FORMAT(5X,I5,3E20.4)
C
C     ELEMENT DATA INPUT FROM DATA FILE
C
      WRITE(IPT,2000)
      DO 60 I=1,NELE
      READ(IRD,*)N,NODN(I,1),NODN(I,2),LN(I),WD(I),NTYP
      AREA(I) = LN(I)*WD(I)
C     type 1 = balsa;  type 2 = spruce;  type 3 = plywood
      DENS(I) = 0.0058
      EMOD(I) = 65000.0
      SMAX(I) = 400.0
      IF(NTYP .EQ. 2) THEN
      DENS(I) = .0231
      EMOD(I) = 1.3E6
      SMAX(I) = 6000.0
      ELSEIF(NTYP .EQ. 3) THEN
      DENS(I) = 0.016
C     DENS(I) = 0.001
      EMOD(I) = 2.01E6
      SMAX(I) = 2500.0
```

```
            ENDIF
            MOI(I) = 1./12.*WD(I)*LN(I)**3.
            TMOI = 1./12.*LN(I)*WD(I)**3.
            IF(TMOI .LT. MOI(I)) THEN
            MOI(I) = TMOI
            ENDIF
C           WRITE(IWR,53)N,NODN(I,1),NODN(I,2),LN(I),WD(I),AREA(I),EMOD(I)
            WRITE(IPT,53)N,NODN(I,1),NODN(I,2),AREA(I),EMOD(I)
60          CONTINUE
53          FORMAT(/,I5,4X,2I5,4E14.4)
C
C           GENERATION OF INFORMATION FOR ASSEMBLING GLOBAL STIFFNESS
C
            ICON=0
            DO 20 I=1,NNOD
            DO 20 J=1,3
            K=IBOU(I,J)
            IF (K.EQ.0) GOTO 20
            ICON=ICON+1
            IBOU(I,J)=ICON
20          CONTINUE
            NDOF=ICON
54          FORMAT(/5X," NUMBER OF FREE DEGREES OF FREEDOM",I5)
            WRITE(IWR,54)NDOF
            WRITE(IPT,54)NDOF
            DO 30 I=1,NELE
            I1=NODN(I,1)
            I2=NODN(I,2)
            DO 30 J=1,3
            ICOR(I,J)=IBOU(I1,J)
            ICOR(I,J+3)=IBOU(I2,J)
30          CONTINUE
            IF(IPR1.EQ.0) GOTO 75
            WRITE(IPT,2000)
            WRITE(IWR,61)
            WRITE(IPT,61)
61          FORMAT(/5X,"ELEMENT",5X,"NODAL DEGREES OF FREEDOM")
            WRITE(IWR,63)
            WRITE(IPT,63)
63          FORMAT(5X,"NUMBER     1     2     3     4     5     6")
            DO 70 I=1,NELE
            WRITE(IWR,62)I,(ICOR(I,J),J=1,6)
            WRITE(IPT,62)I,(ICOR(I,J),J=1,6)
70          CONTINUE
62          FORMAT(/6X,7I5)
75          CONTINUE
C
C           INITIALIZING GLOBAL STIFFNES MATRIX
C
            DO 80 I=1,NDOF
            DO 80, J=1,NDOF
80          SYTF(I,J)=0.
C
C           DEVELOP  ELEMENTAL STIFFNESS MATRIX IN GLOBAL SYSTEM
C
            IF(IPR1.EQ.1) WRITE (IPT,2001)
            DO 400 IE=1,NELE
C
            I1=NODN(IE,1)
            I2=NODN(IE,2)
            X1=XNOD(I1)
            X2=XNOD(I2)
            Y1=YNOD(I1)
            Y2=YNOD(I2)
```

```
      Z1=ZNOD(I1)
      Z2=ZNOD(I2)
C
C     DEVELOP DIRECTION COSINES
C
      ELEL=SQRT((X2-X1)**2+(Y2-Y1)**2+(Z2-Z1)**2)
      LAMX=(X2-X1)/ELEL
      LAMY=(Y2-Y1)/ELEL
      LAMZ=(Z2-Z1)/ELEL
      AA=AREA(IE)
      AE=EMOD(IE)
C
C     THE FOLLOWING CALL DEVELOPS THE STIFFNESS MATRIX
C
      CALL ELESTF(ELEL,AA,AE,LAMX,LAMY,LAMZ,ESTFT)
C
      IF(IPR1.EQ.1)WRITE(IWR,103) IE,((ESTFT(I,J),J=1,6),
     $ I=1,6)
      IF(IPR1.EQ.1)WRITE(IPT,103) IE,((ESTFT(I,J),J=1,6),
     $ I=1,6)

103   FORMAT(/5X,"TRANSFORMED STIFFNESS MATRIX OF ELEMENT "
     $ , I5,/6(/1X,6E13.4))

C
C     ADD ELEMENT TO CONSTRAINED GLOBAL STIFFNESS MATRIX
C
      DO 200 I=1,6
      DO 200 J=1,6
      K=ICOR(IE,I)
      L=ICOR(IE,J)
      IF(K*L.EQ.0) GOTO 200
      SYTF(K,L)=SYTF(K,L)+ESTFT(I,J)
200   CONTINUE
400   CONTINUE
      IF(IPR2.EQ.0)GOTO 230
210   CONTINUE
      WRITE(IWR,201)
201   FORMAT(/5X,"GLOBAL STIFFNESS MATRIX")
      DO 220 I=1,NDOF
      WRITE(IWR,202) I
      WRITE(IPT,202) I
202   FORMAT(/5X,I5," - ROW NUMBER")
      WRITE(IWR,203) (SYTF(I,J),J=1,NDOF)
      WRITE(IPT,203) (SYTF(I,J),J=1,NDOF)
203   FORMAT(1X,6E10.3)
220   CONTINUE
230   CONTINUE
C
C     ASSEMBLING THE LOAD VECTOR
C
      DO 500 I=1,NNOD
      DO 500 J=1,3
      K=IBOU(I,J)
      IF(K.EQ.0) GOTO 500
      SLOD(K)=FORC(I,J)
500   CONTINUE
      IF(IPR2.EQ.1) WRITE(IWR,501)
      IF(IPR2.EQ.1) WRITE(IPT,501)
501   FORMAT(/5X,"ASSEMBLED LOAD VECTOR")
      IF(IPR2.EQ.1)WRITE(IWR,502) (SLOD(I),I=1,NDOF)
      IF(IPR2.EQ.1)WRITE(IPT,502) (SLOD(I),I=1,NDOF)
502   FORMAT(/5X,E12.4)
C
```

```
C           SOLUTION FOR GLOBAL DISPLACEMENTS
C
            CALL SIMEQ(SYTF,SOLU,SLOD,NDOF,ND)
            IF(NDOF.GT.1000) WRITE(IWR,507)
  507       FORMAT(" THE MATRIX IS SINGULAR - STOP")
            IF(NDOF.GT.1000) GOTO 999
C
C           SORT THE SOLUTION FOR NODAL DISPLACEMENTS
C
            WRITE(IPT,2001)
            WRITE(IPT,2000)
            WRITE(IWR,506)
            WRITE(IPT,506)
  506       FORMAT(/,5X,"NODAL DISPLACEMENTS")
            WRITE (IWR,503)
            WRITE (IPT,503)
  503       FORMAT(6X,"NODE",15X,"DISPLACEMENTS")
            WRITE(IWR,504)
            WRITE(IPT,504)
  504       FORMAT(8X,"NO",11X,"U",13X,"V",15X,"W")
            DO 700 I=1,NNOD
            DO 600 J=1,3
            NODIS(I,J)=0.
            K=IBOU(I,J)
            IF(K.EQ.0) GOTO 600
            NODIS(I,J)=SOLU(K)
  600       CONTINUE
            WRITE(IWR,601) I,(NODIS(I,L),L=1,3)
            WRITE(IPT,601) I,(NODIS(I,L),L=1,3)
  601       FORMAT(/,5X,I5,3F15.8)
  700       CONTINUE
C
C         . COMPUTATION OF ELEMENTAL FORCES AND STRESSES
C
            WRITE(IPT,2000)
            WRITE(IWR,804)
            WRITE(IPT,804)
  804       FORMAT(/1X,"ELEMENT FORCES AND AXIAL STRESS(LOCAL COORD.)")
            WRITE(IWR,801)
            WRITE(IPT,801)
  801       FORMAT(/1X,"ELEMENT",2X,"INTERNAL FORCE",2X,"BUCKLING",
          $ 4X,"AXIAL STRESS",6X,"YIELD",5X,"WEIGHT",4X,"FOS",/1X)

            VOL = 0.0
            TVOL1 = 0.0
            TVOL2 = 0.0
            TVOL3 = 0.0
            FOSM = 999.0
            NVIOL = 0

            DO 900 IE=1,NELE
            I1=NODN(IE,1)
            I2=NODN(IE,2)
            X1=XNOD(I1)
            X2=XNOD(I2)
            Y1=YNOD(I1)
            Y2=YNOD(I2)
            Z1=ZNOD(I1)
            Z2=ZNOD(I2)
C
C           RECOMPUTE DIRECTION COSINES
C
            ELEL=SQRT((X2-X1)**2+(Y2-Y1)**2+(Z2-Z1)**2)
            LAMX=(X2-X1)/ELEL
```

```
      LAMY=(Y2-Y1)/ELEL
      LAMZ=(Z2-Z1)/ELEL
      AA=AREA(IE)
      AE=EMOD(IE)
      DU=NODIS(I2,1)-NODIS(I1,1)
      DV=NODIS(I2,2)-NODIS(I1,2)
      DZ=NODIS(I2,3)-NODIS(I1,3)
C
C     COMPUTE INTERNAL AXIAL FORCE AND DIRECT STRESS
C
      ELEFOR=(AE*AA/ELEL)*(LAMX*DU+LAMY*DV+LAMZ*DZ)
      ELESTR=ELEFOR/AA

      VOL = ELEL*AREA(IE)
      WGT(IE) = VOL*DENS(IE)
      IF(EMOD(IE) .EQ. 65000.) TVOL1 = TVOL1 + VOL
      IF(EMOD(IE) .EQ. 1.3E6) TVOL2 = TVOL2 + VOL
      IF(EMOD(IE) .EQ. 2.01E6) TVOL3 = TVOL3 + VOL

      PCR = 9.8696*EMOD(IE)*MOI(IE)/ELEL/ELEL
      IF(ELEFOR .LT. 0.0) PCRTST = ABS(ELEFOR)

C     write(iwr,*) ie, pcr, pcrtst, elefor, abs(elefor)

      IF(PCRTST .GT. PCR) THEN
      WRITE(IWR,*) ' MEMBER ',IE,' BUCKLES!!!'
      NVIOL = NVIOL + 1
      ENDIF
      PCRTST = 0.0

      IF(ABS(ELESTR) .GT. SMAX(IE)) THEN
      NVIOL = NVIOL + 1
      WRITE(IWR,*) ' MEMBER ',IE,' EXCEEDS YIELD STRESS!!!'
      ENDIF

      FOS = SMAX(IE)/ABS(ELESTR)
      IF(FOS .LT. FOSM) THEN
      FOSM = FOS
      MFOSM = IE
      ENDIF
      IF(FOS .LT. (1.2/SRF)) THEN
      NVIOL = NVIOL + 1
      WRITE(IWR,*) ' MEMBER ',IE,' FOS VIOLATION!!!'
      ENDIF

      WRITE(IWR,803)IE,ELEFOR,PCR,ELESTR,SMAX(IE),WGT(IE), FOS
C     write(iwr,*) ie, elel
      WRITE(IPT,803)IE,ELEFOR,ELESTR
 803  FORMAT(1X,I5, 4F14.3,2F10.3, /)

      TWGT = TWGT + WGT(IE)

 900  CONTINUE
      WRITE(IWR,*) ' TOTAL WEIGHT = ',TWGT, '   POUNDS'
      WRITE(IWR,*) ' TOTAL WEIGHT = ',TWGT*16., '   OUNCES'
      WRITE(IWR,*) ' TOTAL VOLUME TYPE 1 = ', TVOL1, '   IN^3'
      WRITE(IWR,*) ' TOTAL VOLUME TYPE 2 = ', TVOL2, '   IN^3'
      WRITE(IWR,*) ' TOTAL VOLUME TYPE 3 = ', TVOL3, '   IN^3'
      WRITE(IWR,*) ' MIN FACTOR OF SAFETY ALLOWED = ',1.2/SRF
      WRITE(IWR,*) ' MIN FACTOR OF SAFETY = ', FOSM,'    IN MEMBER:',MFOSM
      IF(NVIOL .GT. 0) THEN
      WRITE(IWR,*) NVIOL, ' VIOLATIONS !!!'
      ENDIF
```

```
  999 CONTINUE
      STOP
      END
C
C
      SUBROUTINE ELESTF(ELEL,AA,AE,LAMX,LAMY,LAMZ,ESTFT)
      REAL*8 ESTFT(6,6),TRAN(2,6),LAMX,LAMY,LAMZ,K(2,2),D(2,6)
C
C     UNIFORM 3-D TRUSS ELEMENT STIFFNESS MATRIX
C     AA = AREA
C     ELEL = ELEMENT LENGTH
C     AE=MODULUS
C     LAMX,LAMY,LAMZ ARE THE DIRECTION COSINES OF THE ELEMENT
C     K = ELEMENTAL STIFFNESS MATRIX IN LOCAL COORDINATES
C     TRAN = LOCAL TO GLOBAL TRANSFORMATION MATRIX
C
C
C     ELEMENTAL STIFFNESS MATRIX IN LOCAL COORDINATES
C
      K(1,1)=AA*AE/ELEL
      K(2,1)=-K(1,1)
      K(1,2)=K(2,1)
      K(2,2)=K(1,1)
C
C     TRANSFORMATION MATRIX TO GLOBAL COORDINATES
C
      DO 20 I=1,2
      DO 20 J=1,6
   20 TRAN(I,J)=0.
      TRAN(1,1)=LAMX
      TRAN(1,2)=LAMY
      TRAN(1,3)=LAMZ
      TRAN(2,4)=LAMX
      TRAN(2,5)=LAMY
      TRAN(2,6)=LAMZ
C
C     PERFORM MATRIX MULTIPLICATION (TRAN)TRANSPOSE*K*TRAN
C
      DO 30 I=1,2
      DO 30 J=1,6
      D(I,J)=0.
      DO 30 L=1,2
   30 D(I,J)=D(I,J)+K(I,L)*TRAN(L,J)
      DO 40 I=1,6
      DO 40 J=1,6
      ESTFT(I,J)=0.
      DO 40 L=1,2
   40 ESTFT(I,J)=ESTFT(I,J)+TRAN(L,I)*D(L,J)
      RETURN
      END
C
C
      SUBROUTINE SIMEQ(A,X,F,N,NDIM)
C
C     SIMULTANEOUS EQUATION SOLVER FOR
C          [A] {X} = {F}
C
C     GAUSS ELIMINATION WITH PARTIAL PIVOTING
C
C     A = MATRIX OF COEFFICIENTS
C     X = UNKNOWNS - SOLUTION VEXTOR
C     F = RHS VECTOR
C     NDIM = DIMENSION OF A,X AND F
C     N = NUMBER OF EQUATIONS TO BE SOLVED
```

```
C
      REAL*8 A(NDIM,NDIM),X(NDIM),F(NDIM)
      DO 7 L=2,N
100   FORMAT(1X,I5)
      LM1=L-1
      AMAX=ABS(A(LM1,LM1))
      JMAX=LM1
      DO 2 J=L,N
      ATEMP=ABS(A(J,LM1))
      IF(ATEMP.LE.AMAX) GOTO 2
      AMAX=ATEMP
      JMAX=J
2     CONTINUE
      IF(AMAX.LE.1.E-6) GOTO 10
      IF(JMAX.EQ.LM1) GOTO 4
      ATEM=F(LM1)
      F(LM1)=F(JMAX)
      F(JMAX)=ATEM
      DO 3 K=LM1,N
      ATEM=A(LM1,K)
      A(LM1,K)=A(JMAX,K)
3     A(JMAX,K)=ATEM
4     CONTINUE
      DO 6 J=L,N
      Q=A(J,LM1)/A(LM1,LM1)
      DO 5 K=L,N
5     A(J,K)=A(J,K)-Q*A(LM1,K)
6     F(J)=F(J)-Q*F(LM1)
7     CONTINUE
      X(N)=F(N)/A(N,N)
      DO 9 M=2,N
      J=N-M+1
      JP1=J+1
      S=0.0
      DO 8 K=JP1,N
8     S=S+A(J,K)*X(K)
9     X(J)=(F(J)-S)/A(J,J)
      GOTO 11
10    N=9999
11    CONTINUE
      RETURN
      END
```

FUSE.dat

```
FUSELAGE: SIDE PANEL : N = 4 : Clmax : Vel = 50 fps: SRF = 0.825 : Pos Tail L

42      94      0      0      0.825

1    0    0    0    7.     0.0    0.0       0.      0.    -.36
2    1    0    1    7.     0.0    4.125     0.      0.    -.28
3    1    0    1    7.     0.0    5.25      0.      0.    0.

4    1    0    1    10.    0.0    0.0       0.      0.    -.72
5    1    0    1    10.    0.0    4.125     0.      0.    -.28
6    1    0    1    10.    0.0    5.25      0.      0.    0.

7    1    0    1    13.    0.0    0.0       0.      0.    -.72
8    1    0    1    13.    0.0    4.125     0.      0.    0.
9    1    0    1    13.    0.0    5.25      0.      0.    0.

10   1    0    1    16.    0.0    0.0       0.      0.    -.72
11   1    0    1    16.    0.0    4.125     0.      0.    0.
12   1    0    1    16.    0.0    5.25      0.      0.    0.

13   1    0    0    40.    0.0    0.0       0.      0.    -.36
14   1    0    1    40.    0.0    4.125     0.      0.    0.
15   1    0    1    40.    0.0    5.25      0.      0.    0.

16   1    0    1    44.    0.0    4.125     0.      0.    0.
17   1    0    1    44.    0.0    5.25      0.      0.    0.

18   1    0    1    47.    0.0    4.125     0.      0.    0.
19   1    0    1    47.    0.0    5.25      0.      0.    0.

20   1    0    1    19.    0.0    0.0       0.      0.    -.72
21   1    0    1    19.    0.0    4.125     0.      0.    0.
22   1    0    1    19.    0.0    5.25      0.      0.    0.

23   1    0    1    22.    0.0    0.0       0.      0.    -.72
24   1    0    1    22.    0.0    4.125     0.      0.    0.
25   1    0    1    22.    0.0    5.25      .1465   0.    4.52

26   1    0    1    25.    0.0    0.0       0.      0.    -.72
27   1    0    1    25.    0.0    4.125     0.      0.    0.
28   1    0    1    25.    0.0    5.25      .1465   0.    4.52

29   1    0    1    28.    0.0    0.0       .1352   0.    1.48
30   1    0    1    28.    0.0    4.125     0.      0.    0.
31   1    0    1    28.    0.0    5.25      .1465   0.    4.52

32   1    0    1    31.    0.0    0.0       .1352   0.    1.48
33   1    0    1    31.    0.0    4.125     0.      0.    0.
34   1    0    1    31.    0.0    5.25      0.      0.    2.45

35   1    0    1    34.    0.0    0.0       0.      0.    -.72
36   1    0    1    34.    0.0    4.125     0.      0.    -.46
37   1    0    1    34.    0.0    5.25      0.      0.    0.

38   1    0    1    37.    0.0    0.0       0.      0.    -.72
39   1    0    1    37.    0.0    4.125     0.      0.    -.46
40   1    0    1    37.    0.0    5.25      0.      0.    0.

41   1    0    1    50.    0.0    4.125     .0585   0.    1.56
42   1    0    1    50.    0.0    5.25      .0585   0.    1.56
```

FUSE.dat

```
1    1    2    .1875   .1875   2
2    2    3    .1875   .1875   2
3    3    6    .125    .1875   2
4    2    5    .125    .1875   1
5    1    4    .125    .1875   2

6    4    5    .125    .1875   2
7    5    6    .125    .1875   2
8    6    9    .125    .1875   2
9    5    8    .125    .1875   1
10   4    7    .125    .1875   2

11   7    8    .125    .1875   2
12   8    9    .125    .1875   2
13   9    12   .125    .1875   2
14   8    11   .125    .1875   1
15   7    10   .125    .1875   2

16   10   11   .125    .1875   2
17   11   12   .125    .1875   2
18   12   22   .125    .1875   2
19   11   21   .125    .1875   1
20   10   20   .125    .1875   2

21   20   21   .125    .1875   2
22   21   22   .125    .1875   2
23   22   25   .125    .1875   2
24   21   24   .125    .1875   1
25   20   23   .125    .1875   2

26   23   24   .125    .1875   2
27   24   25   .125    .1875   2
28   25   28   .125    .1875   2
29   24   27   .125    .1875   1
30   23   26   .125    .1875   2

31   26   27   .125    .1875   2
32   27   28   .125    .1875   2
33   28   31   .125    .1875   2
34   27   30   .125    .1875   1
35   26   29   .125    .1875   2

36   29   30   .125    .1875   2
37   30   31   .125    .1875   2
38   31   34   .125    .1875   2
39   30   33   .125    .1875   1
40   29   32   .125    .1875   2

41   32   33   .125    .1875   2
42   33   34   .125    .1875   2
43   34   37   .125    .1875   2
44   33   36   .125    .1875   1
45   32   35   .125    .1875   2

46   35   36   .125    .1875   2
47   36   37   .125    .1875   2
48   37   40   .125    .1875   2
49   36   39   .125    .1875   1
50   35   38   .125    .1875   2

51   38   39   .125    .1875   2
52   39   40   .125    .1875   2
53   40   15   .125    .1875   2
```

FUSE.dat

54	39	14	.125	.1875	1
55	38	13	.125	.1875	2
56	13	14	.1875	.1875	2
57	14	15	.1875	.1875	2
58	15	17	.125	.1875	2
59	14	16	.125	.1875	1
60	13	16	.1875	.1875	1
61	13	18	.1875	.1875	2
62	16	17	.125	.1875	2
63	17	19	.125	.1875	2
64	16	18	.125	.1875	1
65	18	19	.125	.1875	2
66	3	5	.125	.1875	2
67	2	4	.125	.1875	2
68	6	8	.125	.1875	2
69	5	7	.125	.1875	2
70	9	11	.125	.1875	2
71	8	10	.125	.1875	2
72	12	21	.125	.1875	2
73	11	20	.125	.1875	2
74	22	24	.125	.1875	2
75	21	23	.125	.1875	2
76	25	27	.125	.1875	2
77	24	26	.125	.1875	2
78	28	30	.125	.1875	2
79	27	29	.125	.1875	2
80	31	33	.125	.1875	2
81	30	32	.125	.1875	2
82	34	36	.125	.1875	2
83	33	35	.125	.1875	2
84	37	39	.125	.1875	2
85	35	39	.125	.1875	2
86	40	14	.125	.1875	2
87	38	14	.125	.1875	2
88	14	17	.125	.1875	2
89	16	19	.125	.1875	2
90	19	42	.125	.1875	2
91	18	41	.125	.1875	1
92	41	42	.125	.1875	1
93	13	41	.1875	.1875	2
94	18	42	.125	.1875	2

Appendix F

Catapult Analysis

Appendix F

Catapult Analysis

The geometry, aerodynamic characteristics, and some stability characteristics of the F-92 Reliant were used to predict how the aircraft would behave if catapulted from a height of 50 feet. This information can be used to predict the behavior of the plane if catapulted from the ground, and later, a catapult test from the ground will be performed on the aircraft. It was determined from the catapult program that an elevator deflection of 10^{o} up is necessary in order to maximize distance flown and to ensure that the plane flies when catapulted. The predicted behavior of the plane is shown in the following graphs of velocity vs. time and y distance vs. x distance for the catapult flight trajectory. It is clear from these graphs that the plane does have some damping characteristics, but at the same time, it is obvious that the damping is not very great. 35 seconds and over 900 feet downrange from the launch, the oscillations continue. These oscillations are both in position and in velocity. An input data file is also included behind the graphs. The accuracy of the catapult program will be determined when the catapult tests occur.

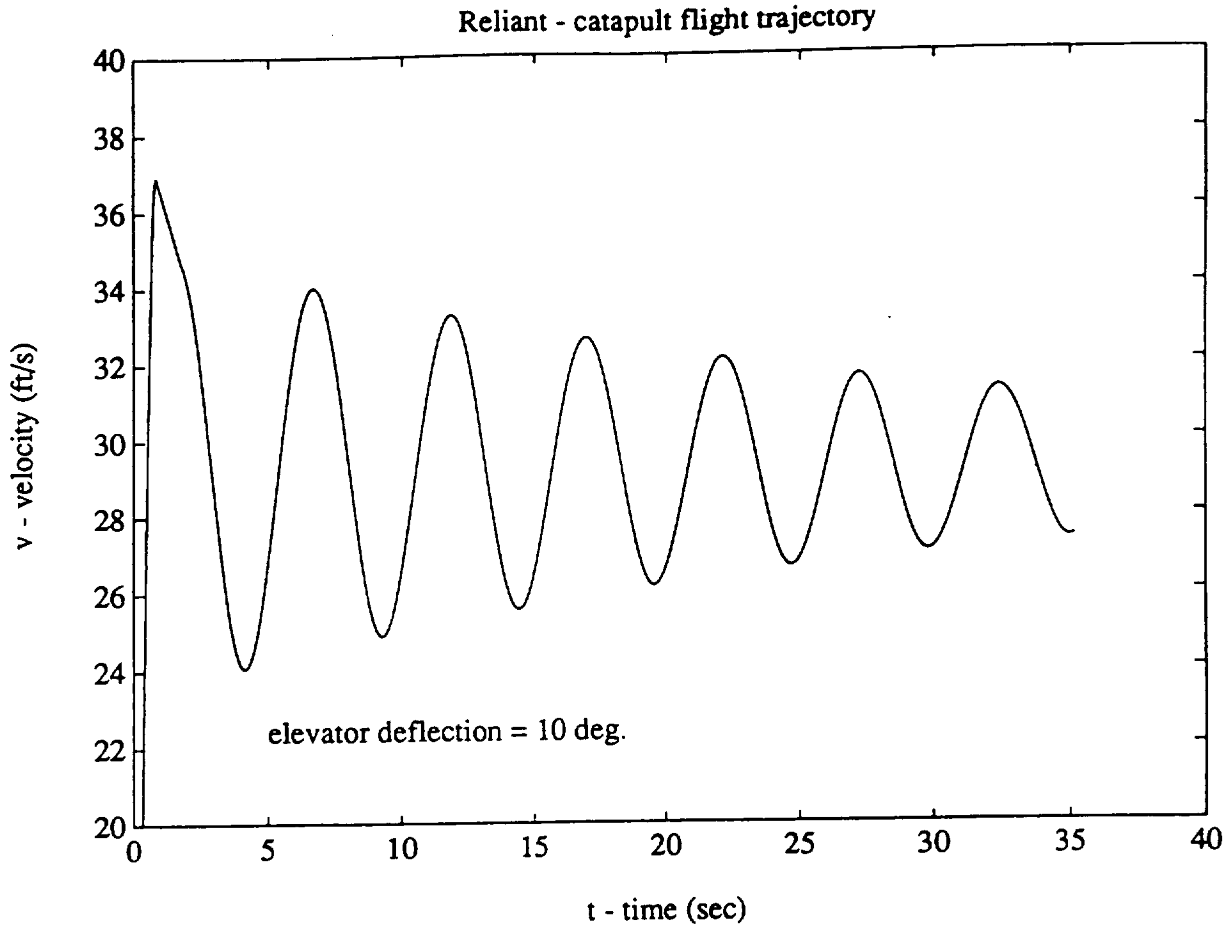
Reliant - catapult flight trajectory
v - velocity (ft/s)
t - time (sec)
elevator deflection = 10 deg.

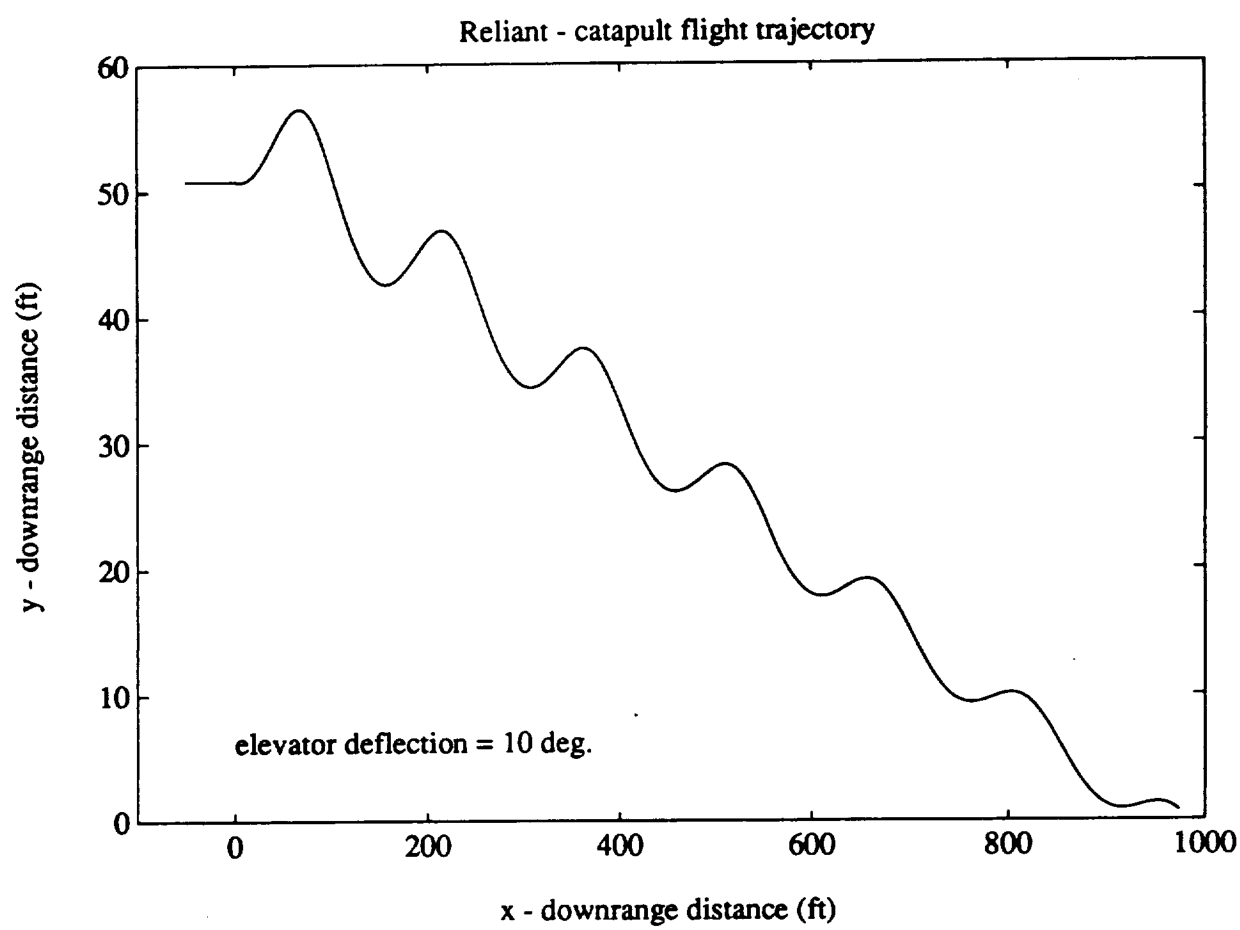
Reliant - catapult flight trajectory
y - downrange distance (ft)
x - downrange distance (ft)
elevator deflection = 10 deg.

```
0              canard flag-enter 1 for canard, any other number for tail
-32.17         gravity (ft/s**2)
0.00238        density (slugs/ft**3)
1.29167        x dist. from plane cg to attach pt. (ft)
-.2867         y dist. from plane cg to attach pt. (ft)
35.1875        catapult 'spring' undeformed length (ft)
20.0           distance between sling hardpoints (ft)
15.0           catapult-plane attachment cable (ft)
50.767         y position of top of catapult pins (ft) - **
0.767          height of catapult pins (ft)
32.0           catapult deformation <x dir.> (ft)
0.78           RPV c.g. height above ground when parked (ft)
50.78          initial altitude (ft) - **
0.0698         initial pitch angle (radians)
0.0            initial x velocity (ft/s)
0.0            initial y velocity (ft/s)
0.0            initial theta velocity (rad/s)
8.45           wing reference area (ft**2)
0.3837         body reference area (ft**2) - frontal area
2.25           tail reference area (ft**2)
2.757          body planform area (ft**2)
0.993          body volume (ft**3)
0.65           finite to infinite body drag ratio - DATCOM 4.2.3.2
1.2            body cross flow drag coefficient - DATCOM 4.2.3.2
0.0105         wing cdo
0.21           body cdo - based on frontal area
0.009          tail cdo
11.834         wing aspect ratio
4.0            tail aspect ratio
0.887          wing efficiency factor
0.8            tail efficiency factor
0.0835         wing clo
0.0            body clo - based on frontal area
0.0            tail clo
0.2094         wing stall angle (radians)
0.1745         tail stall angle (radians)
3.38           wing lift curve slope (per radian)
0.10886        body lift curve slope (per radian) - DATCOM 4.2.1.1
3.8            tail lift curve slope (per radian)
2.41           tail lift slope - elv. defl. (per rad.) - DATCOM 6.1.4.1
0.0349         wing angle of incidence (radians)
0.0            tail angle of incidence (radians)
0.0            elevator deflection (radians) (positive down)
-0.06          wing moment coefficient
0.0            tail moment coefficient
0.845          wing mean chord (ft)
0.75           tail mean chord (ft)
4.083          body length (ft)
1.875          distance from body nose to rpv c.g. (ft)
0.04167        x position of wing ac <from cg> (ft)
0.854          x position of body ac <from cg> (ft)
-2.208         x position of tail ac <from cg> (ft)
0.109          y position of wing ac <from cg> (ft)
0.0            y position of body ac <from cg> (ft)
0.109          y position of tail ac <from cg> (ft)
1.0            tail/wing dynamic pressure ratio - Nelson p.47
0.1734         rpv mass (slugs)
0.289          rpv pitching moment of inertia <about cg> (slugs*ft**2)
0.1            dynamic coefficient of friction
0.01           time step (s)
0.0            initial time value (s)
6              # of 1st order differential eqns. in system
```

Appendix G

Primary Data Items

Effect of Payload on Range

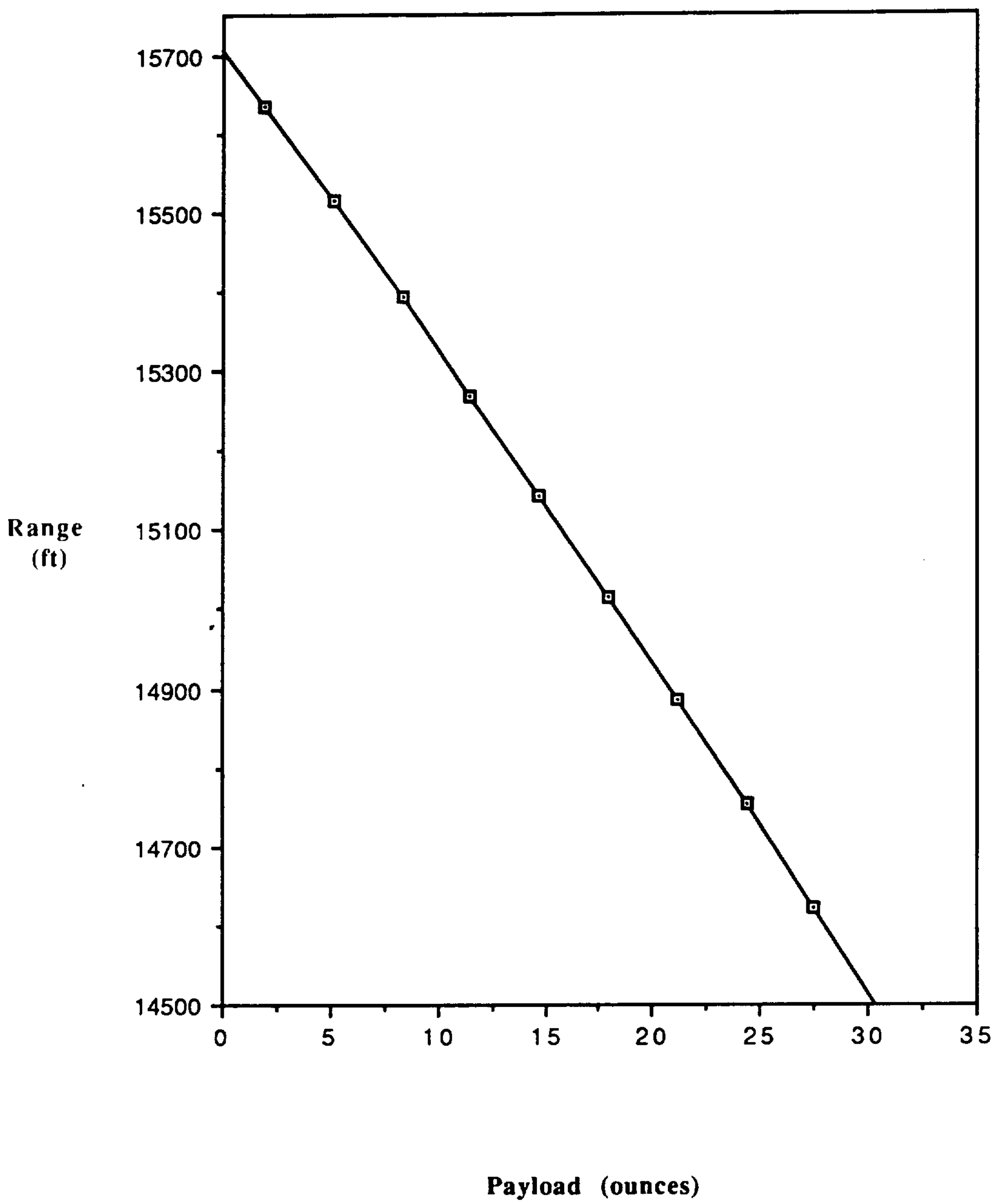

NACA 64-418 AIRFOIL LIFT CURVE

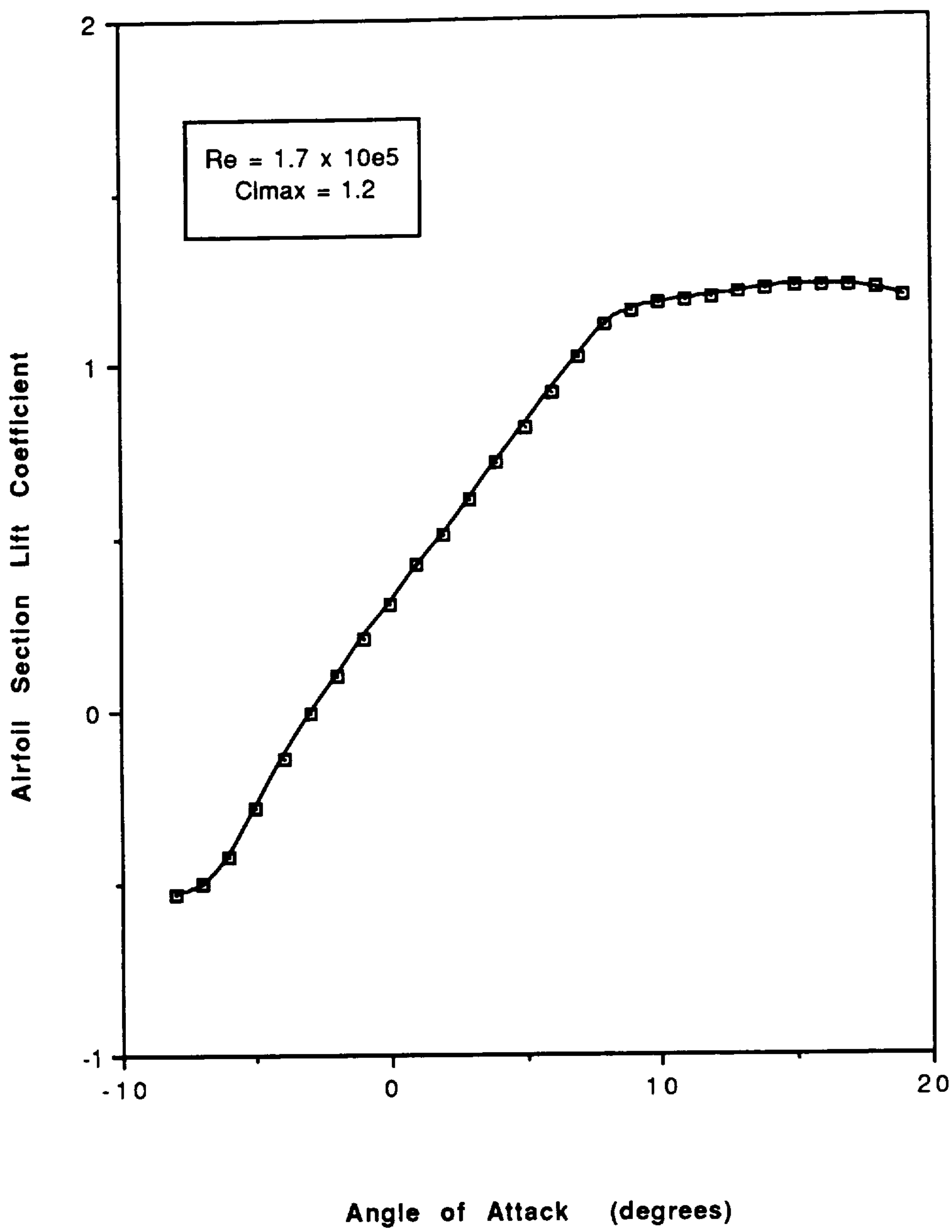

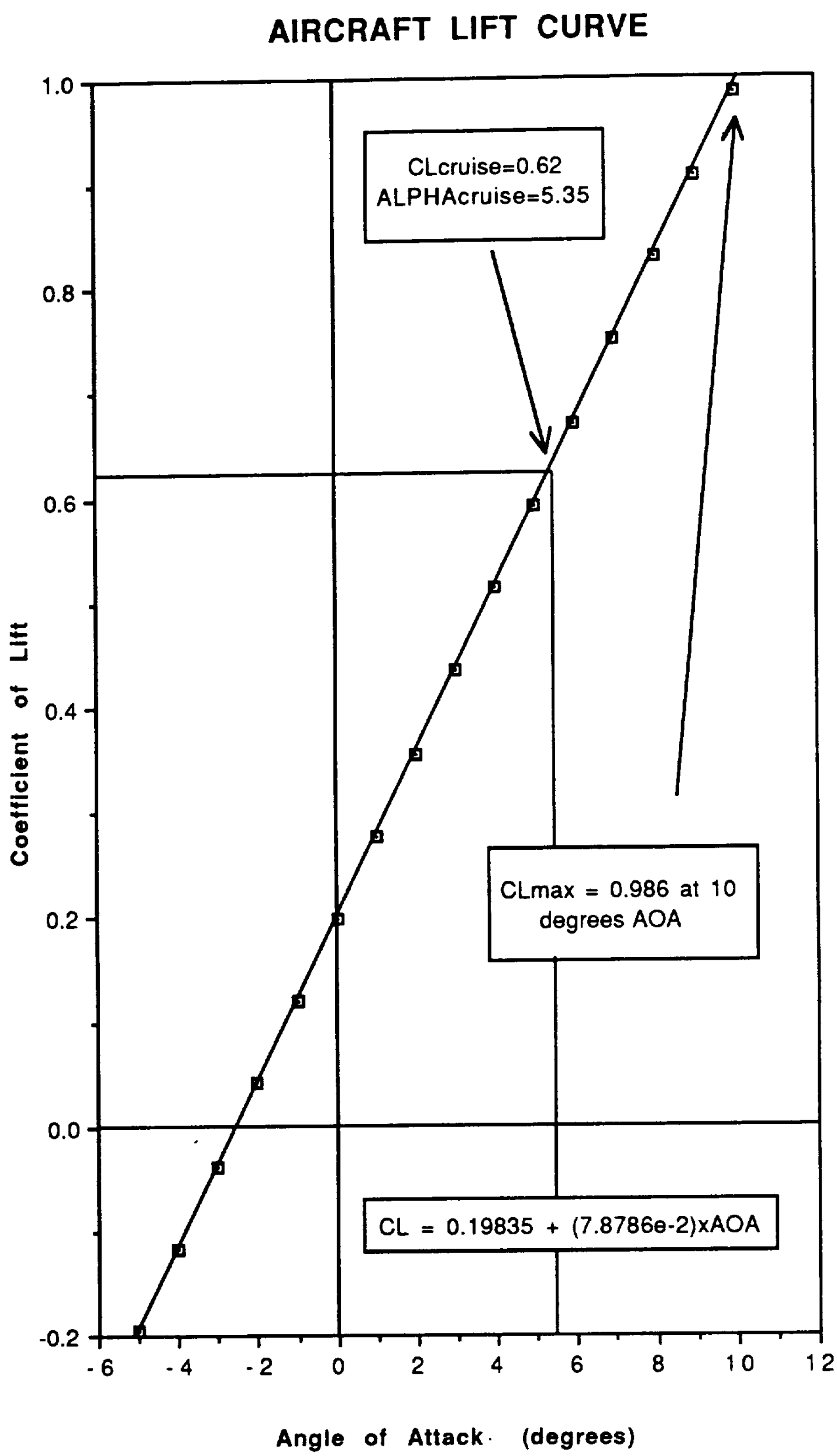
AIRCRAFT LIFT CURVE
CLcruise=0.62
ALPHAcruise=5.35
CLmax = 0.986 at 10
degrees AOA
CL = 0.19835 + (7.8786e-2)xAOA
Coefficient of Lift
Angle of Attack (degrees)
1.0
0.8
0.6
0.4
0.2
0.0
-0.2
-6
-4
-2
0
2
4
6
8
10
12

AIRCRAFT DRAG POLAR

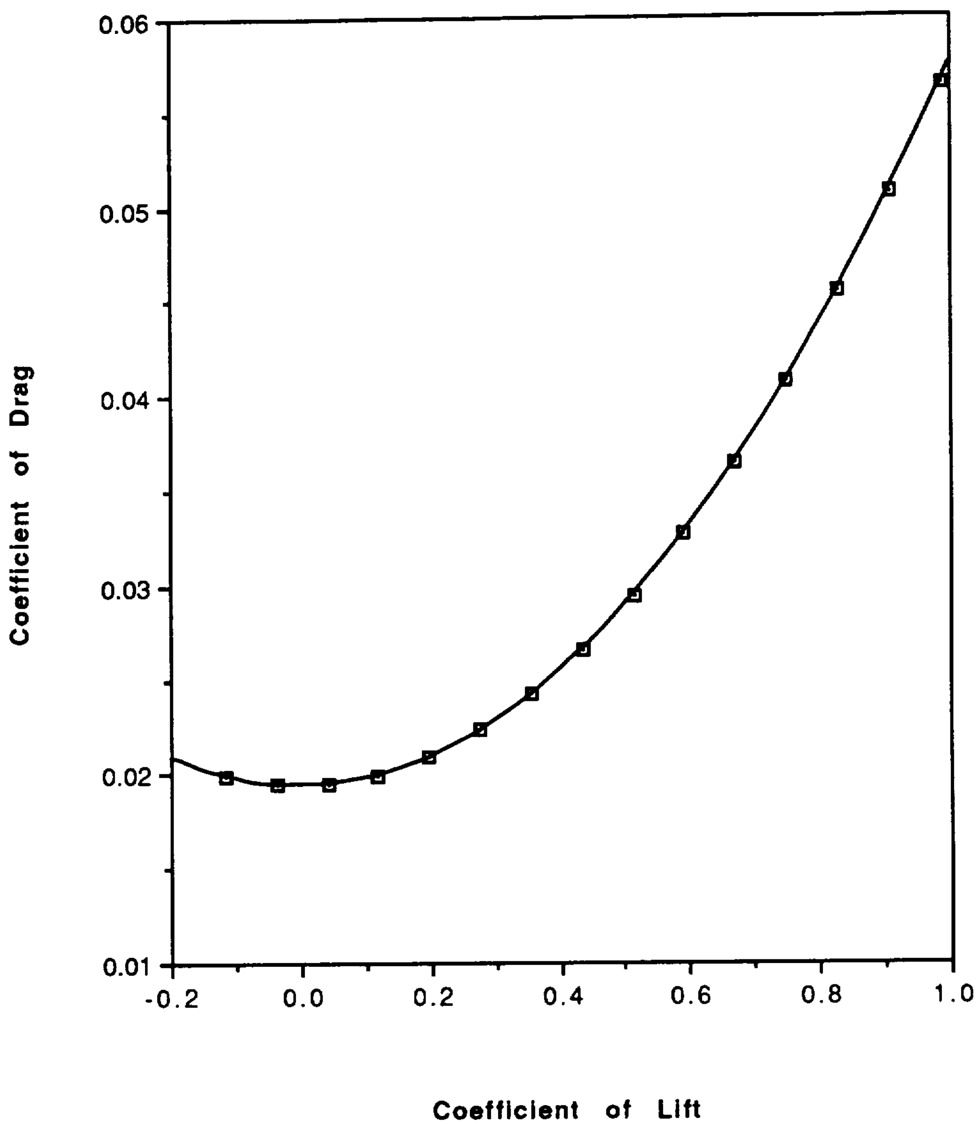

AIRCRAFT LIFT TO DRAG RATIO

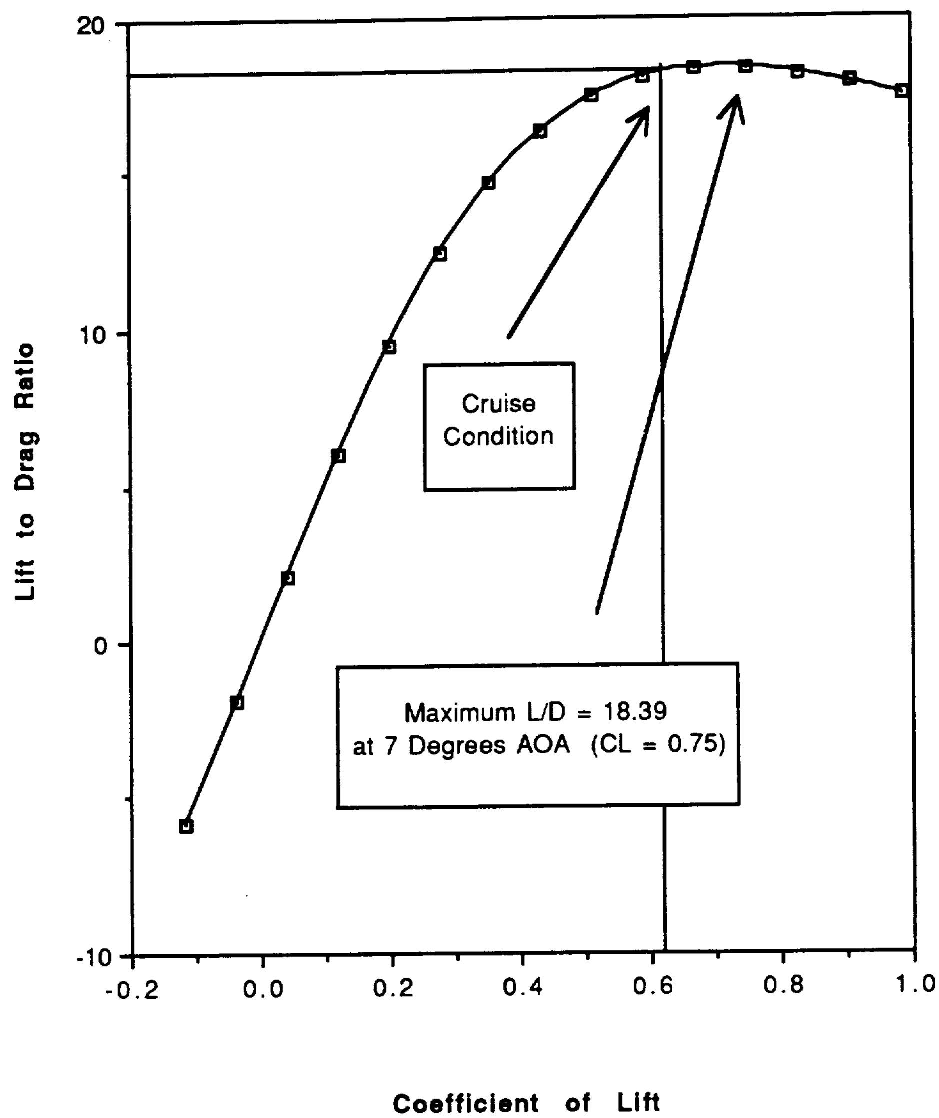

Figure 7.1.1 :
Cm-alpha curve for most forward CG location

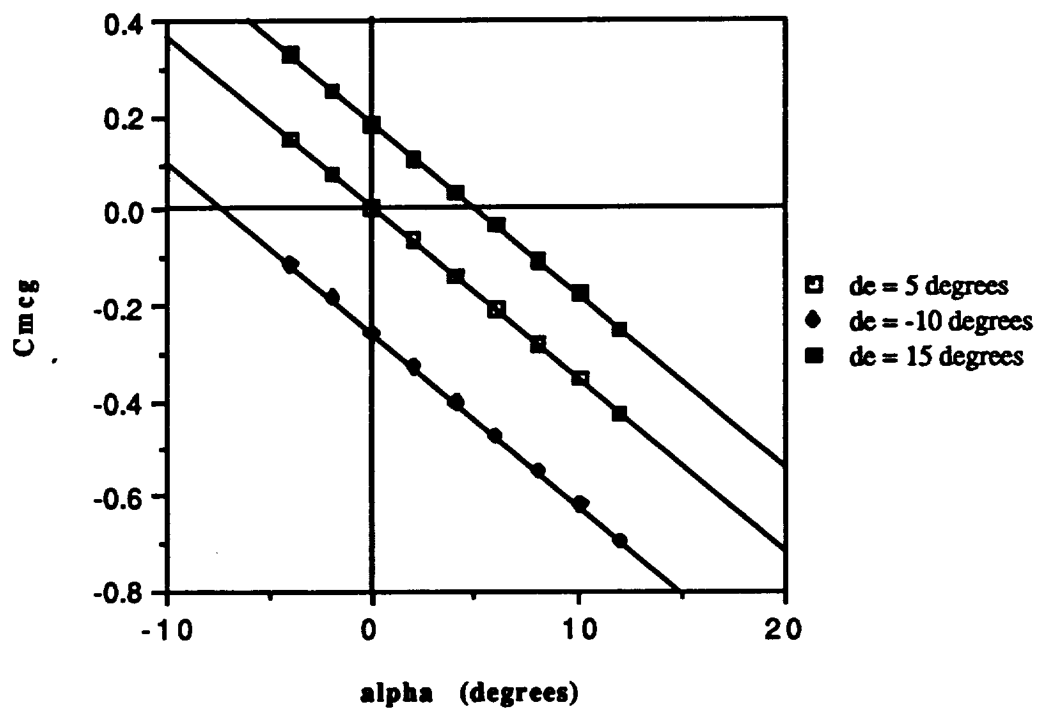

Figure 7.1.2:
Cm-alpha curve for most aft CG location

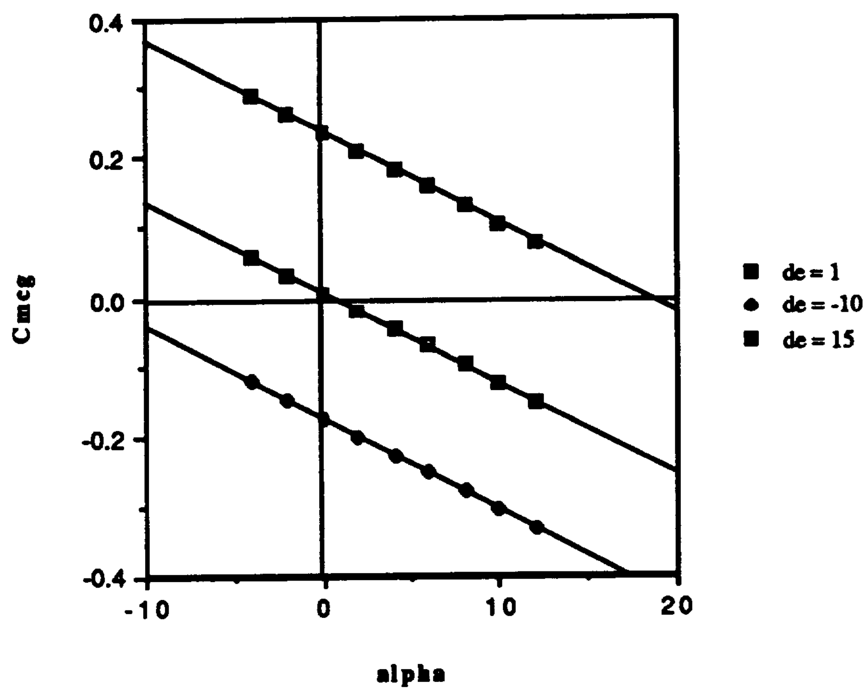

Power Required and Power Available for Various Throttle Positions

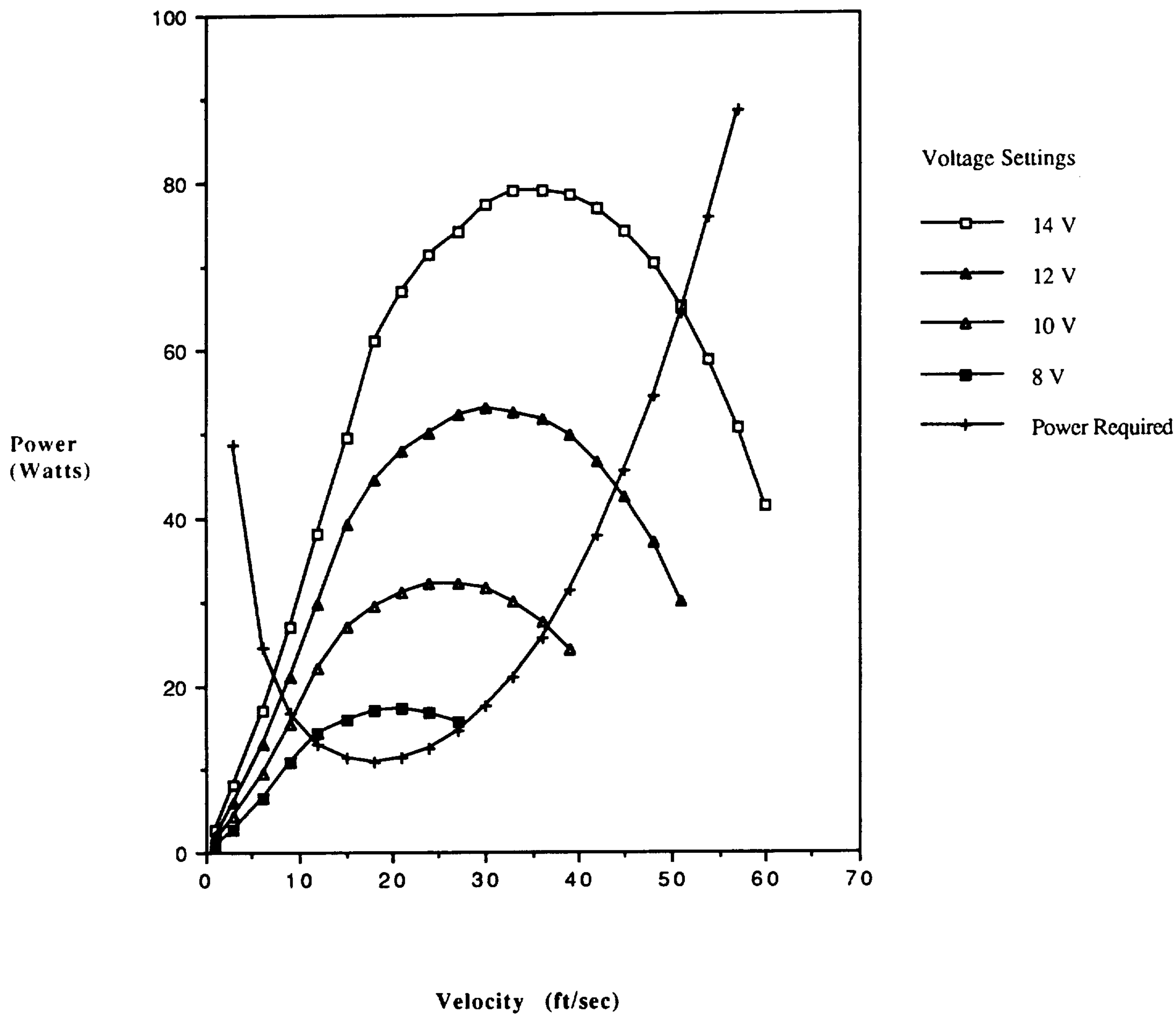

Propeller Efficiency Curve

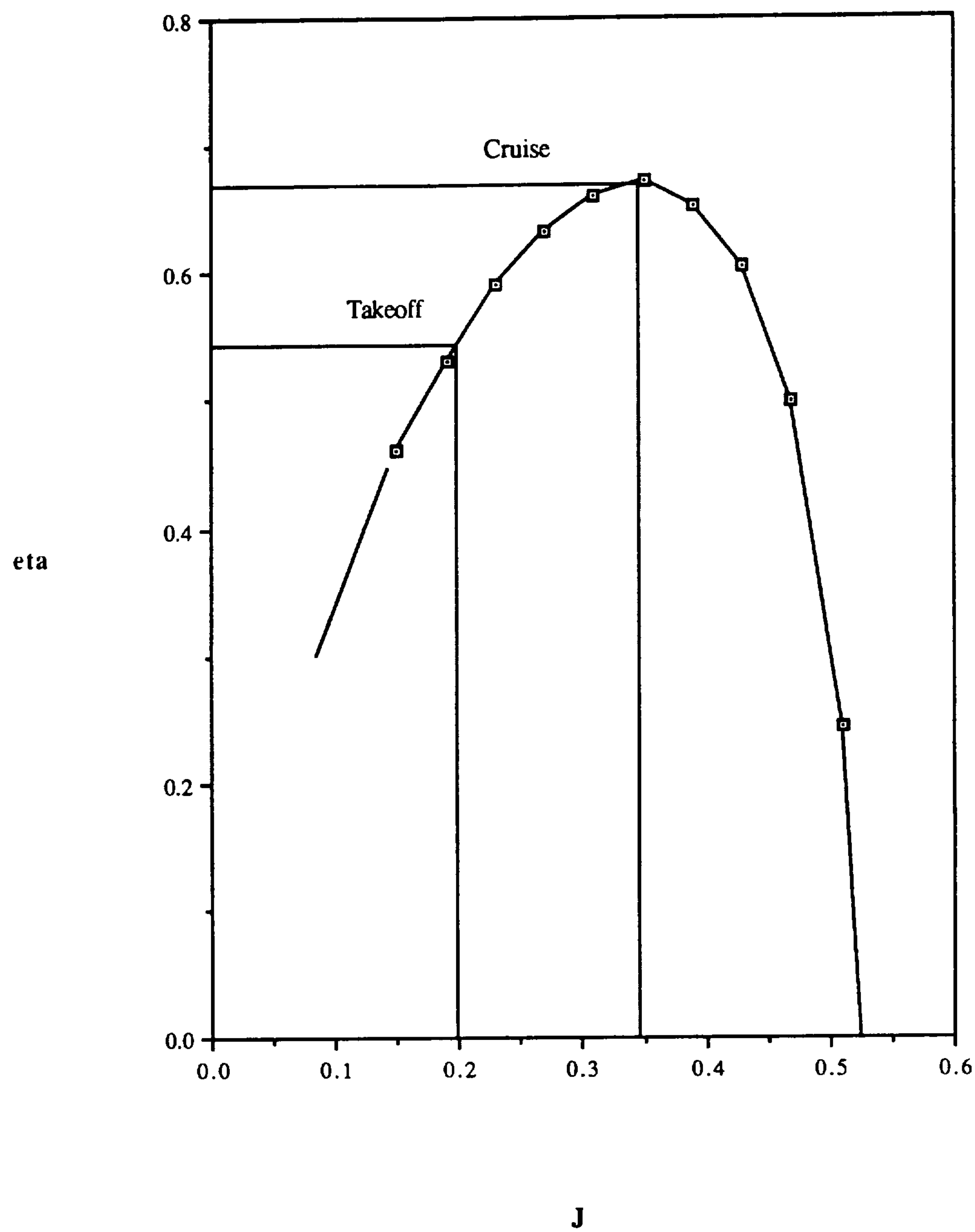

Figure 6.2 : Weight Balance Diagram

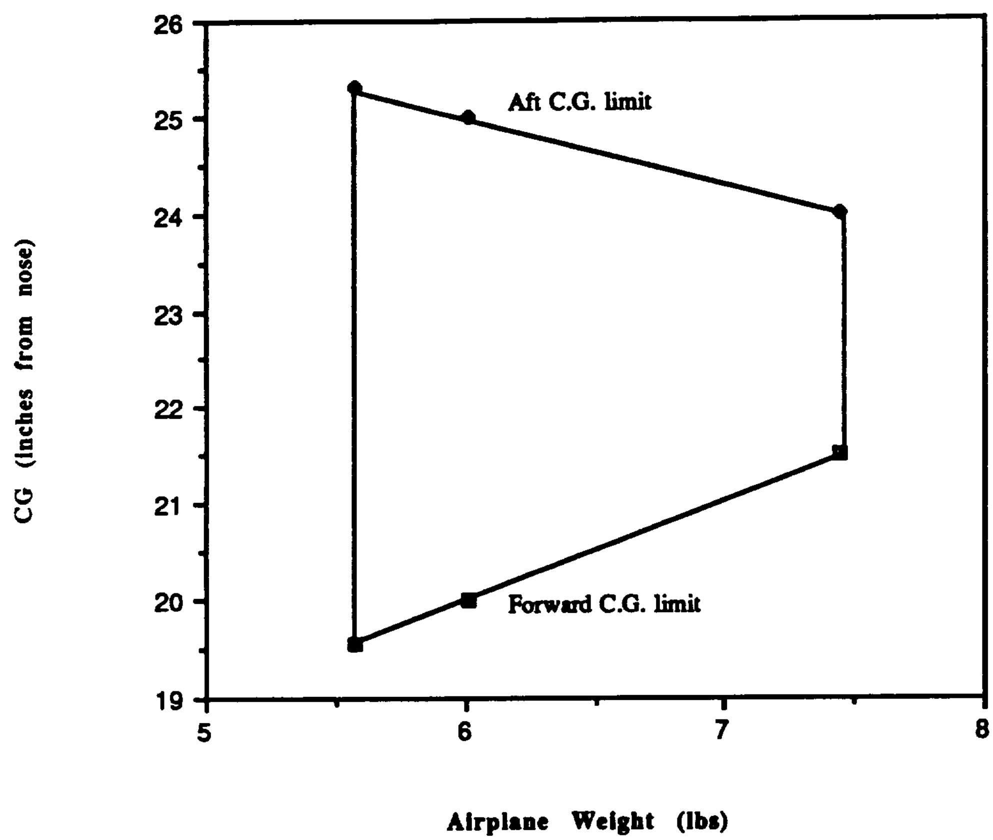

TABLE 13.2 **Component Weights, Positions, & Center of Gravity For Technology Demonstrator**

Component	Weight (lbf)	Weight (oz)	Xpos (inches)	Zpos (inches)	m*X (oz-in)	m*Z (oz-in)
---	---	---	---	---	---	---
Receiver & Antenna	0.061	0.98	10.00	5.00	9.80	4.90
Radio Battery	0.132	2.11	8.00	5.00	16.88	10.55
Servo (Elevator)	0.041	0.65	11.00	5.00	7.15	3.25
Servo (Rudder&Steering)	0.041	0.65	11.00	5.00	7.15	3.25
Pushrod (Elevator)	0.047	0.75	30.50	5.00	22.88	3.75
Pushrod (Rudder&Steering)	0.047	0.75	30.50	5.00	22.88	3.75
Fuselage & Motor Mount	1.094	17.50	23.00	2.50	402.50	43.75
Main Wing - High	0.813	13.00	22.00	6.00	286.00	78.00
Main Wing Mount	0.266	4.25	23.00	6.00	97.75	25.50
Secondary Wing - Low	0.419	6.70	29.00	-0.75	194.30	-5.03
Secondary Wing Mount	0.125	2.00	29.00	-0.75	58.00	-1.50
Vertical Tail & Rudder	0.088	1.40	46.00	12.60	64.40	17.64
Horizontal Tail & Elevator	0.253	4.05	50.00	5.75	202.50	23.29
Main Gear	0.394	6.30	11.00	-4.00	69.30	-25.20
Tail Gear & Steering	0.175	2.80	38.00	-2.00	106.40	-5.60
Engine & Clamp	0.563	9.00	3.00	2.00	27.00	18.00
Speed Control	0.110	1.76	6.50	3.00	11.44	5.28
Propeller	0.057	0.91	0.50	1.75	0.46	1.59
Battery (P90SCR) x 6	0.567	9.07	34.50	4.75	312.92	43.08
Battery (P90SCR) x 6	0.567	9.07	34.50	4.75	312.92	43.08
Battery Cable	0.144	2.30	20.75	4.50	47.73	10.35
Ballast	0.563	9.00	3.00	3.25	27.00	29.25
	Total Weights:				Centers of Gravity:	
Design Configuration:	6.000	96.00			23.75	3.14
(Both Wings/No Ballast)	Pounds	Ounces			= CG: X	= CG: Z
Altered Configuration:	6.144	98.30			21.50	3.42
(Main Wing Only/Ballast)	Pounds	Ounces			= CG: X	= CG: Z

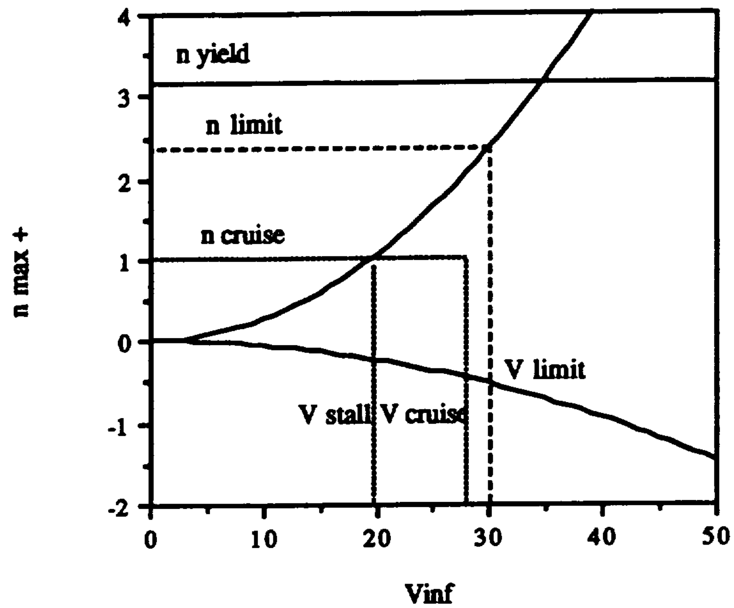

(a) Fully loaded

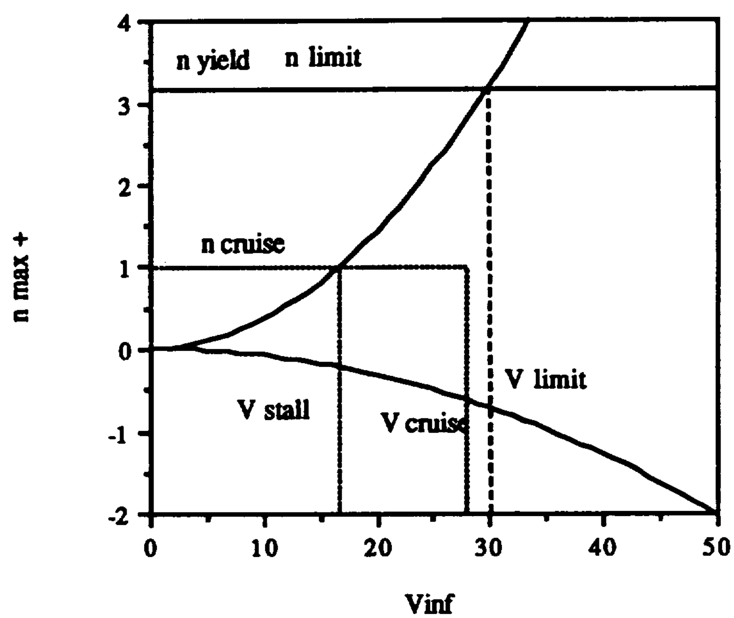

(b) Empty - no cargo

FIGURE 9.1.1.1 V-n DIAGRAMS FOR EXTREME WEIGHT CONDITIONS

TECHNOLOGY DEMONSTRATOR
PRIMARY COMPONENT COSTS

COMPONENT	COSTS
FUSELAGE	$32.46
LIFTING SURFACES	$31.50
EMPENNAGE	$11.71
LANDING GEAR	$10.51
MOTOR	$272.00
BATTERIES	$125.00
AVIONICS	$40.00

TOTAL $523.18

TECHNOLOGY DEMONSTRATOR
PRIMARY COMPONENT CONSTRUCTION TIMES

COMPONENT	TIME (LABOR-HOURS)
LIFTING SURFACES	72.5
FUSELAGE	33.5
EMPENNAGE	13.5
LANDING GEAR	6.75
AVIONICS	3.75

TOTAL 130

FIGURE 1.0.1

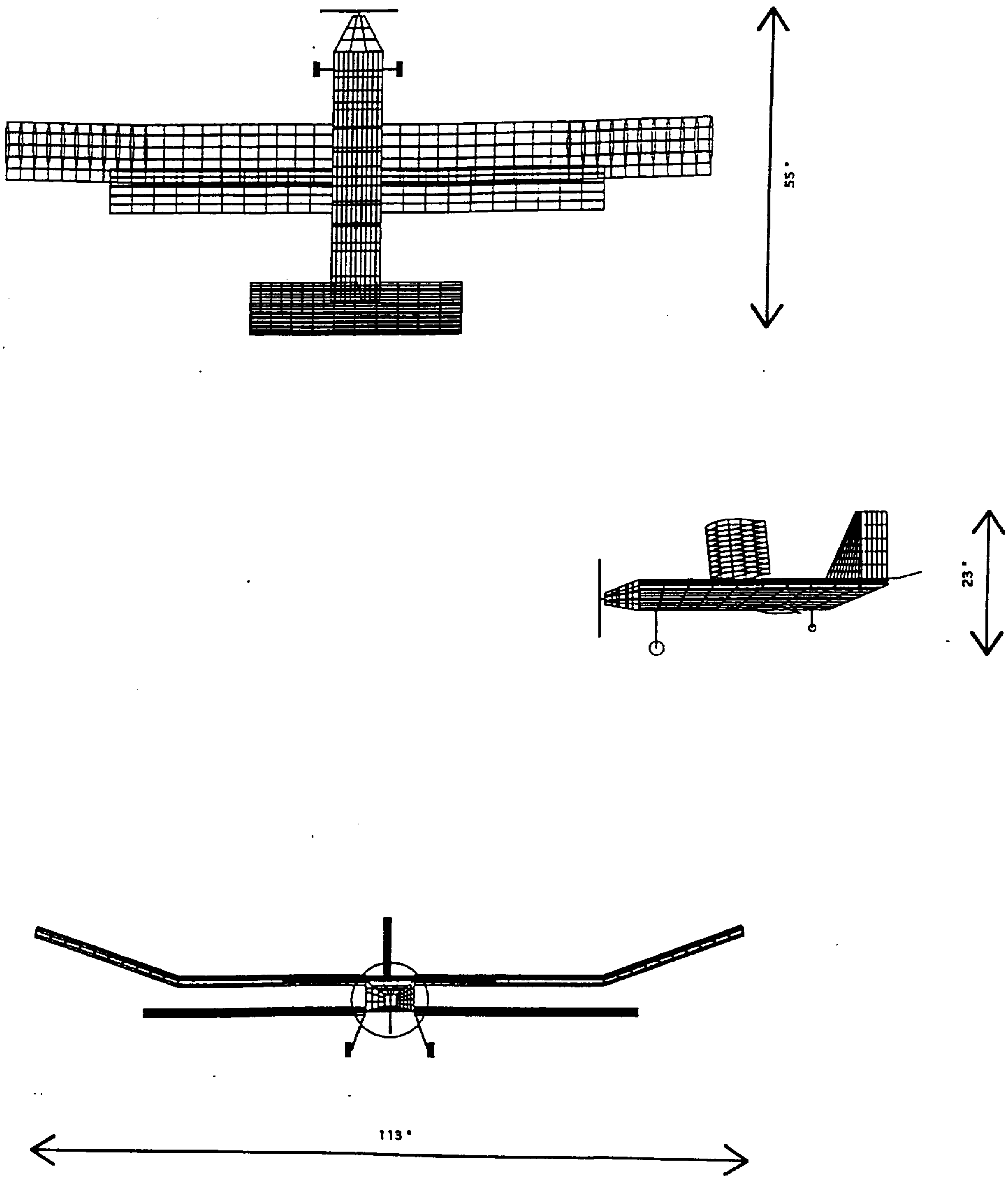

Appendix H

References

1. Anderson, John D. *Introduction to Flight*, 3rd Ed.McGraw-Hill, INC, 1989, NY.

2. Gere and Timoshenko, *Mechanics of Materials*, 2nd Ed.Wadsworth, INC, 1982 Belmont CA.

3. McCormick, Barnes W., *Aerodynamics, Aeronautics, and Flight Mechanics*, John Wiley & Sons, 1979, NY.

4. Merriam and Kreig, *Mechanics, Vol I Statics*, John Wiley & Sons, 1980, NY.

5. Model Aviation,(Magazine), Academy of Model Aeronautics, "Dihedral", Aug,Sep,Oct,Nov 1988.

6. Nelson, Robert C, *Flight Stability and Automatic Control*, McGraw-Hill, 1989, NY.

7. Niu, Michael C., *Airframe Structural Design*, Conmilit Press LTD. 1988, Los Angeles CA.

8. Nietsch, E. and Gillmer, T.C., *Simplified Theory of Flight*, D. Van Nostrand Company, INC., 1942, NY.

9. Miley, S.J., *A Catalog of Low Reynolds Number Airfoil Data for Wind Turbine Applications*, Texas A&M University, 1982, College Station TX.

10. Jensen, D.T., *A Drag Prediction Methodology for Low Reynolds Number Flight Vehicles*, A Master's Thesis, 1990, University of Notre Dame.